Quantum corrections to Drell-Yan production of Z bosons

Dissertation
zur Erlanung des Doktorgrades
des Fachbereichs Physik
der Universität Hamburg

vorgelegt von
Elena S. Shcherbakova
aus Kujbyshev (USSR)

Hamburg 2011

.

Erstgutachter der Dissertation:	Prof. Dr. B. A. Kniehl
Zweitgutachter der Dissertation:	Prof. Dr. A. Mirizzi
Erstgutachter der Disputation:	Prof. Dr. B. A. Kniehl
Zweitgutachter der Disputation:	Prof. Dr. G. Moorgat-Pick
Datum der Disputation:	22. Juli 2011
Vorsitzender des Prüfungsausschusses:	Prof. Dr. G. Sigl
Vorsitzender des Promotionsausschusses:	Prof. Dr. G. Hauschildt
Dekan der MIN-Fakultät:	Prof. Dr. H. Graener

Abstract

In this thesis, we present higher-order corrections to inclusive Z-boson hadroproduction via the Drell-Yan mechanism, $h_1+h_2 \to Z+X$, at large transverse momentum (q_T). Specifically, we include the QED, QCD and electroweak corrections of orders $O(\alpha_S\alpha, \alpha_S^2\alpha, \alpha_S\alpha^2)$. We work in the framework of the Standard Model and adopt the $\overline{\rm MS}$ scheme of renormalization and factorization. The cross section of Z-boson production has been precisely measured at various hadron-hadron colliders, including the Tevatron and the LHC. Our calculations will help to calibrate and monitor the luminosity and to estimate of backgrounds of the hadron-hadron interactions more reliably. Besides the total cross section, we study the distributions in the transverse momentum and the rapidity (y) of the Z boson, appropriate for Tevatron and LHC experimental conditions. Investigating the relative sizes of the various types of corrections by means of the factor $K = \sigma_{\rm tot}/\sigma_{\rm Born}$, we find that the QCD corrections of order $\alpha_S^2\alpha$ are largest in general and that the electroweak corrections of order $\alpha_S\alpha^2$ play an important role at large values of q_T, while the QED corrections at the same order $\alpha_S\alpha^2$ are small, of order 2% or below. We also compare our results with the existing literature. We correct a few misprints in the original calculation of the QCD corrections, and find the published electroweak corrections to be incomplete. Our results for the QED corrections are new.

Zusammenfassung

In dieser Arbeit präsentieren wir die Korrekturen höherer Ordnungen zur inklusiven Hadroproduktion von Z-Bosonen über den Drell-Yan-Mechnismus, $h_1 + h_2 \to Z + X$, bei hohem Transversalimpuls (q_T). Insbesondere nehmen wir die QED, QCD und elektroschwachen Korrekturen der Ordnungen $O(\alpha_S\alpha, \alpha_S^2\alpha, \alpha_S\alpha^2)$ mit. Wir arbeiten im Rahmen des Standardmodels und verwenden das $\overline{\text{MS}}$-Schema der Renormierung und Faktorisierung. Der Wirkungsquerschnitt der Z-Bosonerzeugung wurde bereits bei mehreren Hadronen-Speicherringen, einschließlich dem Tevatron und dem LHC, gemessen. Unsere Rechnungen werden dazu beitragen, die Luminosität zuverlässiger zu eichen und zu überwachen und die Untergründe der Hadron-Hadron-Wechselwirkung zuverlässiger abzuschätzen. Neben dem totalen Wirkungsquerschnitt untersuchen wir auch die Verteilungen im Transversalimpuls und in der Rapidität (y) des Z-Bosons unter den experimentellen Bedingungen des Tevatron und des LHC. Indem wir die relative Größe der verschiedenen Korrekturtypen mit Hilfe des Faktors $K = \sigma_{\text{tot}}/\sigma_{\text{Born}}$ untersuchen, finden wir, daß die QCD-Korrekturen der Ordnung $\alpha_S^2\alpha$ im allgemeinen am größten sind und daß die elektroschwachen Korrekturen der Ordnung $\alpha_S\alpha^2$ bei großen Werten von q_T eine wichtige Rolle spielen, während die QED-Korrekturen derselben Ordnung $\alpha_S\alpha^2$ klein sind, von der Ordnung 2% und darunter. Wir vergleichen unsere Ergebnisse auch mit der vorhandenen Literatur. Wir korrigieren einige Druckfehler in der Originalrechnung der QCD-Korrekturen und finden, daß die veröffentlichten, elektroschwachen Korrekturen unvollständig sind. Unsere Ergebnisse für die QED-Korrekturen sind neu.

Contents

List of Figures

Chapter 1

Introduction

The topic of this thesis is a precision investigation of Z boson production in hadron-hadron interactions. In particular, we calculated transverse momentum q_T and rapidity y distribution as well as the total cross section of Z boson production in proton-proton and proton-antiproton collisions, where QED, QCD and electroweak corrections were taken into account up to the orders $O(\alpha_S\alpha, \alpha_S^2\alpha, \alpha_S\alpha^2)$ of the perturbation theory. The accuracy of calculation for the theoretical description of this process is very important for the modern physics. The measurements of the Z boson production and jets are fundamental probes of the electroweak sector of the Standard Model (SM) and are an essential starting point for searches of new physics beyond the SM. The exploring of the electroweak symmetry breaking and search for physics beyond the Standard Model are significant goals of experimental research. For this purpose the detectors systematics should be under control. One of the ways to achieve it is the study very precisely the well-understood standard processes like W or Z boson production. The cross section of the Z boson production with the high transverse momenta q_T and well-isolated leptons decay modes can be very easy triggered in detectors such as ATLAS [1] and CMS [2]. This provide a clean experimental signature with rather low background especially for the Z boson production.

The Drell-Yan process occurs in high energy hadron-hadron scattering. It takes place when a parton of one hadron and another parton of the other hadron annihilate with creating a boson (virtual photon or neutral weak boson) which then decay into a pair of oppositely-charged leptons. This process was first suggested by Sidney Drell and Tung-Mow Yan in 1970 [3] to describe the production of lepton-antilepton pairs in high-energy hadron collisions. Experimentally, this process was first observed by J.H. Christenson et al. [4] in proton-uranium collisions at the Brookhaven National Laboratory, Alternating Gradient Synchrotron. The production of leptons pairs of invariant mass around 95 GeV was discovered and studied in other experiments [5].

The first theoretical calculation of the corrections to the Z boson production in the Drell-Yan process was done in the paper of Altarelli at al. [6], where the cross section $d\sigma/dQ^2$ was calculated for the prediction of a muons pair production of invariant mass Q^2 via the Drell-Yan mechanism in QCD.

The next-to-leading (NLO) QCD corrections for the large q_T vector boson production

have been computed in [7] by R. K. Ellis at al., then by R. J. Gonsalves at al. in [8] and by P. B. Arnold and M. H. Reno in [9]. The QCD corrections at the next-to-leading order to this process are the prime necessity for the correct description and amount to several tens of percent depending on the observable under consideration.

The corrections of order $O(\alpha_S^2)$ to the Drell-Yan K-factor were considered in [10] by W. L. van Neerven and others. This result was checked by R. V. Harlander and W. B. Kilgore in [11], where they fixed a mistake. Next step of corrections, the calculation of additional jets to Z/W production in hadrons collisions, was considered in papers [12]. The next-to-next-to-leading corrections including two-loop QCD diagrams were firstly computed for the total cross-section by T. Matsuura and others in [13].

To make a certain prediction in the calculation of the multiple gluon emission, which plays significant role in the region of small transverse momenta q_T, the contributions of arbitrary many gluon's must be re-sum ([14], [15]).

The dilepton differential distributions are calculated by C. Anastasiou et al. in papers [16]. The pure weak one-loop corrections were considered by J. H. Kuhn et al. in [17] while in [18] the leading logarithmic corrections were found. These works show that the electroweak corrections at high energies can amount few percent. The complete mixed $O(\alpha^2\alpha_s)$ corrections are not yet available. The virtual two-loop form factor of order $\alpha\alpha_s$ has been computed in [19] in terms of finite sums which have been then summed up analytically using explanation in [20].

We confine our attention to the large q_T and calculate the second order $O(\alpha_S^2\alpha)$ and $O(\alpha_S\alpha^2)$ corrections to Z boson production in Drell-Yan process. Using our calculated expressions together with the parton distributions functions, we make the prediction for q_T distributions at Tevatron and LHC colliders. We work in the framework of the SM in the $\overline{\rm MS}$ scheme. The cancellation of the divergences was carry out in the dimensional regularization scheme, where for the implementation of γ_5 matrix we used the idea of 't Hooft-Veltman method. The result of calculations includes:

– the QCD corrections of the order $O(\alpha_S^2\alpha)$ in the perturbation theory, where we considered loops and bremsstrahlung corrections to the QCD $i+j \to Z+k$ Born process (here i, j and k are gluons, quarks or antiquarks);

– the QED corrections of the order $O(\alpha_S\alpha^2)$ in the perturbation theory, where we considered loops and bremsstrahlung photonic corrections to the QCD $i+j \to Z+k$ Born process and QCD corrections to QED $i+j \to Z+\gamma$ Born process.

– the EW corrections of the same order $O(\alpha_S\alpha^2)$, where we considered loops diagrams in the exchange of weak bosons, and mixed EW-QCD corrections of the interference diagram $q+q \to q+q+Z$ with exchange of Z boson and the same diagram with exchange of gluon.

As a result of our calculations we present the total cross section $\sigma^{\rm tot}(q_T^{cut})$ of the Z boson production up to the order $O(\alpha_S\alpha^2, \alpha_S^2\alpha)$. The cut transverse momentum q_T^{cut} comes from the upper limit of the integration over kinematic parameters. We plotted also the rapidity and transverse momentum distributions of the differential cross sections $\frac{{\rm d}\sigma}{{\rm d}q_T}$ and $\frac{{\rm d}\sigma}{{\rm d}y}$. We investigated the relative size of the various types of the contributions with a help of the so-called K factor: $K = \frac{\sigma^{tot}}{\sigma^{Born}}$. The analysis of the numerical calculations showed

that however the corrections of the QCD order are the biggest in all region of transverse momentum q_T or rapidity y, the EW corrections are also very important at high q_T and can reach values up to 20%. The QED corrections are small and can be visible only by high transverse momenta q_T, where they reach $1-2\%$.

The thesis will be organized as follows.

In Chapter 2 we discuss the general method for calculating the cross section in the perturbation theory. In section (2.1) we give the master formula for the calculation of the hadronic cross section with a help of convolution of the partonic cross section (which is given in section 2.3) and the parton distribution functions. The Dokshitzer-Gribov-Lipatov-Altarelli-Parisi (DGLAP) equations for the parton distribution functions are given in the section (2.2). In section (2.4) we discuss Integration By Part procedure, which reduces all integrals to the set of master integrals, and gives the set of scalar integrals, which was used by loop calculation. Section (2.5) is devoted to the the method of integration the bremsstrahlungen corrections to the Born processes. We used Passarino-Veltman reductions scheme [21] to calculate loops integrals in dimensional regularization. The phase space integrals are considered in d dimensional space by using the van Neerven [22] method. In section (2.6) we discuss the way to calculate traces with γ_5 matrix in d dimensional space.

In Chapter 3 we discuss the steps of our calculation in more detail. At first, we give the Lagrangian of the SM and Feynman rules which were used in the calculation of QCD and EW corrections to the Z boson production (section 3.1). Then, in section (3.2) we introduce relevant Feynman diagrams. Section (3.3) contains the details of singularities consideration and the factorization of collinear singularities.

In Chapter 4 we present the analytical results of the calculated corrections. Namely, we give the formulae for the QCD corrections (Section (4.2)), for the QED correction (Section (4.3)) and for the EW corrections (Section (4.4)).

The numerical analysis is given in Chapter 5, where we present the total cross section $\sigma^{tot}(q_T^{cut})$, where q_T^{cut} is cutted transverse momentum, the differential rapidity distribution $\frac{\mathrm{d}\sigma}{\mathrm{d}y}$ and the transverse momentum distributions $\frac{\mathrm{d}\sigma}{\mathrm{d}q_T}$. To see the values of different contributions to total result we analyze the K factor for the total cross section.

Finally we present the summary in Chapter 6.

The appendix contains the full analytical formula for QED and EW corrections.

Chapter 2

Cross section

The first observations of the deep-inelastic lepton-nucleon scattering with non hadronic final states shown that its dependence the transverse momentum q_T^2 decline slower in distinction from the elastic scattering cross sections, which slopes steeply down by high q_T^2. This means that inside hadrons must be point-like subparticles, which later were named by Feynman "partons".

In the current theoretical framework, the high energy lepton-hadron and hadron-hadron cross sections are related to calculable fundamental parton interaction cross section $\sigma_{i,j}$ by the QCD factorization theorems as a sum of the convolution partonic cross section with universal parton distribution functions.

In this Chapter we will explain how the hadronic cross section can be calculated throw consideration of the partonic interactions and will give formulae for integrated partonic cross sections.

2.1 Parton distributions in the hadrons

The collision of one hadron h_1 with momentum P_1 and another hadron h_2 with momentum P_2 at high energies with a production of a weak boson, so-called Drell-Yan process, can be described in the frame of the parton model. According to this model, in the limit of big collision energy S and high value of virtual bosons mass $q^2 \to \infty$ (with fixed relation q^2/S), the reaction is going throw interaction of partons with production of a vector boson V with momentum q (see Fig. (2.1)). The vector boson decaying into lepton pair can be observed at the detectors in experiments. Each of partons is emitted from parent hadrons and contains the part x of momenta of hadron.

The Drell-Yan process can be written as

$$h_1(P_1) + h_2(P_2) \longrightarrow V(q) + X, \tag{2.1}$$

where for our case V is the Z boson with transverse momentum q_T and mass $q^2 = m_Z^2$; X are unobservable particles which arise together with the vector boson. We have to integrate over their momenta.

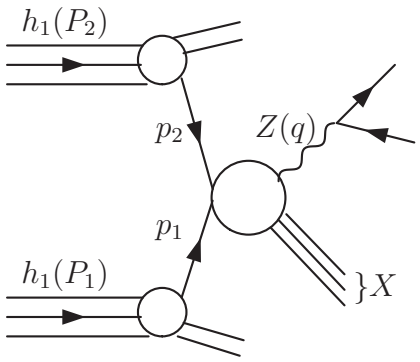

Figure 2.1: Production of the weak boson Z in hadron-hadron interaction.

In the framework of the particle interaction we can rewrite this process as a partons interaction:

$$i(p_1) + j(p_2) \longrightarrow V(q) + X; \tag{2.2}$$

here $i(j)$ is the mass-less parton with momentum $p_{i(j)} = x_{i(j)}P_{i(j)}$, which emits from the corresponding hadron $h_{i(j)}$ $(i, j = 1, 2)$. Let us denote $f_i(x, \mu_F^2)$ the probability of density to find the parton i with momentum fraction x if it is probes at factorization scale μ_F^2. Then the hadronic cross-section of the Z boson production in the Drell-Yan process (2.1) can be written as a convolution of parton densities functions with the partonic cross-section:

$$\frac{d\sigma}{dq_T^2\, dy} = \sum_{i,j} \int dx_1\, dx_2\, f_i(x_1, \mu_F^2) f_j(x_2, \mu_F^2) \frac{s\, d\hat{\sigma}_{i,j}}{dt\, du}(x_1 P_1, x_2 P_2, \mu_F^2). \tag{2.3}$$

Here the hadronic cross section σ is wrote as a derivative distribution of transverse momentum of observable boson q_T and rapidity y. The parameters s, t and u are common Mandelstam variables, which are composed of partonic momenta. The sum runs over all parton flavors i and j, and the "hat" at the partonic differential cross-section $\hat{\sigma}_{i,j}$ means that calculations were done in the $\overline{\text{MS}}$ scheme, which we will discuss later.

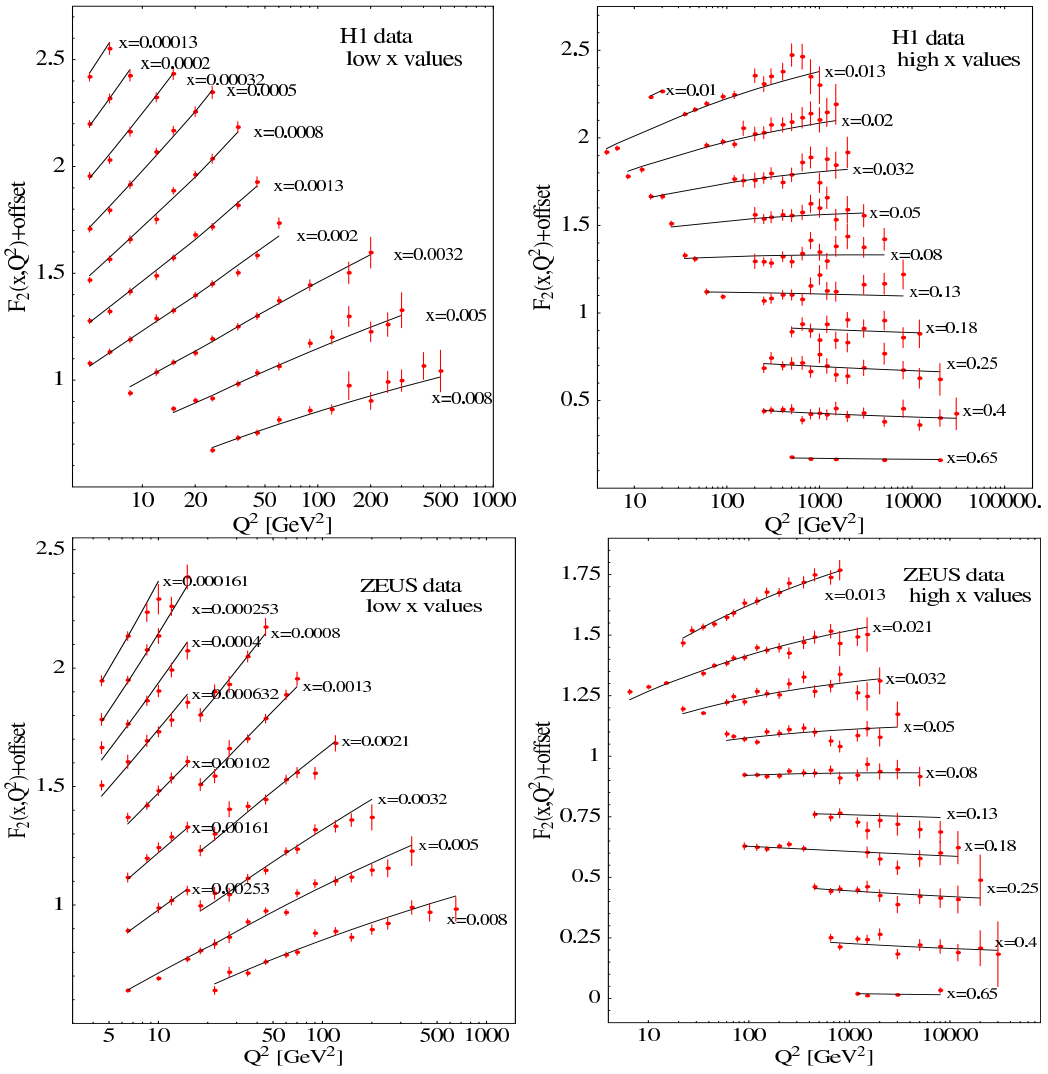

Figure 2.2: Comparison of the CTEQ6M fit to the H1 data [23] (above) and the ZEUS data [24] (below) in separate x bins. The data points include the estimated corrections for systematic errors. The error bars contain statistical only. [25].

Because of the inherent non-perturbative effect in a QCD binding states, the parton distribution functions (PDF) cannot be obtained by the perturbative QCD. Due to the limitations in present lattice QCD calculations, the known PDFs are instead obtained by using experimental data. The parton distributions can be determined from analyzing of a set of standard experiments:

– deep inelastic scattering (DIS),
– lepton-pair production,
– high-p_t direct-photon production,
– W- and Z-production,

– high-p_t jet-production,

– etc.

The Fig. (2.2) shows, as an example, the comparison of the theoretical PDF's fit CTEQ6m to the data of the H1 experiment [23] and data of ZEUS [24] experiment.

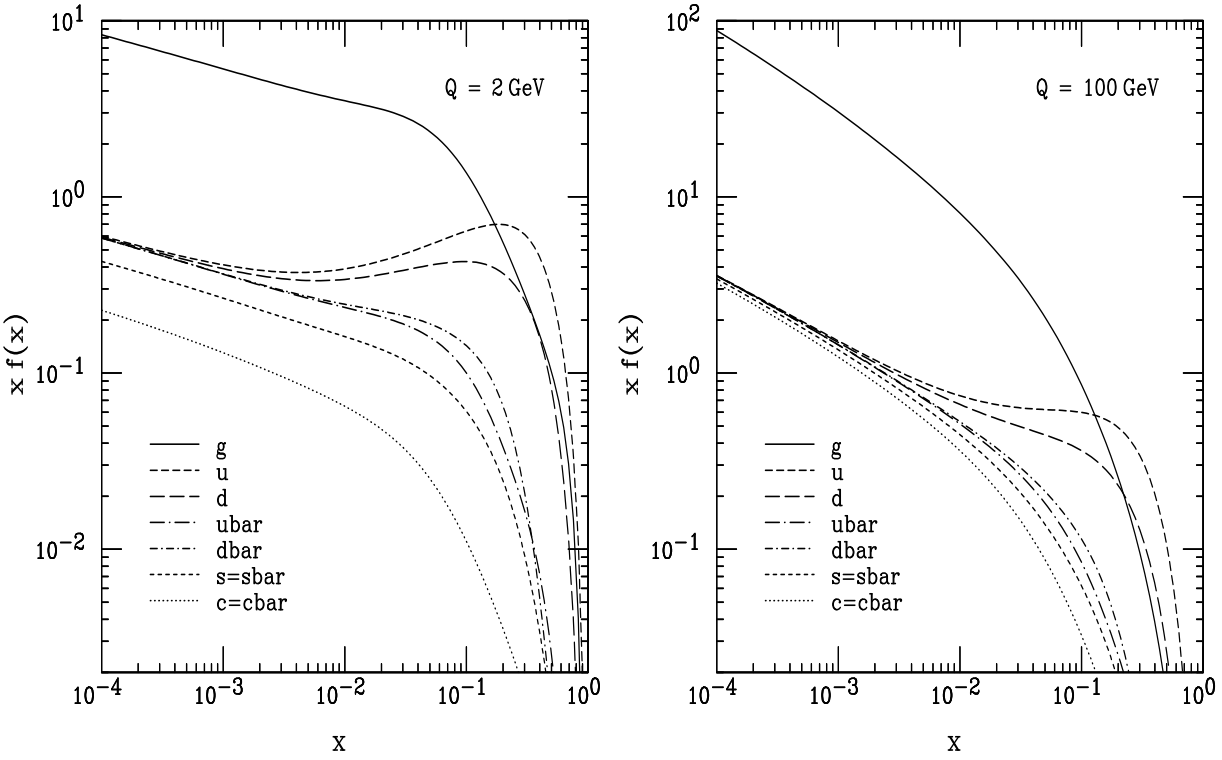

Figure 2.3: Overview of the CTEQ6M parton distribution functions at $Q = 2$ and $Q = 100GeV$ [25].

There are a lot of groups that estimate the PDFs from experiments. In our calculation we used the results of two groups. The first one is a CTEQ collaboration (G. Sterman, J. Smith, J. C. Collins, W. Vogelsang, J. Huston, J. Pomplin etc. [25]), which parton distribution functions were accounted in our main result. For our problem we used the standard set of parton distributions in the $\overline{\text{MS}}$ scheme for proton and antiproton (CTEQ6). At the Fig. 2.3 is shown the overall view of these PDF's, at two scales $Q = 2GeV$ and $Q = 100GeV$.

The PDF from another group, MRS collaboration (A. Martin, J. Stirling, R. Thorne, G. Watt [26]), was used in the special part of QED contributions, a photoproduction. We will be discuss it in more detail below.

In the Appendix A are operators definitions [27] of the parton distribution functions for reference.

2.2 DGLAP functions

The parton distribution functions obey to DGLAP equations [28]. This equations describe the evolution of the parton distribution $f_f(x,Q)$, $f_{\bar{f}}(x,Q)$ for quarks and antiquarks of every flavor f ($\bar{f}$), where particles can be considered at the Q scale as mass-less, together with parton distributions of gluons $f_g(x,Q)$ in an explicit form:

$$\begin{aligned}
\frac{d}{d\ln Q} f_g(x,Q) &= \frac{\alpha_S(Q^2)}{\pi}\int\limits_x^1 \frac{dz}{z}\left\{ P_{g\leftarrow q}(z)\sum_f \left[f_f(\frac{x}{z},Q) + f_{\bar{f}}(\frac{x}{z},Q)\right]\right. \\
&\qquad \left. + P_{g\leftarrow q}(z) f_g(\frac{x}{z},Q)\right\}, \\
\frac{d}{d\ln Q} f_f(x,Q) &= \frac{\alpha_S(Q^2)}{\pi}\int\limits_x^1 \frac{dz}{z}\left\{ P_{q\leftarrow q}(z) f_f(\frac{x}{z},Q) + P_{q\leftarrow g}(z) f_g(\frac{x}{z},Q)\right\}, \\
\frac{d}{d\ln Q} f_{\bar{f}}(x,Q) &= \frac{\alpha_S(Q^2)}{\pi}\int\limits_x^1 \frac{dz}{z}\left\{ P_{q\leftarrow q}(z) f_{\bar{f}}(\frac{x}{z},Q) + P_{q\leftarrow g}(z) f_g(\frac{x}{z},Q)\right\},
\end{aligned} \tag{2.4}$$

where the splitting functions $P_{i\leftarrow j}$ are here:

$$\begin{aligned}
P_{q\leftarrow q}(y) &= C_F\left(\frac{1+y^2}{(1-y)_+} + \frac{3}{2}\delta(y-1)\right), \\
P_{g\leftarrow q}(y) &= C_F\frac{1+(1-y)^2}{y}, \\
P_{g\leftarrow g}(y) &= 2C_A\left(\frac{1}{(1-y)_+} + \frac{1}{y} + y(1-y) - 2\right) + \delta(y-1)\left(\frac{11}{6}C_A - \frac{2}{3}T_F\right), \\
P_{q\leftarrow g}(y) &= n_f\frac{y^2+(1-y)^2}{2}.
\end{aligned} \tag{2.5}$$

The color factors C_A and C_F are associated with $SU(2)$ group, n_F is a number of flavors. The " $+$ " distribution in the splitting functions is defined by the relation

$$\int\limits_0^1 dy \frac{f(y)}{(1-y)_+} = \int\limits_0^1 dy \frac{f(y)-f(1)}{(1-y)}. \tag{2.6}$$

The DGLAP equations describe the evolution of distribution functions in QCD for any flavor, or any hadron components with an accuracy up to corrections of order α_S, which are not strong of large logarithms.

The DGLAP functions predict the generic view of partons distribution function evolution, which is shown at the Fig. (2.3). By high x the partons radiate and are going to states with lower x. At the same time, as a result of these radiation, new partons product with small value of x. So, with increase of Q^2, the parton distribution functions fall off at

high x and grow much stronger at small x. By considering the wave function of proton at the more smaller scales, we will have the proton, which contains the larger number of partons, which momenta are shared the full momenta of the proton.

2.3 Partonic cross section

The partonic cross section $d\sigma_{i,j}$ in the Eq. (2.3) can be found with a help of the general formula

$$d\sigma_{i,j} = \frac{1}{2E_i 2E_j |v_i - v_j|} |M(p_i, p_j \to \{p_f\})|^2 d\Phi^{(n)} \tag{2.7}$$

where $2E_i 2E_j|v_i - v_j|$ is the flux factor, $|M(p_i, p_j \to \{p_f\})|^2$ is the partonic matrix elements of interaction particles p_i and p_j with production of a set of final particles $\{p_f\}$, E_i and E_j are the energies of incoming particles.

The integration under momenta of final states has following general structure:

$$\int d\Phi^{(n)} = \Big(\prod_f \int \frac{d^3 p_f}{(2\pi)^3} \frac{1}{2E_f}\Big) (2\pi)^4 \delta^{(4)}\big(p_i + p_j - \sum_f (p_f)\big). \tag{2.8}$$

This integral is known as relativistic-invariant phase volume of n-particles and it is distinctly Lorentz-invariant, cause constructed from invariant integrals under 3-momenta, which are connected with delta-function of 4-momenta. This delta-function of 4-momenta points at the energy conserving law.

Matrix elements $|M(p_i, p_j \to \{p_f\})|^2$ are constructed of squared scattering amplitudes for the process $i + j \to \{f\}$. By convention, the scattering amplitudes are expressed with a help of so-called Feynman diagrams, which depend of model in which the calculations is made. In the Chapter 3 we will consider the interactions and the set diagrams, which was taken into account in Z boson production. In this chapter of discussion we will give common consideration of basic steps by calculation of cross section.

In the Fig. (2.4) the scheme of calculation matrix elements is shown. Here the parameter g marks the order in the perturbation theory of calculations. For calculation of the first level in perturbation theory, we have to square tree diagrams. For calculation of the second order of correction, we divided them to virtual and collinear (bremsstrahlung) corrections. The loop diagrams can contain bubble, triangle, box corrections. They multiply by tree diagram to obtain next order correction of g. The bremsstrahlung corrections contain additional emitted particle.

We will describe the structure of diagrams, which we used by calculations, in more detail in the next Chapter.

2.4 Virtual integrations

The virtual corrections of the Z boson production include calculations of loop integrals over a phase space $\mathrm{d}\Phi^2$. Let us firstly consider kinematic correlations, then we give the phase

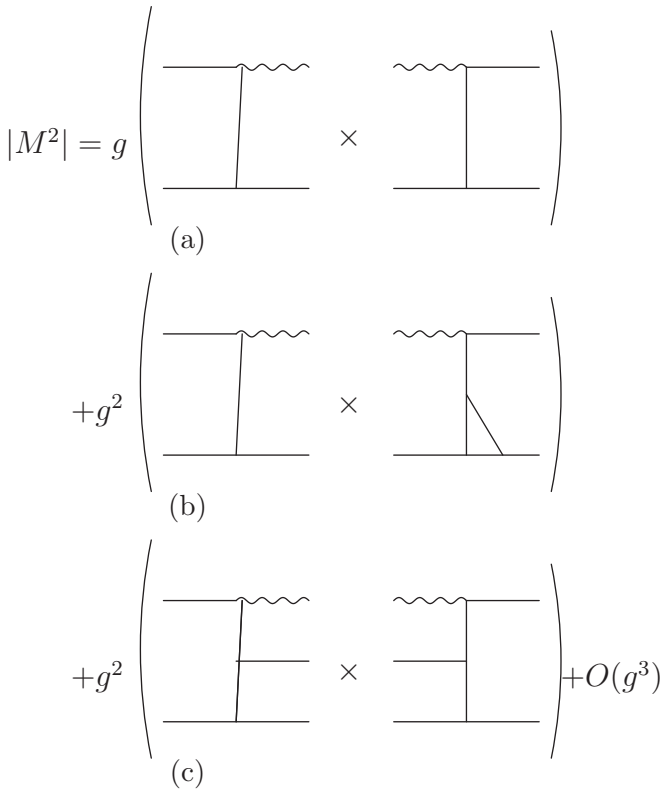

Figure 2.4: Matrix elements structure. See explanation in the text.

space formula for the two-to-two process. Then we consider one of the ways of calculating of the loop integrals.

2.4.1 Phase space with two final particles

In the center-of-mass framework of incoming hadrons h_1 and h_2 for the process which was shown in the Fig. 2.1, we have for momenta following formulations:

$$\begin{aligned} P_1 &= \frac{1}{2}\sqrt{S}(1;0,0,1), \\ P_2 &= \frac{1}{2}\sqrt{S}(1;0,0,-1), \\ q &= (q_0;\vec{q}_T,q_3), \qquad q^2 = Q^2, \end{aligned} \tag{2.9}$$

where q is momentum of boson, which we consider, S is summarized energy of incoming particles. S can be found in definition:

$$S \;=\; (P_1+P_2)^2; \tag{2.10}$$

and other global Mandelstam variables are defined as follows:

$$T = (P_1 - q)^2, \tag{2.11}$$
$$U = (P_2 - q)^2. \tag{2.12}$$

For partonic processes (2.2) in the center-of-mass framework of incoming partons i and j momenta p_1 and p_2 can be written as

$$p_1 = \frac{\sqrt{s}}{2}(1;0,0,1), \tag{2.13}$$
$$p_2 = \frac{\sqrt{s}}{2}(1;0,0,-1).$$

For partonic momenta we introduced "small" Mandelstam variables as usual:

$$s = (p_1 + p_2)^2, \tag{2.14}$$
$$t = (q - p_1)^2,$$
$$u = (q - p_2)^2,$$
$$s_2 = p_X^2,$$

which can be rewritten in the center of mass of incoming particles system:

$$t = Q^2 - \sqrt{s}(q^0 - |\vec{q}|\cos\theta), \tag{2.15}$$
$$u = Q^2 - \sqrt{s}(q^0 + |\vec{q}|\cos\theta),$$
$$q^0 = \frac{2Q^2 - t - u}{2\sqrt{s}}, \qquad \cos\theta = \frac{u-t}{u+t},$$

The energy conserve principle give us the formula, which obey invariants:

$$s + t + u = s_2 + Q^2\,. \tag{2.16}$$

The relations between global and "small" Mandelstam parameters are following:

$$s = x_1 x_2 S, \qquad t = x_1(T - Q^2) + Q^2, \qquad u = x_2(U - Q^2) + Q^2; \tag{2.17}$$
$$(T - Q^2) = -\sqrt{S}(Q^2 + q_T^2)^{1/2} e^{-y}, \quad (U - Q^2) = -\sqrt{S}(Q^2 + q_T^2)^{1/2} e^{y},$$

where the rapidity y is denoted as

$$y = \frac{1}{2}\ln\frac{q_0 + q_3}{q_0 - q_3} = \frac{1}{2}\ln\frac{Q^2 - U}{Q^2 - T}, \tag{2.18}$$

and for our case of Z boson production Q^2 is equal to M_Z^2, the squared mass of the Z boson.

Let us consider the form of phase space for process $1 + 2 \to 3 + 4$, where the first two particles are partons with momenta p_1 and p_2, one of the produced particles is a boson with momenta q and another one is a parton with momenta q_1, which have to be integrated.

For this case we can write the phase volume as follows:

$$d\Phi^{(2)} = (2\pi)^d \delta^{(d)}(p_1 + p_2 - q - q_1) \frac{d\vec{q}}{(2\pi)^{d-1} 2q^0} \frac{d\vec{q_1}}{(2\pi)^{d-1} 2q_1^0}. \tag{2.19}$$

After integration over q_1 we have

$$d\Phi^{(2)} = \frac{1}{(2\pi)^{d-2}} \delta_+(q_1^2) \frac{d\vec{q}}{2q^0}\bigg|_{q_1 = p_1 + p_2 - q}. \tag{2.20}$$

For two-to-two process the correlation $q_1^2 = s + t + u - Q^2$ is realized, so we can rewrite our formula as

$$\frac{d\vec{q}}{2q^0} = \frac{|\vec{q}|^{d-2} d|\vec{q}| d\Omega_{d-2}}{2q^0} = \frac{\Omega_{d-2}}{2} |\vec{q}^{d-3}| dq^0 (\sin\theta)^{d-4} d\cos\theta, \tag{2.21}$$

where θ is the angle between three-space momenta $\vec{p_1}$ and $\vec{q}$. After substitution this result to (2.20) we obtain:

$$\mathrm{d}\Phi^{(2)} = \frac{d\Omega_{d-2}}{2(2\pi)^{d-2}} \delta(s + t + u - Q^2) \vec{q}^{d-3} dq^0 (\sin\theta)^{d-4} d\cos\theta. \tag{2.22}$$

In the partonic central of mass scheme using kinematic formulae (2.15) we can write the final result for phase volume two-to-two:

$$\mathrm{d}\Phi^{(2)} = \frac{1}{8\pi s} \frac{(4\pi)^{2-d/2}}{\Gamma(d/2 - 1)} \left(\frac{tu - s_2 Q^2}{s} \right)^{d/2-2} \delta(s_2) dt du. \tag{2.23}$$

2.4.2 Integration By Part procedure

The estimation corrections leads to calculation of large number loop integrations over the momenta of virtual particles, and phase-space integrations over the momenta of particles in the final state. The methods for the analytic calculation of loop and phase-space integrals are complicated. A solution to this problem can be constructing algorithms which reduce the number of all integrals of the process to a few master integrals. This master integrals can be calculated directly.

The famous method for the reduction loop integrals to some master integrals is integration by parts (IBP), which was introduced in papers [29], [30]. The integrals with common propagators satisfy linear algebraic identities. These identities can be derived with the IBP method and can be cleverly combined to produce reduction identities to master integrals.

Let us consider the integrals of type:

$$B(\nu_1, \nu_2, \nu_3, \nu_4) = \int \mathrm{d}^d k \frac{1}{[k^2]^{\nu_1} [(k + p_1)^2]^{\nu_2} [(k + p_{12})^2]^{\nu_3} [(k + p_{123})^2]^{\nu_4}}, \tag{2.24}$$

where sum of momenta was denoted as $p_{ij\ldots k} = p_i + p_j + \ldots + p_k$. The momentum k is a loop momentum. All external momenta p_i are incoming to the loop and mass-less. The powers ν_i can be positive or negative. Scalar bubble or triangle integrals correspond to

zero powers ν_i. Negative powers correspond to triangle or bubble integrals with irreducible numerators. To find the algebraic equations for the integrals we can use Integration By Part procedure. The total derivatives of integrand (2.24) multiplied with combination of a loop or external momentum integrate to zero:

$$0 = \int \mathrm{d}^d k \frac{\partial}{\partial k_\mu} \frac{\eta^\mu}{[k^2]^{\nu_1}[(k+p_1)^2]^{\nu_2}[(k+p_{12})^2]^{\nu_3}[(k+p_{123})^2]^{\nu_4}}, \tag{2.25}$$

where $\eta^\mu = k,\, k+p_1,\, k+p_{12},\, k+p_{123}$. After derivation we have four IBP identities:

$$T1 \;:\; 0 = [s\nu_1 \mathbf{1}^+ + (\mathbf{d} - \nu_{\mathbf{12334}}) - (\nu_1 \mathbf{1}^+ + \nu_2 \mathbf{2}^+ + \nu_4 \mathbf{4}^+)\mathbf{3}^-]\mathbf{B} \tag{2.26}$$

$$T2 \;:\; 0 = [t\nu_2 \mathbf{2}^+ + (\mathbf{d} - \nu_{\mathbf{12344}}) - (\nu_1 \mathbf{1}^+ + \nu_2 \mathbf{2}^+ + \nu_3 \mathbf{3}^+)\mathbf{4}^-]\mathbf{B} \tag{2.27}$$

$$T3 \;:\; 0 = [s\nu_3 \mathbf{3}^+ + (\mathbf{d} - \nu_{\mathbf{11234}}) - (\nu_2 \mathbf{2}^+ + \nu_3 \mathbf{3}^+ + \nu_4 \mathbf{4}^+)\mathbf{1}^-]\mathbf{B} \tag{2.28}$$

$$T4 \;:\; 0 = [t\nu_4 \mathbf{4}^+ + (\mathbf{d} - \nu_{\mathbf{12234}}) - (\nu_2 \mathbf{1}^+ + \nu_3 \mathbf{3}^+ + \nu_4 \mathbf{4}^+)\mathbf{2}^-]\mathbf{B} \tag{2.29}$$

where the notation $\nu_{iijk\ldots}$ means the sum of indexes $\nu_i + \nu_i + \nu_j + \nu_k + \ldots$. The operator $\mathbf{i}^+(\mathbf{i}^-)$ increases (decreases) ν_i by one in the integral B:

$$\mathbf{3}^\pm \mathbf{B} = \mathbf{B}(\nu_\mathbf{1}, \nu_\mathbf{2}, \nu_\mathbf{3} \pm \mathbf{1}, \nu_\mathbf{4}), \tag{2.30}$$

products of operators have a straightforward interpretation:

$$\mathbf{3}^+\mathbf{1}^-\mathbf{B} = \mathbf{B}(\nu_\mathbf{1} - \mathbf{1}, \nu_\mathbf{2}, \nu_\mathbf{3} + \mathbf{1}, \nu_\mathbf{4}). \tag{2.31}$$

The IBP Eqs. (2.26)-(2.29) are sufficient to reduce any integral of the box topology to master integrals by using the algorithm of Laporta [31].

One of the computer program which used the method IBP is the Automatic Integral Reduction (AIR) [32]. In our computations we made reductions of loop integrals with a help of AIR.

2.4.3 Loop Integrals

The loop integrals, which are created by the calculating of corrections to the Born diagrams, had to be integrated over a loop momentum. In the loop integrals we have terms which give us a divergences at high ($\to \infty$) or small ($\to 0$) value of momentum. Because the final result (the cross section which we will calculate) is finite, we have to regularize our integrals. One of the way to make this is the technique of dimension regularization suggested by 't Hooft and Veltmann in 1972 [33]. One of the advantage of this regularization is that it conserves gauge invariance. The dimensional regularization bases on the analytical extension from four to arbitrary value d of the dimensionality,

$$\int \mathrm{d}^4 k \to \mu^{4-d} \int \mathrm{d}^d k,$$

where μ is a regularization mass. The integratable momentum can be presented as

$$\mathrm{d}^d k = \mathrm{d}k_0 |k|^{d-2} \mathrm{d}|k| \mathrm{d}\phi \prod_{k=1}^{d-3} \sin^k \theta_k \mathrm{d}\theta_k.$$

The d dimensional integrals are convergent. After integration in d dimensional space we can put $d = 4 - 2\varepsilon$ to the answer and we get separately finite and infinite parts of integrals after integration on soft and collinear corrections.

The loop diagrams which are coming from considering of QED and QCD corrections can be calculated in the mass-less limit of initial momentum k: $m_k = 0$. According to the Passarino-Veltman reduction scheme [21], we can find the solution for two-, three- and four-point mass-less loop integrals [13], [33].

In the below formula we presented two-, three- and four-point integrals which was used by our calculations. All momenta of particles are incoming. In the below formulae we didn't write the regularization mass μ.

For the self-energy bubble diagram with the input momentum p, we can write following formula of scalar integral:

$$\int \frac{d^d k}{(2\pi)^d} \frac{1}{k^2(k+p)^2} = -i(4\pi)^{-d/2}(-p^2)^{\varepsilon/2} \frac{2}{\varepsilon} \frac{\Gamma(1-\varepsilon/2)\Gamma^2(1+\varepsilon/2)}{\Gamma(2+\varepsilon)} \tag{2.32}$$

where $\varepsilon = (4-d)/2$ and for Gamma function $\Gamma(y)$ the follows expansions can be used:

$$\begin{aligned} &\Gamma(\varepsilon) = \frac{1}{\varepsilon} - \gamma_e, \quad \varepsilon \to 0, \\ &\Gamma(y+1) = y\Gamma(y) \end{aligned} \tag{2.33}$$

with Euler-Mascheroni constant $\gamma_e \approx 0.577216$.

The triangle diagrams correspond to three point function. For the diagram with incoming momenta p_1, p_2 and p_3 if $p_1^2 = p_2^2 = 0$, $p_3^2 \neq 0$ we have formula

$$\begin{aligned} &\int \frac{d^d k}{(2\pi)^d} \frac{1}{k^2(k+p_1)^2(k-p_2)^2} = \\ &-i(4\pi)^{-d/2}(-p_3^2)^{-1+\varepsilon/2} \frac{4}{\varepsilon^2} \frac{\Gamma(1-\varepsilon/2)\Gamma^2(1+\varepsilon/2)}{\Gamma(1+\varepsilon)}. \end{aligned} \tag{2.34}$$

For the triangle diagram with incoming momenta p_1, p_2 and p_3 in the case $p_1^2 \neq 0$, $p_2^2 \neq 0$, $p_3^2 = 0$, the scalar integral is here:

$$\begin{aligned} &\int \frac{d^d k}{(2\pi)^d} \frac{1}{k^2(k+p_1)^2(k-p_2)^2} = \\ &-i(4\pi)^{-d/2}((-p_1^2)^{-\varepsilon/2} - (-p_2^2)^{\varepsilon/2}) \frac{1}{(p_1^2 - p_2^2)} \frac{4}{\varepsilon^2} \frac{\Gamma(1-\epsilon/2)\Gamma^2(1+\varepsilon/2)}{\Gamma(1+\varepsilon)}. \end{aligned} \tag{2.35}$$

And for the four point function with incoming momenta p_1, p_2, p_3 and p_4 for case $p_1^2 =$

$p_2^2 = p_3^2 = 0$, $p_4^2 \neq 0$, we have following expression:

$$\int \frac{d^dk}{(2\pi)^d} \frac{1}{k^2(k+p_1)^2(k-p_2)^2(k-p_2-p_3)^2} = \tag{2.36}$$
$$-i(4\pi)^{-d/2} \frac{8}{\varepsilon^2} \frac{\Gamma(1-\varepsilon/2)\Gamma^2(1+\varepsilon/2)}{\Gamma(1+\varepsilon)} \left(\frac{(-p_4^2)^{\varepsilon/2}}{P_{12}P_{23}} F\left(1, \frac{\varepsilon}{2}; 1+\frac{\varepsilon}{2}; -\frac{P_{13}p_4^2}{P_{12}P_{23}}\right) \right.$$
$$\left. -\frac{(-P_{12})^{\varepsilon/2}}{P_{12}P_{23}} F\left(1, \frac{\varepsilon}{2}; 1+\frac{\varepsilon}{2}; -\frac{P_{13}}{P_{23}}\right) - \frac{(-P_{23})^{\varepsilon/2}}{P_{12}P_{23}} F\left(1, \frac{\varepsilon}{2}; 1+\frac{\varepsilon}{2}; -\frac{P_{13}}{P_{12}}\right) \right),$$

with $P_{ij} = (p_i + p_j)^2$. The hyper-geometric function $F(a, b; c; x)$ can be presented as

$$F(a,b;c;x) = \frac{\Gamma(c)}{\Gamma(b)\Gamma(c-b)} \int_0^1 t^{b-1}(1-t)^{c-b-1}(1-tz)^{-a}dt; \tag{2.37}$$
$$Re(c) > Re(b) > 0 \wedge |arg(1-z)| < \pi.$$

By calculation loop diagrams of EW corrections to the Born process of Z boson production, loops with massive initial and lines are arisen. In this case we can not neglect the mass in propagators as in pure QED or QCD calculations. The master integrals for this loop calculation can be found in papers [33], [34], [35]. Here we presented some integrals which was used in our calculations.

For the bubble integrals with one massive initial line and nonzero incoming momenta p_1 we have the formula:

$$\begin{aligned} I_2^D(p_1^2; m_1^2, m_2^2) &= \frac{\mu^{4-D}}{i\pi^{D/2}}\Gamma(1-\varepsilon) \int \frac{d^Dl}{(l^2-m_1^2+i\varepsilon)((l+q_1)^2-m_2^2+i\varepsilon)}\Big|_{m_1^2=0} \\ &= \left(\frac{\mu^2}{m_2^2}\right)^{\varepsilon} \Big[\frac{1}{\varepsilon} + 2 + \frac{m^2-p_1^2}{p_1^2} \ln\Big(\frac{m_2^2-p_1^2-i\varepsilon}{m_1^2}\Big)\Big] + O(\varepsilon), \end{aligned} \tag{2.38}$$

where l is initial momentum, $q_n = \sum_{i=1}^{n}(p_i)$.

The triangle diagram with one massive initial line and two nonzero incoming to loop momenta can be calculated with a help of this formula:

$$I_3^D(p_1^2, p_2^2, p_3^2; m_1^2, m_2^2, m_3^2) = \frac{\mu^{4-D}}{i\pi^{D/2}}\Gamma(1-\varepsilon) \tag{2.39}$$
$$\times \int \frac{d^Dl}{(l^2-m_1^2+i\varepsilon)((l+q_1)^2-m_2^2+i\varepsilon)((l+q_2)^2-m_3^2+i\varepsilon)}\Big|_{p_1^2=m_1^2=m_2^2=0}$$
$$= \frac{1}{p_2^2-p_3^2}\Big(\frac{\mu^2}{m_2^2}\Big)^{\varepsilon}\Big[\frac{1}{\varepsilon}\ln\left(\frac{m^2-p_3^2}{m^2-p_2^2}\right) + \mathrm{Li}_2\left(\frac{p_2^2}{m^2}\right) - \mathrm{Li}_2\left(\frac{p_3^2}{m^2}\right)$$
$$+ \ln^2\left(\frac{m^2-p_2^2}{m^2}\right) - \ln^2\left(\frac{m^2-p_3^2}{m^2}\right)\Big] + O(\varepsilon),$$

And also we give here one example of box integral with two initial masses and three nonzero incoming momenta is here:

$$
\begin{aligned}
& I_4^D(p_1^2,p_2^2,p_3^2,p_4^2;s_{12},s23;m_1^2,m_2^2,m_3^2,m_4^2) = \frac{\mu^{4-D}}{i\pi^{D/2}}\Gamma(1-\varepsilon) \qquad (2.40)\\
\times & \int \frac{d^Dl}{(l^2-m_1^2+i\varepsilon)((l+q_1)^2-m_2^2+i\varepsilon)((l+q_2)^2-m_3^2+i\varepsilon)((l+q_3)^2-m_4^2+i\varepsilon)}\Big|_{p_1^2=m_1^2=m_2^2=0}\\
= & \frac{1}{\Delta}\Big[\frac{1}{\varepsilon}\ln\left(\frac{(m_3^2-p_2^2)(m_4^2-p_4^2)}{(m_3^2-s_{12})(m_4^2-s_{23})}\right)\\
- & 2\mathrm{Li}_2\left(1-\frac{m_3^2-p_2^2}{m_3^2-s_{12}}\right)-\mathrm{Li}_2\left(1-\frac{m_3^2-p_2^2}{m_4^2-s_{23}}\frac{\gamma_{34}^+}{\gamma_{34}^+-1}\right)-\mathrm{Li}_2\left(1-\frac{m_3^2-p_2^2}{m_4^2-s_{23}}\frac{\gamma_{34}^-}{\gamma_{34}^--1}\right)\\
- & 2\mathrm{Li}_2\left(1-\frac{m_4^2-p_4^2}{m_4^2-s_{23}}\right)-\mathrm{Li}_2\left(1-\frac{m_4^2-p_4^2}{m_3^2-s_{12}}\frac{\gamma_{43}^+}{\gamma_{43}^+-1}\right)-\mathrm{Li}_2\left(1-\frac{m_4^2-p_4^2}{m_3^2-s_{12}}\frac{\gamma_{43}^-}{\gamma_{43}^--1}\right)\\
+ & \mathrm{Li}_2\left(1-\frac{(m_3^2-p_2^2)(m_4^2-p_4^2)}{(m_3^2-s_{12})(m_4^2-s_{23})}\right)+2\ln\left(\frac{m_3^2-s_{12}}{\mu^2}\right)\ln\left(\frac{m_4^2-s_{23}}{\mu^2}\right)\\
- & \ln^2\left(\frac{m_3^2-p_2^2}{\mu^2}\right)-\ln^2\left(\frac{m_4^2-p_4^2}{\mu^2}\right)+\ln\left(\frac{m_3^2-p_2^2}{m_4^2-s_{23}}\right)\ln\left(\frac{m_3^2}{\mu^2}\right)+\ln\left(\frac{m_4^2-p_4^2}{m_3^2-s_{12}}\right)\ln\left(\frac{m_4^2}{\mu^2}\right)\\
- & \frac{1}{2}\ln^2\left(\frac{\gamma_{34}^+}{\gamma_{34}^+-1}\right)-\frac{1}{2}\ln^2\left(\frac{\gamma_{34}^-}{\gamma_{34}^--1}\right)\Big]+O(\varepsilon),
\end{aligned}
$$

where

$$
\gamma_{ij}^{\pm}=\frac{1}{2}\left\{1-\frac{m_i^2-m_j^2}{p_3^2}\pm\sqrt{(1-\frac{m_i^2-m_j^2}{p_3^2})^2-\frac{4m_j^2}{p_3^2}}\right\},
$$

$$
\Delta=(m_3^2-s_{12})(m_4^2-s_{23})-(m_3^2-p_2^2)(m_4^2-p_4^2).
$$

In the Appendix C there are other integrals with massive initial lines which were computed by calculation of EW corrections to Z boson production.

2.5 Bremsstrahlung integrations

The next type of corrections to the Born level is the emission of an additional particle. In this case the phase space contains three final particles, the Z boson and two other, over which momenta we have to integrate in d phase space to fixed divergences.

2.5.1 Phase space with three final particles

Let us consider the case of production of three particles like $1+2\to 3+4+5$. In the process (2.2) we put at place X two particles with momenta q_1 and q_2. For this case the phase volume can be presented as:

$$
\mathrm{d}\Phi^{(3)}=(2\pi)^d\delta^{(d)}(p_1+p_2-q-q_1-q_2)\frac{d\vec{q}}{(2\pi)^{d-1}2q^0}\frac{d\vec{q_1}}{(2\pi)^{d-1}2q_1^0}\frac{d\vec{q_2}}{(2\pi)^{d-1}2q_2^0}. \qquad (2.41)
$$

For the integration over momenta q_1 and q_2, firstly we introduce the vector $K = q_1 + q_2$ and rewrite the $\mathrm{d}\Phi_3$, splitted two parts:

$$\begin{aligned} \mathrm{d}\Phi^{(3)} &= \frac{1}{(2\pi)^(2d-3)} \underbrace{\delta^{(d)}(p_1+p_2-q-K)\delta_+(q_2-Q^2)d^dqd^dK}_{} \\ &\underbrace{\delta^{(d)}(K-q_1-q_2)\delta_+(q_1^2)\delta_+(q_2^2)d^dq_1d^dq_2}. \end{aligned} \tag{2.42}$$

For the second part we have

$$\begin{aligned} I_2 &= \delta^{(d)}(K-q_1-q_2)\delta_+(q_1^2)\delta_+(q_2^2)d^dq_1d^dq_2 && (2.43)\\ &= \delta_+(q_1^2)\delta_+((K-q_1)^2)dq_1^2 && (2.44)\\ &= \frac{1}{2}\delta_+(K^2-2Kq_1)(q_1^0)^{d-3}dq_1d^{d-2}\Omega_{q_1} \end{aligned}$$

In the central mass scheme of momenta $q_1 + q_2$ (this means that is satisfied $\vec{K} = 0$), we have

$$\begin{aligned} I_2 &= \frac{1}{4K_0}\delta(q_0-K_0/2)(q_1^0)dq_1^0d^{d-2}\Omega_{q_1} = \frac{1}{4}2^{3-d}K_0^{d-4}d^{d-2}\Omega_{q_1} && (2.45)\\ &= \frac{\Omega_{d-3}}{4}2^{3-d}K_0^{d-4}\sin^{d-3}\beta_1d\beta_1\sin^{d-4}\beta_2d\beta_2 && (2.46)\\ &= \frac{s_2^{d/2-2}\pi^{d/2-2}\Gamma(d/2-1)}{4\Gamma(d-3)}\sin^{d-3}\beta_1d\beta_1\sin^{d-4}\beta_2d\beta_2, \end{aligned}$$

where was assumes $K^2 = s_2$. For the first part from (2.42) we have

$$\begin{aligned} I_1 &= \delta^{(d)}(p_1+p_2-q-K)\delta_+(q_2-Q^2)d^dqd^dK && (2.47)\\ &= \frac{1}{2}\Omega_{d-2}|\vec{q}|^{d-3}dq_0\sin^{d/2-2}\theta d\cos\theta\Big|_{K=p_1+p_2-q} \\ &= \frac{(2\pi)^{d-2}(4\pi)^{2-d/2}}{8\pi s\Gamma(d-3)}\left(\frac{tu-s_2Q^2}{s}\right)^{d/2-2}dtdu, \end{aligned}$$

where was used result (2.23) for 2-to-2 kinematics.

After combining I_1 and I_2 for the phase volume $\mathrm{d}\Phi_3$ we obtain the following integral:

$$\begin{aligned} \int \mathrm{d}\Phi^{(3)} &= \frac{s^{1-d/2}}{(4\pi)^d\Gamma(d-3)}\int\limits_0^\pi \sin^{d-3}\beta_1d\beta_1\int\limits_0^\pi \sin^{d-3}\beta_2d\beta_2 && (2.48)\\ &\int\limits_{-a}^{0}\int\limits_{-a-u}^{\frac{Q^2(-a-u)}{Q^2-u}} dtdus_2^{d/2-2}(tu-s_2Q^2)^{d/2-2}, \end{aligned}$$

which can be integrated in d-dimensional space after calculation of matrix elements.

2.5.2 Van Neerven's Integrals

The bremsstrahlung integration means integration over additional emitted particles in processes like

$$i(p_1) + j(p_2) \to V(q) + x_1(q_1) + x_2(q_2), \tag{2.49}$$

where x_1 and x_2 are unobservable particles, over which momenta we will integrate, V is a boson with $q^2 = Q^2$.

In the central of mass system the momenta in d dimensional space are parametrized as follows

$$\begin{aligned}
p_1 &= \frac{s_2 - u}{2\sqrt{s_2}}(1, 0, ..., 0, 1), \\
p_2 &= \left(\frac{s_2 - t}{2\sqrt{s_2}}, 0, ..., |\vec{q}| \sin\theta, |\vec{q}\cos\theta - \frac{s_2 - u}{2\sqrt{s_2}}\right), \\
q &= \left(\frac{s - Q^2 - s_2}{2\sqrt{s_2}}, 0, ..., |\vec{q}| \sin\theta, |\vec{q}| \cos\theta\right), \\
q_1 &= \frac{\sqrt{s_2}}{2}(1, 0, ..., \sin\beta_2 \sin\beta_1, \cos\beta_2 \sin\beta_1, \cos\beta_1), \\
q_2 &= \frac{\sqrt{s_2}}{2}(1, 0, ..., -\sin\beta_2 \sin\beta_1, -\cos\beta_2 \sin\beta_1, -\cos\beta_1), \\
|\vec{q}| &= \frac{\lambda(s, Q^2, s_2)}{2\sqrt{s_2}}, \quad \cos\theta = \frac{1}{2|\vec{q}|\sqrt{s_2}}\left(\frac{-u(s - Q^2) + s_2(t - 2Q^2)}{s_2 - u}\right),
\end{aligned} \tag{2.50}$$

where $\lambda(x, y, z) = \sqrt{x^2 + y^2 + z^2 - 2xy - 2xz - 2yz}$.

From propagators by calculating real processes, following scalar products are coming:

$$\begin{aligned}
p_1 q_1 &= \frac{s_2 - u}{4}(1 - \cos\beta_1), \\
p_1 q_2 &= \frac{s_2 - t}{4}(1 + \cos\beta_1), \\
p_2 q_1 &= a_0 - b_0 \cos\beta_1 - c_0 \cos\beta_2 \sin\beta_1, \\
p_2 q_2 &= a_0 + b_0 \cos\beta_1 + c_0 \cos\beta_2 \sin\beta_1, \\
Q^2 + 2qq_1 &= \frac{1}{2}(A_0 - B_0 \cos\beta_1 - C_0 \cos\beta_2 \sin\beta_1), \\
Q^2 + 2qq_2 &= \frac{1}{2}(A_0 + B_0 \cos\beta_1 + C_0 \cos\beta_2 \sin\beta_1), \\
Q^2 + 2p_1 q_1 &= a - b \cos\beta_1, \\
Q^2 + 2p_1 q_2 &= a + b \cos\beta_1,
\end{aligned} \tag{2.51}$$

where parameters a, b, a_0, b_0, c_0, A_0, B_0 and C_0 are here:

$$\begin{aligned} &a = Q^2 + \frac{s_2 - u}{2}, \qquad b = \frac{s_2 - t}{2}, \\ &a_0 = \frac{s_2 - t}{4}, \qquad b_0 = \frac{tu - s_2(s + Q^2)}{4(s_2 - u)}, \qquad c_0 = \frac{\lambda}{4}, \\ &A_0 = s + Q^2 - s_2, \qquad B_0 = \lambda \cos\theta, \qquad C_0 = \lambda \sin\theta. \end{aligned} \tag{2.52}$$

The integration of angular integrals was done in according to [22]. The d dimensional integrals with determinants of order k and l can be calculated as

$$\begin{aligned} I_n^{(k,l)} &= \int_0^\pi d\beta_1 \sin^{d-3}\beta_1 \int_0^\pi d\beta_2 \sin^{d-4}\beta_2 \\ &\qquad \times (a + b\cos\beta_1)^{-k} (A + B\cos\beta_1 + C\sin\beta_1\cos\beta_2)^{-l} \\ &= 2^{1-i-j}\pi \frac{\Gamma(d/2-1-i)\Gamma(d/2-1-j)\Gamma(d-3)}{\Gamma(d-2-i-j)\Gamma^2(d/2-1)} {}_2F_1\left(\begin{matrix} i, j \\ d/2-1 \end{matrix}; \cos^2\frac{\chi}{2}\right) \end{aligned} \tag{2.53}$$

where a, b, A, B and C are functions of kinematics variables s, t, u etc. which are coming from the scalar product (see relations (2.52)), ${}_2F_1\left(\begin{smallmatrix} a,b \\ c \end{smallmatrix}; x\right) = {}_2F_1(a, b, c; x)$ is a hyper-geometric function (2.37).

Using the change $\beta_1 \to \pi - \beta_1$, we distinguish two cases for the sets of determinants. In case $((q_1p_1)(q_1p_2))^{-1}$ and $((q_2p_1)(q_2p_2))^{-1}$ we have

$$\cos^2\frac{\chi_+}{2} = \frac{a_0 + b_0}{2a_0} = 1 - \frac{ss_2}{(s_2 - t)(s_2 - u)} = \frac{tu - s_2Q^2}{(s_2 - t)(s_2 - u)}, \tag{2.54}$$

while in cases $((q_1p_1)(q_2p_2))^{-1}$ and $((q_2p_1)(q_1p_2))^{-1}$ we have

$$\cos^2\frac{\chi_-}{2} = \frac{a_0 - b_0}{2a_0} = \frac{ss_2}{(s_2 - t)(s_2 - u)}. \tag{2.55}$$

Denoting $z = cos^2(\chi_-/2) = \frac{ss_2}{(s_2 - t)(s_2 - u)}$, we have two hyper-geometric functions ${}_2F_1(1, 1; 1 - \varepsilon; z)$ and ${}_2F_1(1, 1; 1 - \varepsilon; 1 - z)$. For the former we use the expansion formula

$$\begin{aligned} {}_2F_1\left(\begin{matrix} 1,1 \\ 1-\varepsilon \end{matrix}; z\right) &= \frac{1}{(1-z)^{1+\varepsilon}} \left(1 + \varepsilon^2 \mathrm{Li}_2(z) + \varepsilon^3 \left(\mathrm{Li}_3(z) - \mathrm{S}_{1,2}(z)\right)\right. \\ &\quad \left. + \varepsilon^4 \left(\mathrm{Li}_4(z) - \mathrm{S}_{2,2}(z) + \mathrm{S}_{1,3}(z)\right) + \dots\right), \end{aligned} \tag{2.56}$$

where Nielson's polylogarithms are here:

$$S_{n,m}(z) = \frac{(-1)^{n+m-1}}{(n-m)!m!}\int_0^1 \frac{dx}{x}\ln^{n-1}(x)\ln^m(1-xz), \tag{2.57}$$

$$Li_2(z) = S_{1,1}(z) = -\int_0^1 \frac{dx}{x}\ln(1-xz),$$

$$S_{1,2}(z) = \frac{1}{2}\int_0^1 \frac{dx}{x}\ln^2(1-xz),$$

$$Li_3(z) = S_{2,1}(z) = \int_0^1 \frac{dx}{x}\ln(x)\ln(1-xz) = \int_0^1 Li_2(x),$$

$$Li_4(z) = S_{3,1}(z) = -\frac{1}{2}\int_0^1 \frac{dx}{x}\ln^2(x)\ln(1-xz),$$

$$S_{1,3}(z) = -\frac{1}{6}\int_0^1 \frac{dx}{x}\ln^3(1-xz),$$

$$S_{2,2}(z) = -\frac{1}{2}\int_0^1 \frac{dx}{x}\ln(x)\ln^2(1-xz).$$

In the second case of parametric function, the argument $(1-z)$ is translated to (z) first:

$$\begin{aligned} {}_2F_1\left(\begin{matrix}1,1\\1-\varepsilon\end{matrix};1-z\right) &= \frac{1}{z} - \frac{1-z}{z}{}_2F_1\left(\begin{matrix}1,1\\1+\varepsilon\end{matrix};z\right) \\ &\quad + \Gamma(1-\varepsilon)\Gamma(1+\varepsilon)(1-z)^{\varepsilon}z^{-1-\varepsilon} \end{aligned} \tag{2.58}$$

and expanded as above in Eq. 2.56.

We also used following expansion of hyper-geometric functions:

$$\begin{aligned} {}_2F_1\left(\begin{matrix}1,2\\1-\varepsilon\end{matrix};z\right) &= \frac{1}{(1-z)}\left(-\varepsilon + (1+\varepsilon){}_2F_1\left(\begin{matrix}1,1\\1-\varepsilon\end{matrix};z\right)\right), \\ {}_2F_1\left(\begin{matrix}2,2\\1-\varepsilon\end{matrix};z\right) &= \frac{1}{(1-z)^2}\left(-\varepsilon(2+\varepsilon) + (1+\varepsilon)(1+\varepsilon+z){}_2F_1\left(\begin{matrix}1,1\\1-\varepsilon\end{matrix};z\right)\right). \end{aligned} \tag{2.59}$$

Now we can go directly to integration of bremsstrahlung integrals.

For calculating integrals, the follows presentations were used:

$$\int_{-1}^{1}\frac{(1-z^2)^{-\frac{1}{2}-\varepsilon}}{X+Yz}dz = \pi\frac{4^{\varepsilon}\Gamma(1-2\varepsilon)}{\Gamma^2(1-\varepsilon)}\frac{1}{X}{}_2F_1\left(\begin{matrix}1,\frac{1}{2}\\1-\varepsilon\end{matrix};\frac{Y^2}{X^2}\right) \tag{2.60}$$

$$
\begin{aligned}
{}_2F_1\left(\begin{matrix}1,\frac{1}{2}\\ 1-\varepsilon\end{matrix};z\right) &= 1+\frac{z}{2}\int\limits_0^1 \frac{dt}{(1-t)^{\varepsilon}(1-tz)^{3/2}} \qquad (2.61)\\
&= \frac{1}{\sqrt{1-z}}-\varepsilon\frac{1}{\sqrt{1-z}}\left(\ln\frac{1-\sqrt{1-z}}{1+\sqrt{1-z}}-\ln\frac{x}{1-x}+2\ln 2\right)+O(\varepsilon^2).
\end{aligned}
$$

Some of this integrals can be found in the literature [22], [36]. For our calculation was necessary to compute additional integrals.

The four-dimensional integrals for $a^2\neq b^2$ and $A^2\neq B^2+C^2$ has form:

$$
\begin{aligned}
I_4^{(1,0)} &= \pi\frac{1}{b}\ln\frac{a+b}{a-b}, \qquad (2.62)\\
I_4^{(1,-1)} &= \pi\left[\frac{2B}{b}+\frac{Ab-Ba}{b^2}\ln\frac{a+b}{a-b}\right],\\
I_4^{(1,-2)} &= \pi\left[\frac{4ABb+a(C^2-2B^2)}{b^2}+\frac{2(Ab-Ba)^2+C^2(b^2-a^2)}{2b^3}\ln\frac{a+b}{a-b}\right].
\end{aligned}
$$

The 4-dimensional integrals for case $b\neq -a$ and $A^2\neq B^2+C^2$ give us follow additional integrals:

$$
\begin{aligned}
\bar{I}_4^{(0,1)} &= \frac{\pi}{\sqrt{B^2+C^2}}\ln\frac{A+\sqrt{B^2+C^2}}{A-\sqrt{B^2+C^2}}, \qquad (2.63)\\
\bar{I}_4^{(0,2)} &= \frac{2\pi}{A^2-B^2-C^2},\\
\bar{I}_4^{(-1,1)} &= \pi\left[\frac{B^2+C^2+AB}{(B^2+C^2)^{3/2}}\ln\frac{A+\sqrt{B^2+C^2}}{A-\sqrt{B^2+C^2}}-\frac{2B}{B^2+C^2}\right],\\
\bar{I}_4^{(-1,2)} &= \pi\left[-\frac{B}{(B^2+C^2)^{3/2}}\ln\frac{A+\sqrt{B^2+C^2}}{A-\sqrt{B^2+C^2}}+\frac{2(B^2+C^2+AB)}{(B^2+C^2)(A^2-B^2-C^2)}\right],\\
\bar{I}_4^{(-2,1)} &= \pi\left[\frac{2B^4+5B^2C^2+3C^4+A^2(2B^2-C^2)+4A(B^2+C^2)}{2(B^2+C^2)^{5/2}}\ln\frac{A+\sqrt{B^2+C^2}}{A-\sqrt{B^2+C^2}}\right.\\
&\qquad \left.-\frac{A(2B^2-C^2)+4B(B^2+C^2)}{(B^2+C^2)^2}\right],\\
\bar{I}_4^{(-2,2)} &= \pi\left[\frac{-A(2B^2-C)^2+2B(B^2+C^2)}{2(B^2+C^2)^{5/2}}\ln\frac{A+\sqrt{B^2+C^2}}{A-\sqrt{B^2+C^2}}\right.\\
&\qquad \left.+\frac{2A^2(2B^2-C^2)+2AB(B^2+C^2)+2C^2(B^2+C^2)}{(B^2+C^2)^2(A^2-B^2-C^2)}\right].
\end{aligned}
$$

2.6 d-dimension gamma matrices

The calculation of matrix elements includes also the calculations of traces of Dirac matrices $Tr(\gamma_\mu...\gamma^\nu)$. This Dirac algebra is well known and simple in 4-dimensional space. For d-

dimensional integrations we must be very accurately with substantial 4-dimensional object γ_5.

The Dirac algebra for γ_μ matrices in d-dimensional time-space is presented here:

$$\begin{aligned} \gamma^\mu\gamma_\mu &= d, \\ \gamma^\mu\gamma^\nu\gamma_\mu &= -(d-2)\gamma^\nu, \\ \gamma^\mu\gamma^\nu\gamma^\rho\gamma_\mu &= 4g^{\nu\rho} - (4-d)\gamma^\nu\gamma^\rho, \\ \gamma^\mu\gamma^\nu\gamma^\rho\gamma^\sigma\gamma_\mu &= -2\gamma^\sigma\gamma^\rho\gamma^\nu + (4-d)\gamma^\nu\gamma^\rho\gamma^\sigma, \\ g^{\nu\rho}g_{\nu\rho} &= \delta^\nu_\nu = d. \end{aligned} \tag{2.64}$$

In dimensional regularization the implementation of γ_5 is problematical. This Dirac matrix cannot be continued to $d \neq 4$ dimensions in a consistent and fully covariance way. One of the way of computation traces with γ_5 matrices in d dimension space was suggested by 't Hooft and Veltman in [33]. In this definition the γ_5 matrix is satisfied the conditions

$$\begin{aligned} \gamma_5 &\equiv i\gamma^0\gamma^1\gamma^2\gamma^3, \\ \{\gamma^\mu, \gamma^\nu\} &= 2g^{\mu\nu}, \\ \{\gamma^\mu, \gamma_5\} &= 0, \quad \mu \leq 3, \\ [\gamma^\mu, \gamma_5] &= 0, \quad \mu > 3, \end{aligned} \tag{2.65}$$

this leads to consistent gauge-invariant results. According to commutation relations we can recombine gamma matrices in traces before extension from 4 to d dimension. We count γ_5 as even number of gamma matrices, the pair of γ_5 cancels. Remaining γ_5 can be rewritten with a help of 't Hooft prescription. For our calculation of traces we used the 't Hooft prescription and we assumed that

$$\begin{aligned} Tr(\gamma^\mu\gamma^\nu\gamma^\rho\gamma^\tau\gamma_5) &= -4i\varepsilon^{\mu\nu\rho\tau}, \\ \varepsilon^{0123} &= -\varepsilon_{0123} = 1. \end{aligned} \tag{2.66}$$

By calculating of squared diagrams we considered three cases:

1. The diagrams give us only one trace with γ_5:

$$Tr(...\gamma^\mu...\gamma^\sigma\gamma_5...\gamma^\nu\gamma_5) \tag{2.67}$$

Here we can used commutations relations from (2.65) and cancel double matrices with using relation $\gamma_5\gamma^5 = 1$. The traces without γ_5 can be easy computed in d dimensional space. The traces with only one γ_5 give us antisymmetric tensor $\varepsilon^{\mu\nu\rho\tau}$ which has to be convoluted with external momenta. Once we have performed the phase space integral of the processes $i(p_1) + j(p_2) \to Z(q) + k(q_1)$ (or $i(p_1) + j(p_2) \to Z(q) + k_1(q_1) + k_2(q_2)$ in the bremsstrahlung corrections) over q_1 and q_2 momenta, only three vectors remain: p_1, p_2 and q. There is no non-zero construction of three vectors with antisymmetric tensor $\varepsilon^{\mu\nu\rho\tau}$, so this terms vanish.

2. The squared diagram give us two traces with γ_5.

In this case we cannot neglect the antisymmetric tensor because of $\varepsilon^{\mu\nu\rho\tau}\varepsilon^{\mu\nu\rho\tau} \neq 0$. We have therefore to compute these diagrams using the 't Hooft-Veltman definition of γ_5. Fortunately, in our case of Z boson production, these diagrams are all finite and we can do the traces unambiguously in four dimensions.

Chapter 3

Diagrams, Singularity, Factorization

The calculation was done in the framework of the Standard Model. In this Chapter we give a shortly view about Feynman Diagrams, with which help matrix elements were constructed, about cancellation of divergences and about factorization of the cross section. The ultraviolet coupling renormalization has been done in $\overline{\rm MS}$ scheme. The infrared and collinear singularities have to be canceled in the sum of different contributions. Firstly, let give us an introduction to the SM.

3.1 Interactions

The standard model of particle physics is a theory concerning the electromagnetic, weak, and strong nuclear interactions. The local $SU(3)_c \times SU(2)_L \times U(1)_Y$ gauge symmetry is an internal symmetry that essentially defines the Standard Model. The SM groups two major theories - quantum electroweak theory and quantum chromodynamics - into an internally consistent theory that describes the interactions between all known particles in terms of quantum field theory.

The Standard Model Lagrangian can be presented as a sum of four parts:

$$\mathcal{L}_{\rm SM} = \mathcal{L}_{gauge} + \mathcal{L}_{fermion} + \mathcal{L}_{\rm higgs} + \mathcal{L}_{\rm yukawa}. \tag{3.1}$$

The first part describes the gauge interaction and has term of gluons ($G^a_{\mu\nu}$), gauge bosons ($W^a_{\mu\nu}$) and photon ($B^{\mu\nu}$) fields tensors:

$$\mathcal{L}_{gauge} = -\frac{1}{4} G^a_{\mu\nu} G^{a\,\mu\nu} - \frac{1}{4} W^a_{\mu\nu} W^{a\,\mu\nu} - \frac{1}{4} B^{\mu\nu} B^{\mu\nu}.$$

The gauge invariant gluonic field strength tensor

$$G^a_{\mu\nu} = \partial_\mu A^a_\nu - \partial_\nu A^a_\mu + g f^{abc} A^b_\mu A^c_\nu \tag{3.2}$$

contains the gluon field A^a_μ with a running from 1 to $N_C^2 - 1 = 8$ kinds of gluon (N_C is number of colors). The adjoined representation of the $SU(3)$ color group with generators $t^a = \lambda^a/2$ correspond to eight 3×3 matrices, where matrices λ^a are Gell-Mann matrices.

Generators encode the fact that a gluons interaction with quarks rotates the quark's color in $SU(3)$ space. Generators of $SU(3)$ groups are subject to conditions:

$$\begin{aligned} &\left[t^a, t^b\right] = if^{abc}t^c, \\ &t^a_{i,j}t^a_{j,k} = C_F\delta_{ik}, \\ &f^{acd}f^{bcd} = C_A\delta_{ab}, \\ &t^a_{i,j}, t^b_{i,j} = T_R\delta_{ij}, \end{aligned} \tag{3.3}$$

where f^{abc} are structure constants of $SU(3)$ groups, $C_F = \frac{N_C^2-1}{2N_C}$ is the "Casimir" color factor associated with gluon emission from the quark, $C_A \equiv N_C = 3$ is the color factor associated with gluon emission from a gluon, $T_R = \frac{1}{2}$ is the color factor for a gluon to split to quark-antiquark pair.

The electroweak interaction is describe with the gauge bosons tensor $W^a_{\mu\nu}$ and the electromagnetic field tensor $B_{\mu\nu}$. The unification is accomplished under an $SU(2) \times U(1)$ gauge group. The corresponding gauge bosons are the three W bosons of weak isospin from $SU(2)$ (W^+, W^0, and W), and the B^0 boson of weak hyper-charge from $U(1)$, respectively, all of which are mass-less. The massive bosons W^+, W and Z and the mass-less photon are produced by the spontaneous symmetry breaking of the electroweak symmetry from $SU(2) \times U(1)_Y$ to $U(1)_{em}$, caused by the Higgs mechanism. The generator of $U(1)_{em}$ is given by $Q = Y/2 + I_3$, where Y is the generator of $U(1)_Y$, which is called as the weak hyper-charge, and I_3 is one of the $SU(2)$ generators (a component of weak isospin). The photon γ and weak boson Z are the superposition of W^0 and B^0 bosons:

$$\begin{aligned} Z^0 &= -B^0\sin\theta_W + W^0\cos\theta_W, \\ \gamma &= B^0\cos\theta_W + W^0\sin\theta_W, \end{aligned}$$

where θ_W is the weak mixing angle, $\cos\theta_W = \dfrac{m_W^2}{m_Z^2}$.

The second term of SM Lagrangian (3.1) contains kinematic part of left-handled $SU(2)$ doublets L and right-handled $SU(2)$ singlet r fermions:

$$\mathcal{L}_{fermions} = \sum_L \bar{L}i\gamma^\mu D_\mu L + \sum_r \bar{r}i\gamma^\mu D_\mu r, \tag{3.4}$$

where γ_μ are Dirac gamma matrices, and covariance divergence is here:

$$D_\mu = i\partial_\mu - g_s G^a_\mu t^a - g'\frac{1}{2}Y_W B_\mu - g\frac{1}{2}\vec{\tau}_{\rm L}\vec{W}_\mu$$

with coupling constants g_s, g' and g. The matrices $\vec{\tau}_{\rm L} = \vec{\sigma}/2$ are infinitesimal generators of $SU(2)$ group, so-called Pauli matrices:

$$\sigma_1 = \sigma_x = \begin{pmatrix} 0 & 1 \\ 1 & 0 \end{pmatrix} \quad \sigma_2 = \sigma_y = \begin{pmatrix} 0 & -i \\ i & 0 \end{pmatrix} \quad \sigma_3 = \sigma_z = \begin{pmatrix} 1 & 0 \\ 0 & -1 \end{pmatrix}$$

The summation in formula (3.4) runs over all fermions.

The term of the Higgs sector with scalar doublet field Φ can be written as

$$\begin{aligned} &\mathcal{L}_{\mathrm{h}iggs} = |D\Phi|^2 - V(\Phi^\dagger\Phi), \\ &V(\Phi^\dagger\Phi) = \frac{\lambda^2}{4}\left(\Phi^\dagger\Phi - v^2\right)^2, \end{aligned} \tag{3.5}$$

where Higgs field Φ is a complex spinor of the group $SU(2)_L$, $\Phi = \frac{1}{\sqrt{2}}\begin{pmatrix} \varphi^+ \\ \varphi^0 \end{pmatrix}$; v is a vacuum expectation value and λ is a positive constant.

Yukawa part in the Lagrangian (3.1) describes the interaction between a scalar field Φ and mass-less quark and electron fields:

$$\mathcal{L}_{yukawa} \approx -g_Y \bar{L}\Phi r + h.c. \tag{3.6}$$

The topic of our research is devoted to Z boson production with calculation QCD and EW corrections, so we need only in that part of SM Lagrangian which describe neutral interactions. The Lagrangian of the neutral current can be written as

$$\mathcal{L}_{\mathrm{NC}} = e j_\mu^{\mathrm{EM}} A^\mu + \frac{g}{\cos\theta} j_\mu^{\mathrm{Z}} Z^\mu, \tag{3.7}$$

where electromagnetic j^{EM} and neutral j_μ^{Z} weak boson currents are following

$$\begin{aligned} j_\mu^{\mathrm{EM}} &= j_\mu^3 + \frac{1}{2} j_\mu^{\mathrm{Y}}, \\ j_\mu^{\mathrm{Z}} &= j_\mu^3 - \sin^2\theta j_\mu^{\mathrm{Y}}, \\ j_\mu^3 &= \bar{L}\gamma_\mu \frac{\tau_3}{2} L, \\ j_\mu^{\mathrm{Y}} &= -\bar{L}\gamma_\mu L - 2\bar{r}\gamma_\mu r. \end{aligned} \tag{3.8}$$

From the Lagrangian with a help of the perturbation theory or the path integral method can be achieved the Feynman Rules for calculation matrix elements [37], [38]. In the framework of SM the propagators of quarks with flavor $f_i = u, d, s, ...$, gluons, photons and massive weak bosons are presented here:

$$\begin{aligned} &\text{quark} && \xrightarrow{\mathrm{p}} && : && -i\frac{\gamma^\mu p_\mu + m}{p^2 - m^2 + i\epsilon} \\ &\text{gluon} && \overset{\mathrm{p}}{\text{oooooo}} && : && -i\frac{g_{\mu\nu}t^{ab}}{p^2 + i\epsilon}\left(g_{\mu\nu} + (\xi - 1)\frac{p_\mu p_\nu}{p^2}\right) \\ &\text{photon} && \overset{\mathrm{p}}{\sim\sim\sim} && : && -i\frac{1}{p^2 + i\epsilon}\left(g_{\mu\nu} + (\xi - 1)\frac{p_\mu p_\nu}{p^2}\right) \\ &\text{gauge boson} && \overset{\mathrm{p}}{\sim\sim\sim} && : && -i\frac{1}{p^2 - m^2 + i\epsilon}\left(g_{\mu\nu} - (\xi - 1)\frac{p^\mu p^\nu}{p^2 - \xi m^2}\right) \\ &\text{ghost} && \overset{\mathrm{p}}{\text{- - - - - - -}} && : && -i\frac{1}{p^2 - \xi m^2 + i\epsilon} \end{aligned} \tag{3.9}$$

Here ξ is a gauge parameter, for 't Hooft-Feynman gauge $\xi = 1$, for Landau gauge $\xi = 0$, for unitary gauge $\xi = \infty$.

The couplings of interaction quarks with weak bosons (a), quarks with a photon (b), of triple gauge-bosons interaction (c) and of triple gluons interaction (d) are there:

a) 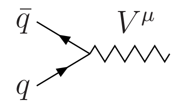

$$: \quad -ie\gamma^\mu\left(L_{f_if_j}\tfrac{1-\gamma_5}{2} + R_{f_if_j}\tfrac{1+\gamma_5}{2}\right),$$

b) 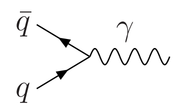

$$: \quad -ig\gamma^\mu t_c,$$

c) 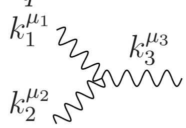

$$: \quad -ieK\Big(g^{\mu_1\mu_2}(k_1-k_2)^{\mu_3} + g^{\mu_2\mu_3}(k_2-k_3)^{\mu_1} + g^{\mu_3\mu_1}(k_3-k_1)^{\mu_2}\Big), \tag{3.10}$$

d) 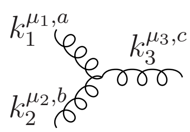

$$: \quad gf^{abc}\Big(g^{\mu_1\mu_2}(k_1-k_2)^{\mu_3} + g^{\mu_2\mu_3}(k_2-k_3)^{\mu_1} + g^{\mu_3\mu_1}(k_3-k_1)^{\mu_2}\Big),$$

where f^{abc} is the color tensor, factor K is equal to 1 for $(WW\gamma)$ vertex and to $\cos\theta_W$ for (WWZ) vertex. The left- and right-handed coupling L and R are different for each type of bosons:

$$\begin{aligned}
W^- &: \; L_{f_if_j} = \frac{1}{\sqrt{2}sin\theta_W}(\tau_+)_{f_if_j}U_{f_if_j}, \qquad R_{f_if_j} = 0, \\
W^+ &: \; L_{f_if_j} = \frac{1}{\sqrt{2}sin\theta_W}(\tau_-)_{f_if_j}U^\dagger_{f_if_j}, \qquad R_{f_if_j} = 0, \\
Z^0 &: \; L_{f_if_j} = \frac{1}{sin2\theta_W}(\tau_3)_{f_if_i} - \delta_{f_if_j}e_{f_j}tan\theta_W, \qquad R_{f_if_j} = -\delta_{f_if_j}e_{f_j}tan\theta_W, \\
\text{photon} &: \; L_{f_if_j} = R_{f_if_j} = \delta_{f_if_j}.
\end{aligned} \tag{3.11}$$

θ_W is the electroweak mixing angle, $\tau_\pm = (\tau_1 \pm i\tau_2)/2$ and τ_3 are weak-isospin Pauli matrices, U is unitary Cabibbo-Kobayashi-Maskawa mixing matrix, δ is Kronecker symbol, e_f is the electromagnetic charge of the quarks in units of electrons charge.

For our calculation of Z boson production, it is more conveniently to rewrite electroweak couplings of interaction quarks with flavor f with neutral boson in following way:

$$i\gamma^\mu(v_f - \gamma_5 a_f), \tag{3.12}$$

where v_f and a_f are

$$v_f = \frac{I_3 - 2Q_f \sin^2\theta_W}{2\sin\theta_W \cos\theta_W}\,, \qquad a_f = \frac{I_3}{2\sin\theta_W \cos\theta_W} \tag{3.13}$$

with I_3 being isospin of a quark.

3.2 Matrix elements construction

By calculation of the Z boson production in the Drell-Yan process, we consider partonic process

$$i(p_1) + j(p_2) \to Z(q) + X(p_X)\,, \tag{3.14}$$

where i, j can be quarks, antiquarks, gluons or photon in depend of considering subprocesses, X is a set of particles, which accompanied to Z boson production, it can be one or two quarks, gluons, etc.

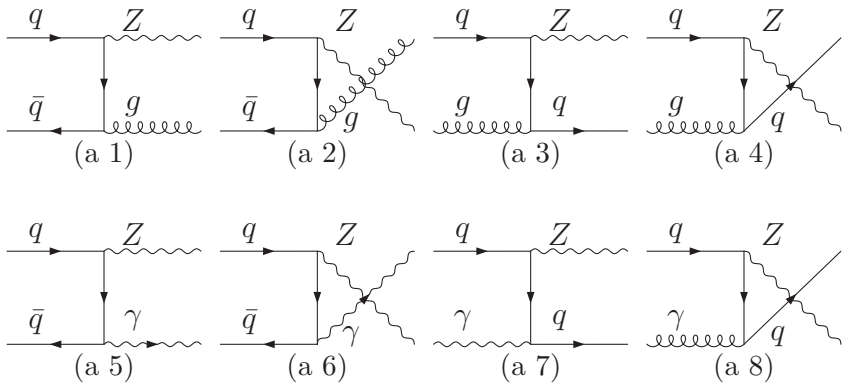

Figure 3.1: Diagrams contributing to the lowest order in Drell-Yan mechanism for Z boson production. The diagrams a_i with $i = 1, ..., 4$ present order $O(\alpha_S\alpha)$, the diagrams a_i with $i = 5, 6$ present order $O(\alpha^2)$.

The lowest order of the partonic process (3.14) can be presented according to Feynman graphical visualization as it shown at the Fig. (3.1). For matrix elements witch give us order $O(\alpha_S\alpha)$ we have squared diagrams of processes $q + \bar{q} \to Z + g$, $q + g \to Z + q$. For the matrix elements which give us order $O(\alpha^2)$, we have to consider Born diagrams with a photon in final state $q+\bar{q} \to Z+\gamma$ and a photoproduction $q+\gamma \to Z+q$. The subprocesses $\bar{q}q$, gq, $\bar{q}g$ and $g\bar{q}$ can be obtain by crossing.

For the calculation of the next order of corrections to the Born level, we must take into account corrections by order α_S and α, so we will have $O(\alpha_S^2\alpha)$ and $O(\alpha_S\alpha^2)$ orders of estimation. The corrections are divided as usual to the virtual and bremsstrahlung types.

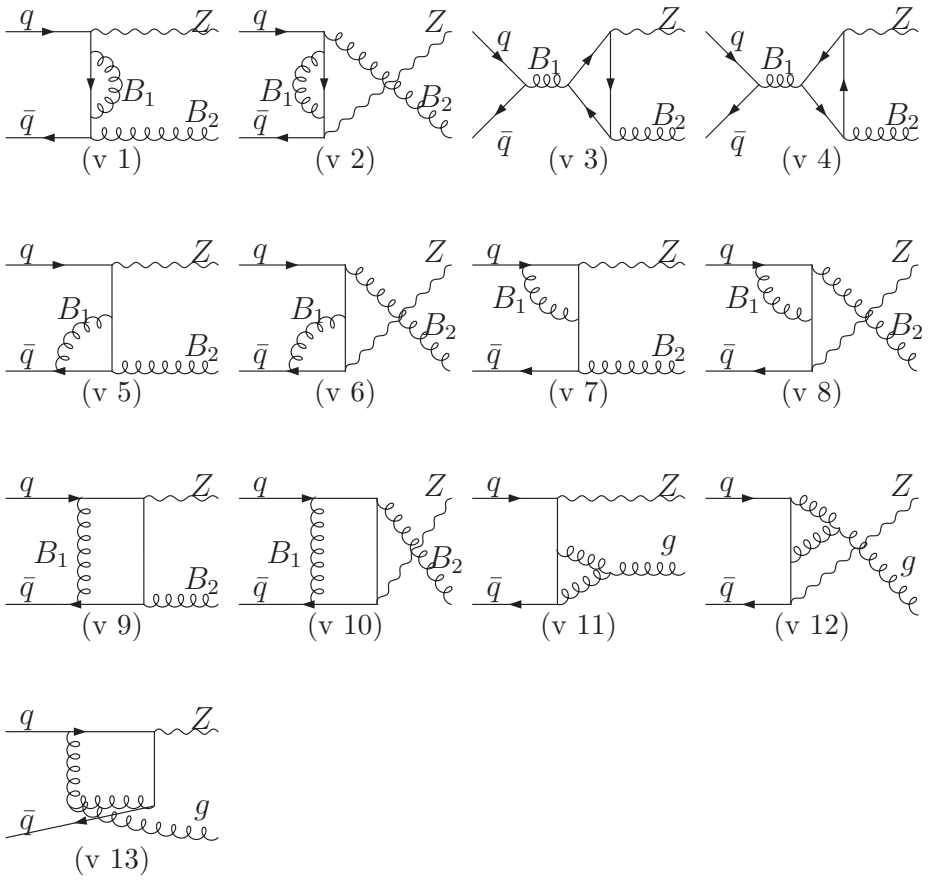

Figure 3.2: Virtual diagrams contributing to the process $q\bar{q} \to BZ$, with boson B as gluon for calculating of order $O(\alpha_S^2\alpha)$ or as photon for calculating of order $O(\alpha_S\alpha^2)$. The diagrams v_{11}, v_{12} and v_{13} correspond only to $O(\alpha_S^2\alpha)$ case.

The first part of contributions come from interference ofi the Born level diagrams with the one-loop diagrams which are presented in the Fig. (3.2) and Fig. (3.3). In these pictures you can see namely the contributions to the subprocess $q + \bar{q} \to Z + g$ and $q + \bar{q} \to Z + \gamma$.

In relation to considering order of estimation, we take into account different types of diagrams. For calculation matrix elements of QCD corrections of order $O(\alpha_S^2\alpha)$, we have to collect Born diagrams a_1, a_2 with all virtual diagrams at the Fig. (3.2), where in the diagrams v_i $(i = 1, ..., 10)$ we put gluons at the both places of bosons B_1 and B_2. Another order of corrections, $O(\alpha_S\alpha^2)$ can be found by the calculations of QED and EW corrections. For the QED part of corrections we consider diagrams v_i, $i = 1, ..., 10$ in the Fig. (3.2) with one signed B line as a photon, and another B line as a gluon. By constructing matrix elements, we square these diagrams with corresponding lowest levels diagrams from the Fig. (3.1):

– for the loop diagram which emit a photon (and has exchanging gluon inside) we take the Born diagrams a_5, a_6;

– for the loop diagrams with an external gluon (and a photon is inside of the loop diagram) we take diagrams a_1, a_2.

Diagrams contributing to the $qg \to qZ$ can be obtained by crossing.

In the Fig. (3.3) the virtual loop diagram which contribute to the order $O(\alpha_S \alpha^2)$ with exchanging weak bosons are presented, so called EW contributions. This diagrams must be squared with the Born diagrams a_1, a_2. By crossing we obtain other subprocesses for the EW corrections calculations.

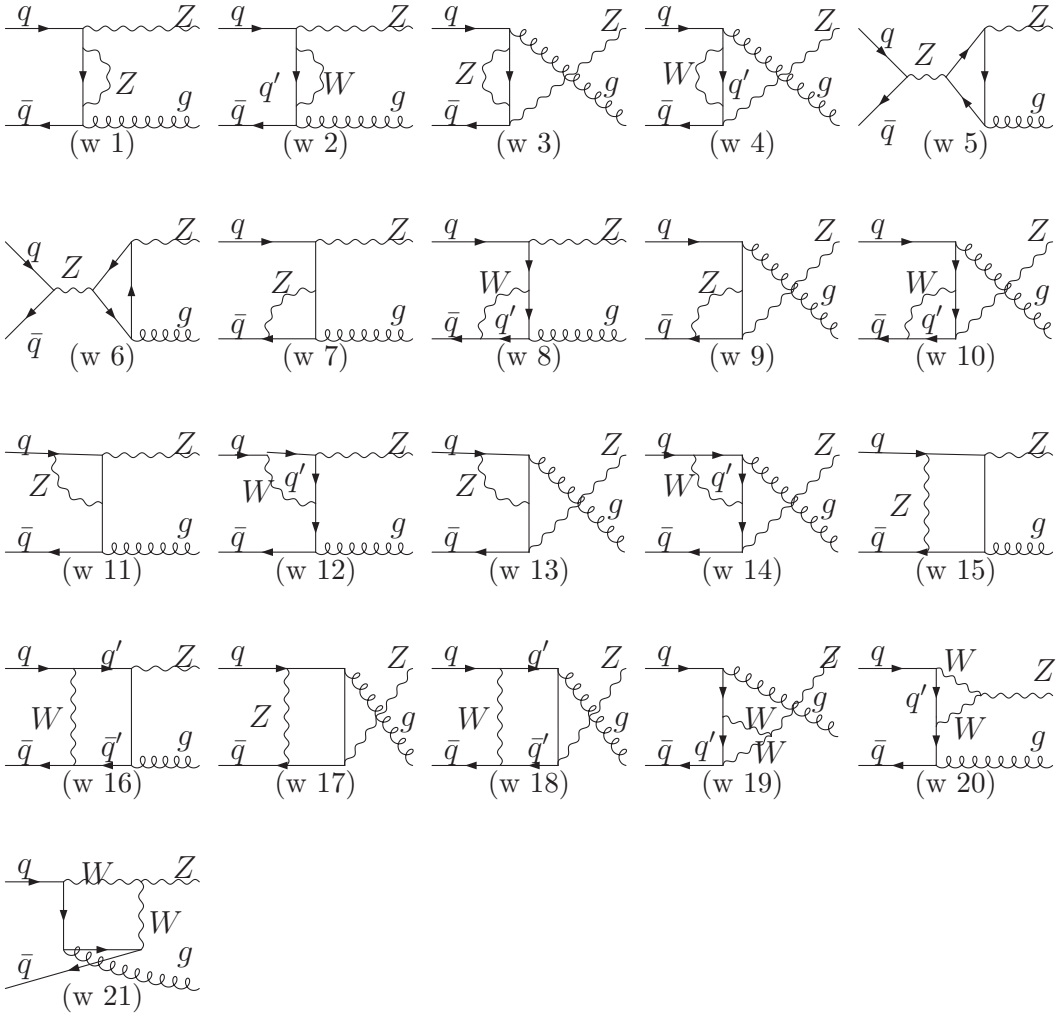

Figure 3.3: Virtual diagrams contributing to the process $q\bar{q} \to gZ$, electroweak case.

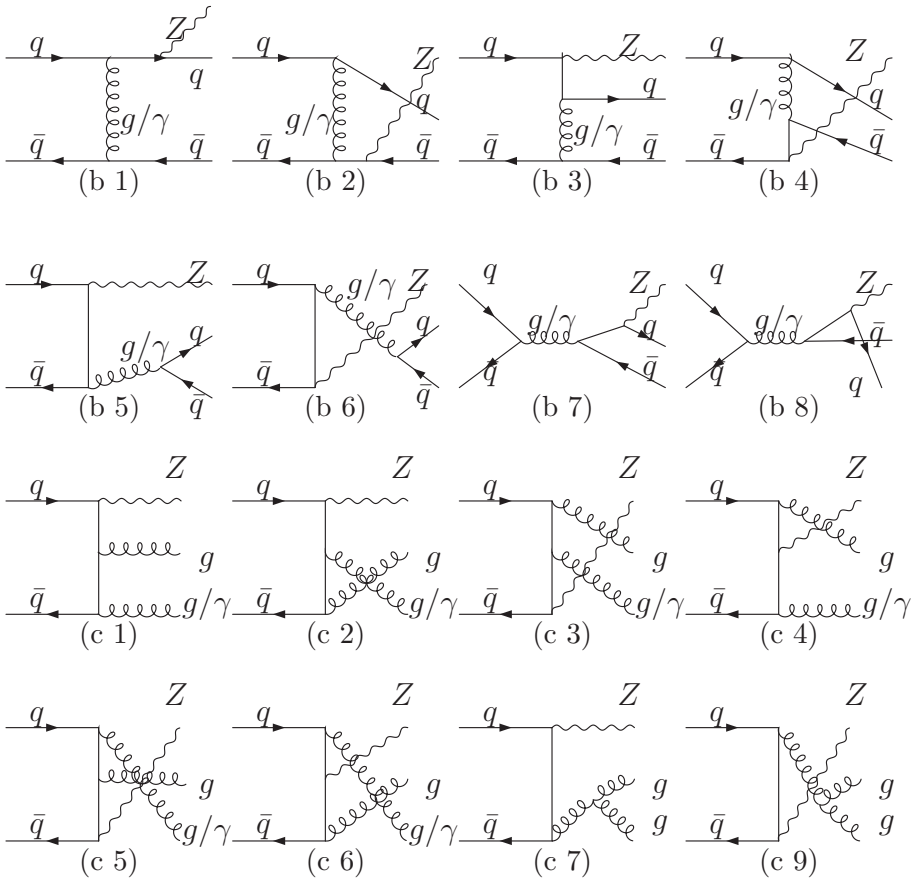

Figure 3.4: a) Diagrams b_i are contributed to the process $q\bar{q} \to Zq\bar{q}$ at the orders $O(\alpha_S^2\alpha)$ and $O(\alpha_S\alpha^2)$ b) Diagrams c_i are contributed to the process $q\bar{q} \to Zgg$ and $q\bar{q} \to Zg\gamma$ at the orders $O(\alpha_S^2\alpha)$ and $O(\alpha_S\alpha^2)$ correspondingly

Another part of contributions of the second order of corrections comes from the two jets productions accompanied Z boson as it shown in the Fig. (3.4), where is presented namely the processes $q\bar{q} \to q\bar{q}Z$ (diagrams b_i), $q\bar{q} \to ggZ$ (diagrams c_i only with $i = 1, ..., 6$) and $q\bar{q} \to g\gamma Z$ (all diagrams c_i). The substitution to the subprocess $gg \to ZX$ can be similarly obtained from c_i alone.

Diagrams contributing to the subprocesses $qg \to qZ$ are obtained by crossing.

As in the virtual case, we collect the diagrams in such way which give us the needful order of corrections, $O(\alpha_S^2\alpha)$ or $O(\alpha_S\alpha^2)$. By considering of the QCD corrections we have gluons in initial exchanging line in the process $q\bar{q} \to Zq\bar{q}$ and additional gluon emissions in suprocesses $q\bar{q} \to Zgg$: we take into account all diagrams from the Fig. (3.4). By calculation the QED corrections for the process $q\bar{q} \to q\bar{q}Z$ we square diagrams b_i, $(i = 1..8)$ in the Fig. (3.4), one with gluon and another with photon in initial line. For subrpocesses

$q\bar{q} \to Zg\gamma$ we take into account only diagrams c_i, $(i = 1, ..., 6)$ in the Fig. (3.4).

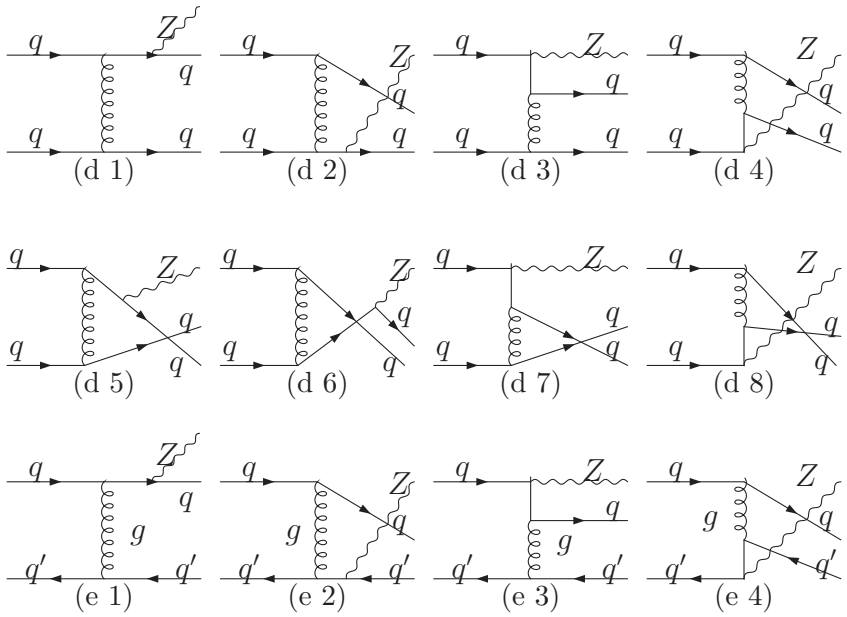

Figure 3.5: a) Diagrams a_i contributing to subprocess $qq \to qqZ$ with exchange g, γ or Z according to considering case; b) diagrams b_i contributing to subprocess $qq' \to qq'Z$.

The next part of the jets contributions of subprocesses (3.14) is presented at the Fig. (3.5), where the production of Z boson in the quark-quark interaction is considered, namely $qq \to qqZ$ and $qq' \to qq'Z$ subprocesses. The circle exchange line between two quarks in the diagrams (d_i) can denote a gluon (for QCD correction of order $O(\alpha_S^2\alpha)$, a photon (for QED correction of order $O(\alpha_S\alpha^2)$) or a Z boson (for EW correction of order $O(\alpha_S\alpha^2)$). As usual, we squared diagrams in such a way that we obtained the needful order of corrections. The mixed QCD/QED corrections due to interference with shown in Fig. (3.5) diagrams with gluon exchange and the same diagrams but with photon and Z boson exchange is involved. This part of EW corrections was missed by Kuhn group in calculation [17]. We included this part corrections to our result and considered the influence of this part to the total cross section. We will show it in discussion of numerical results.

3.3 Singularities

The final result for the cross section is finite in our renormalized model. But by calculation loop and some bremsstrahlung diagrams one can see that integrals has divergences, both ultraviolet and infrared. One of the most convenient and efficient ways to fixed them and

take the right finite answer is calculation with continuing the dimensionality of space-time to $d = 4 - 2\varepsilon$. In this section we discuss how was fixed singularities.

3.3.1 Modified minimal-subtraction scheme

To renormalize the ultraviolet coupling, the calculation of partonic cross section $s\frac{\mathrm{d}\hat{\sigma}}{\mathrm{d}t\mathrm{d}u}$ was done in modified minimal-subtraction scheme $\overline{\mathrm{MS}}$. In this renormalization scheme the $1/\varepsilon$ poles in potentially divergent quantities are removed. The poles are accompanied by terms involving Euler-Mascheroni constant γ_e and $\ln\pi$, which are both also subtracted together with $1/\varepsilon$. So, we have replaces

$$\begin{aligned}\frac{\Gamma(2-\frac{d}{2})}{(4\pi)^{d/2}(m^2)^{2-d/2}} &= \frac{1}{(4\pi)^2}\Big(\frac{2}{\varepsilon} - \gamma + \ln(4\pi) - \ln(m^2)\Big) \\ &\to \frac{1}{(4\pi)^2}\big(-\ln(m^2/M^2)\big),\end{aligned} \tag{3.15}$$

where M is an arbitrary mass parameter that have introduced to make the final equation dimensional correct.

3.3.2 Soft singularities

The final state singularities was considered in accordance to the method which presented in [7], [8]. In the dimensional regularization scheme with $d = 4 - 2\varepsilon$ dimensions, the collinear and soft singularities of the virtual loop corrections to the partonic interactions $2 \to 2$ lead to $1/\varepsilon$ poles. These are to be compensated by contributions coming from subprocesses $2 \to 3$ shown in the Fig. (3.4) and the Fig. (3.5). As it was shown in the section (2.5.1), the phase space $\mathrm{d}\Phi^{(3)}$ can be rewritten so:

$$\mathrm{d}\Phi^{(3)} = \frac{s_2^{-\varepsilon}s^{\varepsilon-1}}{(4\pi)^d\Gamma(1-\varepsilon)(tu - s_2Q^2)^\varepsilon} sin^{1-\varepsilon}\beta_1 d\beta_1 \sin^{1-\varepsilon}\beta_2 d\beta_2 dt du \tag{3.16}$$

Soft or collinear limits in the parton kinematics (2.14) correspond to the case $s_2 \to 0$. Then the factor $s_2^{-\varepsilon}$ in the phase space measure is used to separate explicitly the poles in dimensional regulator ε and finite integrable distribution in $1/\varepsilon$. Namely we have

$$\begin{aligned}\frac{1}{s_2^{1+\varepsilon}} &= \delta(s_2)\left(-\frac{1}{\varepsilon} + \ln s_{2,\max} - \frac{\varepsilon}{2}\ln^2 s_{2,\max} + \dots\right) \\ &\quad + \left(\frac{1}{s_2}\right)_+ + \left(\frac{\ln s_2}{s_2}\right)_+ + \dots,\end{aligned} \tag{3.17}$$

where "+" distributions is defined so that for any smooth test function $f(s_2)$ it takes place

$$\begin{aligned}\int\limits_0^{s_{2,\max}} ds_2 \frac{f(s_2)}{(s_2)_+} &= \int\limits_0^{s_{2,\max}} \frac{ds_2}{s_2}[f(s_2)-f(0)],\\ \int\limits_0^{s_{2,\max}} ds_2 \frac{\ln(s_2)}{(s_2)_+} f(s_2) &= \int\limits_0^{s_{2,\max}} \frac{ds_2}{s_2}[f(s_2)-f(0)]\ln(s_2)\end{aligned}$$

and $s_{2,\max}$ can be determined with a help of kinematic relations. With this definition we can cancel all soft and collinear singularities that are related to the final state radiation.

3.3.3 Factorization of collinear singularities

The remaining collinear singularities in the initial states are eliminated due to the renormalization of the parton distribution functions. This relation reads

$$f_i^h(x,\mu^2) = \sum_j \int\limits_x^1 \frac{dy}{y} f_j^{h,\mathrm{bare}}(x/y)\left(\delta_{ij}\delta(y-1) - \frac{\mu^{-2\varepsilon}}{\varepsilon}\frac{\alpha_s}{2\pi}\frac{\Gamma(1-\varepsilon)}{\Gamma(1-2\varepsilon)}P_{ij}(y)+\dots\right), \quad (3.18)$$

where P_{ij} are the splitting functions in 1-loop approximation

$$\begin{aligned}P_{qq}(y) &= C_F\left(\frac{1+y^2}{(1-y)_+}+\frac{3}{2}\delta(y-1)\right), \quad (3.19)\\ P_{gq}(y) &= C_F\frac{1+(1-y)^2}{y},\\ P_{gg}(y) &= 2C_A\left(\frac{1}{(1-y)_+}+\frac{1}{y}+y(1-y)-2\right)+\delta(y-1)\left(\frac{11}{6}C_A-\frac{2}{3}T_F\right),\\ P_{qg}(y) &= \frac{y^2+(1-y)^2}{2},\end{aligned}$$

and the corresponding QED contributions can be obtained from the above formula with the replacements $\alpha_s \to \alpha$, $C_F \to 1$ and $C_A \to 0$.

The calculation of the factorized cross-section $d\bar{\sigma}$ can be done in a simple way:

$$\begin{aligned}\frac{sd\bar{\sigma}_{i,j}}{dtdu} &= \frac{sd\sigma_{i,j}}{dtdu} \quad (3.20)\\ &-\frac{\alpha_S}{2\pi}\sum_k \int\limits_0^1 dz_1 R_{k\leftarrow i}(z_1,M^2)\frac{sd\sigma^{(1)}_{k,j}}{dt}|_{p_1\to z_1p_1}\delta(z_1(s+t-Q^2)+u)\\ &-\frac{\alpha_S}{2\pi}\sum_k \int\limits_0^1 dz_2 R_{k\leftarrow j}(z_2,M^2)\frac{sd\sigma^{(1)}_{i,k}}{dt}|_{p_2\to z_2p_2}\delta(z_2(s+u-Q^2)+t),\end{aligned}$$

where $d\sigma_{i,j}$ is bare result of Feynman graphs, $d\sigma^{(1)}_{k,j}$ denoted cross-section lowest order and the structure function R has general form:

$$R_{k\leftarrow i}(z,M^2) \;=\; -\frac{1}{\epsilon}P_{k\leftarrow i}(z)\frac{\Gamma(1-\epsilon)}{\Gamma(1-2\epsilon)}\left(\frac{4\pi\mu^2}{M^2}\right)^{\epsilon}+C_{k\leftarrow i}(z). \tag{3.21}$$

The definition of the non-singlet part $C_{k\leftarrow i}(z)$ of (3.21) is undetermined and reflect the freedom of choice in the definition of structure functions. For $\overline{\rm MS}$ scheme there are defined by $C^{\overline{\rm MS}}_{k\leftarrow i}(z)=0$ and DGLAP functions $P_{k\leftarrow i}(z)$ are given in Eq.3.19.

By calculation QED correction, the factorization was done also with adding photonic structure functions. In schematic way we can write:

$$\begin{aligned}\frac{sd\bar{\sigma}^{(2),QED}_{i,j}}{dtdu} \;=\; & \frac{sd\sigma^{(2),QED}_{i,j}}{dtdu} \\ & -\frac{\alpha_S}{2\pi}\sum_k\int_0^1 dz R_{QCD}(z,M^2)\frac{sd\sigma^{(1),QED}_{k,j}}{dt} \\ & -\frac{\alpha}{2\pi}\sum_k\int_0^1 dz R_{QED}(z,M^2)\frac{sd\sigma^{(1),QCD}_{i,k}}{dt},\end{aligned} \tag{3.22}$$

where $\sigma^{(2),QED}$ is the cross section of the order $O(\alpha_S\alpha^2)$, $\sigma^{(1),QED}$ is the cross section of the first order (Born) $O(\alpha_S\alpha)$ and $\sigma^{(1),QCD}$ is the Born cross section of the order $O(\alpha_S^2)$.

The DGLAP splitting function R_{QCD} are done for evolution dispersion in QCD, and R_{QED} – for evolution dispersion in QED.

Chapter 4

Analytical results

In this section we present the analytical result of calculation of the total cross section of the Z boson production in the Drell-Yan process.

The total cross section of the Z boson production includes the tree level (QCD and QED cases), the corrections of order α_S (QCD part of corrections) and the corrections of order α (QED and EW parts of corrections), which all are coming from the loop calculations and from the consideration of the accompanying to boson production jets. In calculation we separated the QCD, QED and EW parts.

The steps of calculations are follows. We started from the Feynman graphs, which was evaluated with a help of DIANA program [39]. The set of diagrams which was considered in the calculations, was discussed in the section (3.2). The output of the DIANA program give us a set of topologies for considering subprocesses. Every type of topologies was recombined with the Integration By Part procedure with a help of the AIR program [32]. The AIR give us the reduction of systems of integrals to the set of master integrals. The Dirac algebra was calculated in the d-dimensional space with 't Hooft-Veltman presentation of γ_5 matrix (see discussion in section (2.5). The phase integrals for processes with accompanying particles to the Z boson and the integration of initial momenta in loop integrals was done also in the d-dimensional time-space. For the virtual integrals we used the Passarino-Veltman reduction scheme [21], Sec. (2.4.3). By calculating phase integrals we followed to the van Neerven method [22], Sec. (2.5.2). The ultraviolet QCD coupling renormalization has been done in $\overline{\rm MS}$ scheme. The final state of singularities was considered in accordance with the method which presented in [7, 8], according to which the singularities were rewritten in terms s_2^ε. This was discussed in Sec. (3.3). The remaining collinear singularities in the initial states are eliminated due to the renormalization of the parton distribution functions.

The analytical result was done as differential cross section by variables t, u and then calculated numerically, what we will discuss in Chapter 5.

4.1 Z boson production at the order $O(\alpha_S\alpha)$. Born level.

In this section we give known formulae for lowest order of calculation of Z boson production. The lowest level of result come from the tree diagrams which was given in the section (3.2) in the Fig. (3.1).

The calculation of the differential partonic cross section of process $i+j \to Z+k$, where i, j and k are quarks or gluons, give us the following formulae:

$$\frac{s\sigma_{ij}^{(1),QCD}}{dt} = \alpha_S^{\overline{\rm MS}}(\mu^2)\frac{K_{ij}}{s}A_{i,j}(s,t,u)(v_q^2+a_q^2), \tag{4.1}$$

where coupling constants v_q and a_q are given in Eq. (3.13) and for actual subprocess we have following kinematic factors:

$$\begin{aligned} A_{q\bar{q}}(s,t,u) &= \frac{u}{t}+\frac{t}{u}+\frac{2Q^2(Q^2-u-t)}{ut}, \\ A_{qg}(s,t,u) &= -A_{q\bar{q}}(u,t,s), \\ A_{gg}(s,t,u) &= 0. \end{aligned} \tag{4.2}$$

Colors coefficients are proportional to color factors C_F and N_C:

$$K_{qq} = \frac{2\pi\alpha C_F}{N_C}, \qquad K_{qg} = \frac{\pi\alpha}{N_C}, \qquad K_{gg} = \frac{\pi\alpha}{2C_FN_C}. \tag{4.3}$$

The QED partonic cross section of the process $q+\bar{q} \to Z+\gamma$ (diagrams a_5 and a_6 in Fig. (3.1)) can be found here:

$$\frac{s\sigma_{q\bar{q}}^{(1),QED}}{dt} = \frac{\alpha(M^2)}{s}\frac{K_{qq}Q_q^2}{C_F}A_{qq}(s,t,u)(v_q^2+a_q^2), \tag{4.4}$$

where Q_q is electric charge of quark q.

Another subprocess is due to the photo-production $\gamma+q \to Z+X$ (Fig. 3.1), which contains the extra power of α, since emission of a photon. It is sufficient to take partonic cross-sections at the tree level approximation. We add the photon spectra form elastic [40] and inelastic [41] scattering in the Weizsäcker-Williams approximation. The cross-section has the following form:

$$\frac{s\sigma_{\gamma q}^{(1)}}{dtdu} = 2\pi\alpha^2(M^2)\frac{Q_q^2}{s}A_\gamma(s,t,u)(v_q^2+a_q^2), \qquad A_\gamma(s,t,u) = A_{qg}(s,t,u). \tag{4.5}$$

The corrections to lowest order of Z boson production must be considered in two ways: with additional gluon interaction ($+\alpha_S$ order, QCD part) or with additional weak interaction ($+\alpha$ order). The last one is divided into photon (QED part) and weak bosons (EW part) interactions. In the next sections we consider this three cases separately.

4.2 Z boson production at the order $O(\alpha_S^2\alpha)$. QCD part

This partonic cross-sections of order $O(\alpha_S^2\alpha)$ was calculated early by any groups (Ellis at al. in [7], Gonsalves at al. in [8], Arnold at al. in [9]) and we have agreement with these final results. Here we will present only short structure of answer, the full formulae are quite big and can be found in given literature.

Firstly, we have to remark the misprint in the paper [8] in the formula (2.12), where in the second line of formula must be sum $\left[\left(B_2^{qG}(s,t,u,Q^2)+C_2^{qG}(s,t,u,Q^2)\right)\sum_{f'<}(1)\right]$ and at the third line must be $C_3^{qG}(s,t,u,Q^2)$ at the place $C_2^{qG}(s,t,u,Q^2)$.

For the calculation of the QCD partonic cross section of the order $(\alpha_S^2\alpha)$ we take into account the virtual and the collinear correction to the Born result, given in the previous section (4.1). In the Fig. (3.2) the loop diagrams for the process $q+\bar{q}\to g+Z$ are shown. In the Fig. (3.4) and the Fig. (3.5) the set of diagrams, which give us the contribution of the collinear correction to the processes $q+\bar{q}\to Z+q+\bar{q}$, $q+\bar{q}\to Z+g+g$, $q+q\to q+q+Z$ and $q+q'\to q+q'+Z$, are presented. The diagrams if other considering process, like $q+g\to q+g+g$, $g+g\to Z+\bar{q}+q$ etc., are not presented since they are simply come from crossing procedure.

For "quark-antiquark" initial state the schematic form of the differential cross section is as follows:

$$\begin{aligned}\frac{s\,d\sigma^{\bar{q}q}}{dt\,du} &= K_{qq}\alpha_S^{\overline{\rm MS}}(\mu^2)\Bigg[\delta(s_2)A_{q\bar{q}}(s,t,u)2(v_q^2+a_q^2)+ \\ &\frac{\alpha_S^{\overline{\rm MS}}(\mu^2)}{2\pi}\Bigg(\delta(s_2)\Bigg(B_1^{q\bar{q}}(s,t,u,Q^2)+n_f B_2^{q\bar{q}}(s,t,u,Q^2)\Bigg)2(v_q^2+a_q^2) \\ &+\Bigg(C_1^{q\bar{q}}(s,t,u,Q^2)+n_f C_2^{q\bar{q}}(s,t,u,Q^2)\Bigg)2(v_q^2+a_q^2) \\ &+C_3^{q\bar{q}}(s,t,u,Q^2)2\sum_{<f}(v_f^2+a_f^2)\Bigg)\Bigg],\end{aligned} \tag{4.6}$$

where $A_{q\bar{q}}$ is the Born result for the quark-antiquark scattering from the Eq. (4.2), analytical formulae B_1, B_2, C_1, C_2 and C_3 are quite big and we don't present them here. They can be found in papers [7–9] for case of production only Z weak boson. The sum $\sum_{<f}$ stands for a sum over quarks with masses less than an appropriately chosen flavor threshold. We take into account five quarks, so for our case $\sum_{<f}(1)=5$.

For "quark-gluon" initial state we have following formula for the differential cross section:

$$\begin{aligned}\frac{s\,\mathrm{d}\sigma^{qg}}{dt\,du} &= K_{qg}\alpha_S^{\overline{\mathrm{MS}}}(\mu^2)\Bigg[\delta(s_2)A_{qg}(s,t,u)2(v_q^2+a_q^2)+ \\ &\frac{\alpha_S^{\overline{\mathrm{MS}}}(\mu^2)}{2\pi}\Bigg(\delta(s_2)\Bigg(B_1^{qg}(s,t,u,Q^2)+n_f B_2^{qg}(s,t,u,Q^2)\Bigg)2(v_q^2+a_q^2) \\ &+C_1^{qg}(s,t,u,Q^2)2(v_q^2+a_q^2)\Bigg)\Bigg],\end{aligned} \tag{4.7}$$

where the Born factor for the qg process A_{qg} was presented in the Eq. (4.2), analytical formula B_1, B_2 and C_1 can be found in the literature [7–9].

The "gluon-gluon" subprocess was calculated for crossed diagrams c_i from the Fig. (3.4). The differential cross section is follows:

$$\frac{s\,d\sigma^{gg}}{dt\,du} = K_{gg}\alpha_S^{\overline{\mathrm{MS}}}(\mu^2)\frac{\alpha_S^{\overline{\mathrm{MS}}}(\mu^2)}{2\pi}B^{gg}(s,t,u,Q^2)2\sum_{f<}(v_f^2+a_f^2)\,. \tag{4.8}$$

For couple quarks subprocesses we divided the result for two cases:

1) both initial quarks has the same flavors ($q+q\to Z+q+q$);

2) initial quarks has different flavors ($q+q'\to Z+q+q'$).

So we have two differential cross sections of the "quark-quark" case with the different color structure:

$$\begin{aligned}\frac{s\,d\sigma^{qq}}{dt\,du} &= K_{qq}\alpha_S^{\overline{\mathrm{MS}}}(\mu^2)\frac{\alpha_S^{\overline{\mathrm{MS}}}(\mu^2)}{2\pi} \\ &\Bigg[B_1^{qq}(s,t,u,Q^2)2(v_q^2+a_q^2)+B_2^{qq}(s,t,u,Q^2)(a_q^2)\Bigg],\end{aligned} \tag{4.9}$$

$$\begin{aligned}\frac{s\,d\sigma^{qq'}}{dt\,du} &= K_{qq}\alpha_S^{\overline{\mathrm{MS}}}(\mu^2)\frac{\alpha_S^{\overline{\mathrm{MS}}}(\mu^2)}{2\pi} \\ &\Bigg[B_1^{qq'}(s,t,u,Q^2)2(v_q^2+a_q^2)+B_2^{qq'}(s,t,u,Q^2)2(v_{q'}^2+a_{q'}^2) \\ &+C_1^{qq'}(s,t,u,Q^2)(v_q a_q)+C_2^{qq'}(s,t,u,Q^2)(v_{q'}a_{q'})\Bigg].\end{aligned} \tag{4.10}$$

4.3 Z boson production at the order $O(\alpha_S\alpha^2)$. QED part

It is a common opinion, that QED contribution can be obtained directly from the QCD one just by manipulating of couplings and color factors. This is obviously true for the pure QED case. But in the mixed QCD/QED corrections some care should be taken. By squaring amplitudes in the mixed case some contributions can drop out due to color traces. To illustrate this effect let us consider, for example, subprocess d_1 at the Fig. (3.5), $q+q \longrightarrow Z+q+q$. The parts for the QED contribution of the order $O(\alpha_S\alpha^2)$ are coming from product of two diagrams, one with a gluon and another (conjugated) with a photon exchange, as it is shown at the Fig. (4.1). After evaluating color factors we can find that it is proportional to $(\mathrm{Tr}t^a)(\mathrm{Tr}t^a)$, where t^a is the color matrix. Since the color matrices are traceless, this contribution vanishes. However if one of the diagrams in the Fig. (4.1) is crossed then the contribution is proportional to another color factor, which is non zero: $\mathrm{Tr}(t^at^a) = C_FN_c$. In this case the QED result cannot be extracted from the QCD formula, if separately diagram contributions are not known. The same situation occurs if we replace a photon by Z boson in the Fig. (4.1).

Since one of the diagrams in the Fig. (4.1) must be crossed, there are not correspond contributions to the flavor not-diagonal process ($q+q' \to Z+q+q'$).

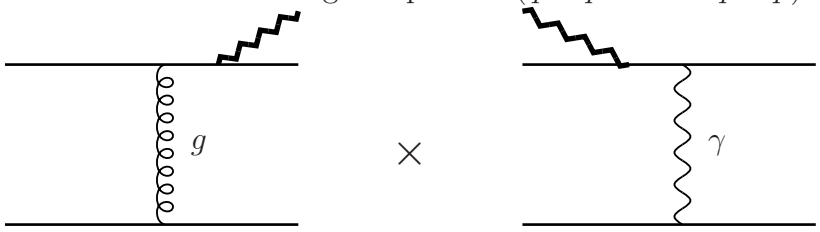

Figure 4.1: Illustration of the color structure in the mixed QED/QCD contribution to the process $q+q \longrightarrow Z+q+q$. See explanation in the text.

In this section we give the order $O(\alpha_S\alpha^2)$ of the QED corrections to Z boson productions. The diagrams for this order of radiative corrections were chosen as it described in the section (3.2): we collect the diagrams with exchanging gluon together with conjugated diagrams with exchanging photon. Let us consider the corrections to Z boson production separately for each subprocesses.

Partonic cross-section $\bar{q}+q \longrightarrow Z+X$

The partonic subprocess $\bar{q}q \longrightarrow Z+X$ of order $O(\alpha_S\alpha^2)$ contain following partonic subprocesses:

$$\begin{array}{lll} a) & \bar{q}q \longrightarrow Zg/\gamma\,, & \text{loops} \\ b) & \bar{q}q \longrightarrow Zg\gamma & \text{bremsstrahlung} \\ c) & \bar{q}q \longrightarrow Z\bar{q}q & \text{bremsstrahlung.} \end{array} \tag{4.11}$$

The first one come from the loop diagrams and divided for two case: with outgoing gluon and virtual photon in loops and with outgoing photon and virtual gluon in loops. They squared with the corresponding conjugated Born process $q+\bar{q}\to Z+g$ or $q+\bar{q}\to Z+\gamma$. The processes a) and b) should be considered together in order to obtain infrared finite cross-section. The last subprocess is finite and gauge invariant itself. Therefore we can present it separately in the formula below the differential cross section

$$\frac{s\,\mathrm{d}\hat{\sigma}^{\bar{q}q}}{dt\,du}=\frac{2\pi\alpha^2Q_q^2(v_q^2+a_q^2)}{N_c}\frac{1}{s}\left\{\delta(s_2)A_{q\bar{q}}(s,t,u)+C_F\frac{\alpha_s}{\pi}\left(\delta(s_2)B_1+B_1'+B_1''\right)\right\} \quad (4.12)$$

where $A_{q\bar{q}}(s,t,u)$ is the Born contribution (4.2), expressions B_1 and B_1' are NLO terms (diagrams c_i and $v_{i=1..10}$ in the Figs. (3.4), (3.2)). The contribution B_1'' comes from the subprocess $\bar{q}+q\to Z+\bar{q}+q$ only (diagrams b_i in Fig. (3.4)). The electroweak coupling constants v_q and a_q are given in Eq. (3.13) and Q_q is the electric charge of a quark.

The analytical presentations of B_1, B_1' and B_1'' are done in the Appendix B

The calculations were done in $\overline{\mathrm{MS}}$ scheme.

Partonic cross-section $qg\longrightarrow Z+X$

For the partonic subprocess $qg\longrightarrow Z+X$ we can present follow QED contributions to the differential cross section:

$$\frac{s\,\mathrm{d}\hat{\sigma}^{qg}}{dt\,du}=\frac{2\pi\alpha\alpha_s Q_q^2(v_q^2+a_q^2)C_F}{N_A}\frac{1}{s}\left\{\delta(s_2)A_{qg}(s,t,u)+\frac{\alpha}{\pi}\left(\delta(s_2)C_1+C_1'\right)\right\} \quad (4.13)$$

where $A_{qg}(s,t,u)$ is the Born contribution (4.2) from diagrams a_3 and a_4 in Fig. 3.1.

The NLO QED corrections, coming from loop and bremsstrahlung diagrams C_1 and C_1' are given in Appendix B.

Partonic cross-section $qq\longrightarrow Z+X$

The mixed QED/QCD contribution to process $qq\longrightarrow Z+q+q$ are due to interference of diagrams which shown in Fig. (3.1) with gluon exchange and the same diagrams but with photon exchange. As discussed in the text this contribution does not follow from QCD calculation because of zero color trace effect. We have the follow differential cross section for the quark-quark interaction:

$$\frac{s\,d\sigma^{qq}}{dt\,du}=\frac{2\pi\alpha_s\alpha^2Q_q^2(v_q^2+a_q^2)C_F}{N_c}C_1'\,, \quad (4.14)$$

where C_1' can be found in Appendix B.

4.4 Z boson production at the order $O(\alpha_S\alpha^2)$. EW part

The next part of corrections of the order $O(\alpha_S\alpha^2)$ is the EW corrections to the main process of the Z boson production. This corrections include the loop diagrams with exchange additional weak boson (see diagrams on the Fig. (3.3)) and the contributions from interference of the process $q+q \longrightarrow Z+q+q$ (the diagrams in the Fig. (3.1)) with Z the boson exchange and the same process with the gluon exchange. This is the mixed QCD/weak parton cross-section.

The virtual weak corrections were calculated by Kuhn et. al in [17]. The comparison of their calculations with our calculations confirms the above result. However, we have different setup form of the infrared singular integrals, which are called $J_{12,13,14}$ in [17] and regularized by introducing the small gluon mass λ. In our approach we used the dimensional regularization and infrared integrals contain additional poles in ε. For practical implementation the formula for the 1-loop scalar integrals from [35] can be used.

In the App.C we shown the result for the EW virtual correction of $q\bar{q}$ initial state. Here we present the new result of the EW corrections which are coming from the interference.

$$\begin{aligned}\frac{s d\sigma^{qq}_{\rm QCD/weak}}{dt\,du} &= \frac{2\alpha^2\alpha_s(v_u^4+6u^2a_u^2+a_u^6)C_F}{N_c s}\times \\ &\Big[\Big\{ f_{ln}(s,t,u)+I_4(1,1,t,1)f_1^{1,1}(s,t,u) \\ &\quad + I_4(1,1,t,-1)f_{-1}^{1,1}(s,t,u) - I_4(1,2,t,-1)f_{-1}^{1,2}(s,t,u)\Big\} \\ &+ \Big\{t\leftrightarrow u\Big\}\Big]\,. \end{aligned} \tag{4.15}$$

The phase space integrals $I_4(i,j,t,k)$ and kinematic functions $f(s,t,u)$ are given in Appendix D.

Chapter 5

Numerical Results

In this Chapter we present the numerical result of our work. We calculated the total hadronic cross-section of the Z boson production in the hadron-hadron interactions with $\sqrt{S} = 14TeV$ for LHC and $\sqrt{S} = 1,96TV$ for Tevatron energies. At the same energies we considered the distributions of the cross section in the rapidity y and the transverse momentum q_T. All results are shown on plots.

5.1 Parameters. Running constants

In this section we will give the parameters which was used by calculations. In the Tab. (5.1) the set of the Standard Model mass parameters, which was used by calculations, is presented. In our estimation we taken into account only five flavors and ignored the top

Leptons	"up" quarks	"down" quarks	Bosons
$m_e = 511\text{keV}$	$m_u = 1.9\text{MeV}$	$m_d = 4.4\text{MeV}$	$m_\gamma = 0$
$m_\mu = 105.7\text{MeV}$	$m_c = 1.32\text{GeV}$	$m_s = 87\text{MeV}$	$m_Z = 91,1876\text{GeV}$
$m_\tau = 1.78\text{GeV}$	$m_t = 172.7\text{GeV}$	$m_b = 4.24\text{GeV}$	$m_W = 80,398\text{GeV}$

Table 5.1: Mass values of quarks and leptons in the Standard Model [42]

quark.

In the framework of the perturbative QCD, the predictions for observables are expressed in the terms of the renormalized coupling $\alpha_S(\mu_R^2)$, a function of an unphysical renormalization scale μ_R. In the renormalization group theory we can write the equations of third order for the strong coupling $\alpha_S = \frac{g_S^2}{4\pi}$ [42]:

$$\mu\frac{d}{d\mu}g(\mu_R) = -\beta_0\frac{g_S^3(\mu_R)}{16\pi^2} - \beta_1\frac{g_S^5(\mu_R)}{128\pi^4} - \beta_2\frac{g_S^7(\mu_R)}{8192\pi^6}. \tag{5.1}$$

where β_i are numerical constants:

$$\begin{aligned}\beta_0 &= 11 - \frac{2}{3}n_f, \\ \beta_1 &= 51 - \frac{19}{3}n_f, \\ \beta_2 &= 2857 - \frac{5033}{9}n_f + \frac{325}{27}n_f^2.\end{aligned} \tag{5.2}$$

Here n_f is a number of quarks with mass less than the energy scale μ. The constants of integration, which are produces by solving this differential equation for the strong coupling, must be obtained from experiments. The most sensible choice for this constant is measure α_S at fixed-reference scale μ_0. The standard one is $\mu_0 = M_Z$. The other values of strong coupling $\alpha_S(\mu)$ at the other values mass μ_R can be obtained from equation

$$\ln\frac{\mu^2}{\mu_0^2} = \int\limits_{\alpha_S(\mu_0)}^{\alpha_S(\mu)} \frac{\mathrm{d}\alpha}{\beta(\alpha)}.$$

To provide a parametrization of the mass μ_R dependence of the strong coupling α_S, one introduce the dimensional parameter Λ. The solution of equation (5.1) can be written as expansion in inverse power of $\ln(\mu^2)$:

$$\begin{aligned}\alpha_S(\mu_R) &\equiv \frac{g^2(\mu_R)}{4\pi} = \frac{4\pi}{\beta_0 \ln(\mu_R^2/\Lambda^2)}\left[1 - \frac{2\beta_1}{\beta_0^2}\frac{\ln[\ln(\mu_R^2/\Lambda^2)]}{\ln(\mu_R^2/\Lambda^2)}\right. \\ &+ \left.\frac{4\beta_1^2}{\beta_0^4 \ln^2(\mu_R^2/\Lambda^2) i}\left(\left(\ln[\ln(\mu_R^2/\Lambda^2)] - 1/2\right)^2 + \frac{\beta_2\beta_0}{8\beta_1^2} - \frac{5}{4}\right)\right].\end{aligned} \tag{5.3}$$

Here we can see the asymptotic freedom property: $\alpha_S \to 0$ as $\mu \to \infty$, QCD becomes strongly coupled at $\mu\ \Lambda$.

The electroweak coupling α can be renormalized with a help of following equations [43]:

$$\alpha(\mu) \equiv \frac{e^2(\mu)}{4\pi}(\delta\alpha_{bos} + \delta\alpha_{lep} + \delta\alpha_{top} + \delta\alpha^{(5)}_{hadrons}(M_Z^2) - \delta\alpha_{udscb}(M_Z^2)), \tag{5.4}$$

where additional contributions of bosons, leptons, quarks interactions were taken into account:

$$\begin{aligned}\delta\alpha_{bos} &= \frac{\alpha}{4\pi}(7\ln\frac{M_W^2}{\mu^2} - \frac{2}{3}), \\ \delta\alpha_{lep} &= -\frac{\alpha}{3\pi}\sum_{l=e,\mu,\tau}\ln\frac{m_l^2}{\mu^2}, \\ \delta\alpha_{top} &= -\frac{4\alpha}{9\pi}\ln\frac{m_t^2}{\mu^2}, \\ \delta\alpha^{(5)}_{hadrons}(M_Z^2) &= 0.027572 \pm 0.000359, \\ \delta\alpha_{udscb}(M_Z^2) &= \frac{11\alpha}{9\pi}\left(\ln\frac{m_Z^2}{\mu^2} - \frac{5}{3}\right).\end{aligned} \tag{5.5}$$

In the evaluating of the distributions we taken $M^2 = M_Z^2$. We have chosen the factorization and renormalization scale masses μ_F^2 and μ_R^2 to be the same as the factorization scale M^2 of the structure functions. And for weak mixing angle θ_W we used $\sin^2\theta_w = 1 - m_W^2/m_Z^2 \approx 0.2226$

5.2 Hadronic cross sections

The analytical calculations give us the distribution of the partonic differential cross section in the Mandelstam variables t and u: $s\frac{\mathrm{d}\hat{\sigma}}{\mathrm{d}t\mathrm{d}u}$. To construct the hadronic cross section, we have to use the master formula(2.3), which con volutes the partonic differential cross section with the parton distribution functions. We put it here again:

$$\frac{d\sigma}{dq_T^2\,dy} = \sum_{i,j}\int dx_1\,dx_2\,f_i(x_1,\mu_F^2)f_j(x_2,\mu_F^2)\frac{s\,d\hat{\sigma}_{i,j}}{dt\,du}(x_1P_1,x_2P_2,\mu_F^2). \tag{5.6}$$

The relations between the Mandelstam variables s, t and u and the integrable parameters momentum fractions x_1, x_2, the transverse momenta q_T and the rapidity y was done in the section (2.4) in the Eq. (2.17). After changing variables, we can integrate (5.6).

Our analytical formulae of partonic cross section contain terms $1/(s_2)_+$, which come from cancellation of the divergences of ε, associated with the limit $s_2 \to 0$. In order to evaluate distributions, it is convenient to rewrite the integrals of variables (x_1, x_2) to (x_1, s_2). The integration bound can be obtained from the conditions

$$0 \le x_1, x_2 \le 1 \quad \text{and} \quad s_2 = x_1x_2S - x_1(Q^2 - T) - x_2(Q^2 - U) + Q^2 \ge 0 \tag{5.7}$$

After that equation (5.6) can be rewritten explicitly in the form

$$\frac{d\sigma}{dq_T^2\,dy} = \sum_{i,j}\int\limits_{x_{1,\min}}^{1} dx_1 \int\limits_0^{s_{2,\max}} \frac{ds_2\;\; f_i(x_1,\mu_F^2)f_j(x_2(s_2),\mu_F^2)}{x_1S + U - Q^2}\frac{s\,d\hat{\sigma}_{i,j}}{dt\,du}(x_1P_1,x_2(s_2)P_2,\mu_F^2) \tag{5.8}$$

where we have now relations

$$\begin{aligned} x_2 &= \frac{s_2 - Q^2 - x_1(T - Q^2)}{x_1S + U - Q^2}\,, \\ x_{1,\min} &= \frac{-U}{S + T - Q^2}\,, \\ s_{2,\max} &= U + x_1(S + T - Q^2)\,, \end{aligned} \tag{5.9}$$

and T and U are given by

$$T = Q^2 - e^{-y}\sqrt{S}\sqrt{Q^2 + Q_T^2}\,, \qquad U = Q^2 - e^{+y}\sqrt{S}\sqrt{Q^2 + Q_T^2}\,. \tag{5.10}$$

5.3 Plots and numerical result

The partonic cross-section was convoluted with the parton distribution functions numerically in FORTRAN and C++ codes. We used generally the PDFs of the CTEQ collaboration (J. C. Collins et al., [25]), which have been derived from the deep inelastic scattering data using a full next-to-leading-order analysis based on $\overline{\text{MS}}$ scheme. We used namely the CTEQ6M data with the standard $\overline{\text{MS}}$ scheme. The calculations were done to be used for two colliders – Tevatron and LHC. According to type of colliders (LHC or Tevatron), the PDFs were chosen for the parton-parton or parton-antiparton distributions. For the calculation of the photoproduction $\gamma + q \to Z + X$ (the diagrams a_7 and a_8 in the Fig. (3.1)), the result of the MRS collaboration (A. Martin et al. [26]) was taken into account. This parton distribution functions incorporate the QED contributions. They considered parton analysis of the deep inelastic and the hard scattering data, including the α corrections to parton evaluation.

The integration of the transverse momenta q_T and the rapidity y was done numerically with a help of CUBA library [44], where we used namely VEGAS and SUAVE algorithms for multidimensional numerical integrations in FORTRAN and C++ codes. These algorithms integrate vector integrands with a help of Monte Carlo method. Vegas uses importance sampling as a variance-reduction technique, each interaction consists of a sampling step followed by refinement of the gird. Suave uses Vegas-like importance sampling combined with a globally adaptive subdivision strategy, the region with the largest error at the time is dominated in considering dimension, before the request accuracy is reached. Both methods give us the same results, but SUAVE algorithm is faster.

The results of the total cross section calculation for the Z boson production in the Drell-Yan process are shown in the Fig. (5.1) and in the Fig. (5.2) for different scale energies $\sqrt{S} = 1.96\,\text{TeV}$ and $\sqrt{S} = 14\,\text{TeV}$ in dependence of the cut momentum q_T^{cut}, which give us the upper limit of integration. The upper plots in these pictures present the full summarized total cross section, which we marked with a solid black heavy line, and contributions of different orders, which all together collect the result:

- the Born contribution is marked with a solid black fine line,

- the QCD corrections of order $O(\alpha_S^2\alpha)$ are marked with a black dashed line,

- the sum of QED and EW corrections of order $O(\alpha_S\alpha)^2$ are marked with a red dashed line

- and also the part of photoproduction correction of order $O(\alpha^2)$ is marked with a green dashed line.

To see the behavior of the different type of contributions at large value of the cut-momenta q_T and to see the behavior of the small contributions, we plotted also their in a logarithmic scale. In the bellow plots at the Fig. (5.1) and at the Fig. (5.2) the same data of Z boson production are presented in the logarithmic scale. Some of the data are negative, so we plot the contributions of the absolute value of corrections, for that reason you can see knees and ankles at some lines.

At the Fig. (5.3) and the Fig. (5.4) we present the plots of a K factor for the total

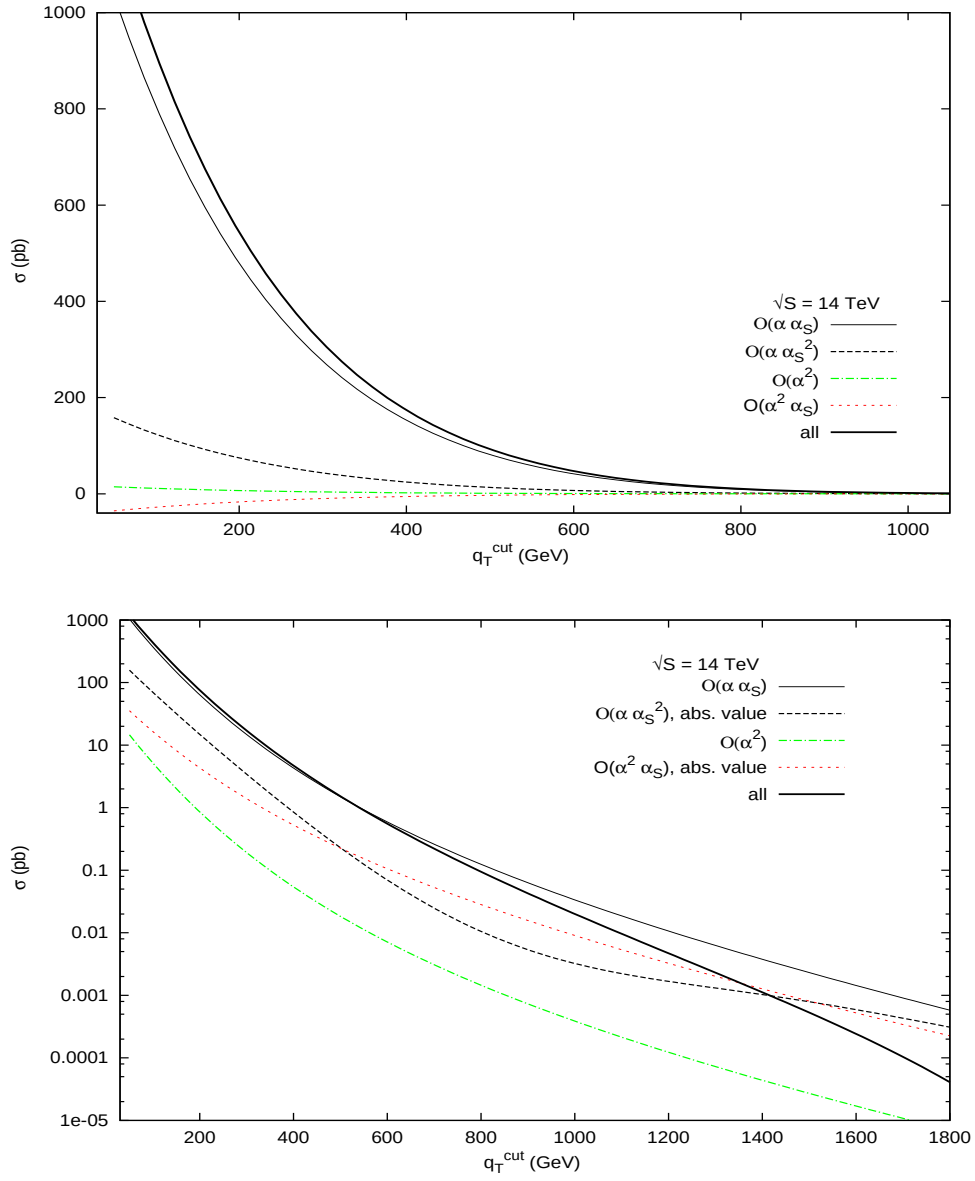

Figure 5.1: The total cross section of Z boson production for $\sqrt{S} = 14\,\mathrm{TeV}$ (LHC energy). The upper picture shows the full value of cross section. The lower one shows the logarithmic values.

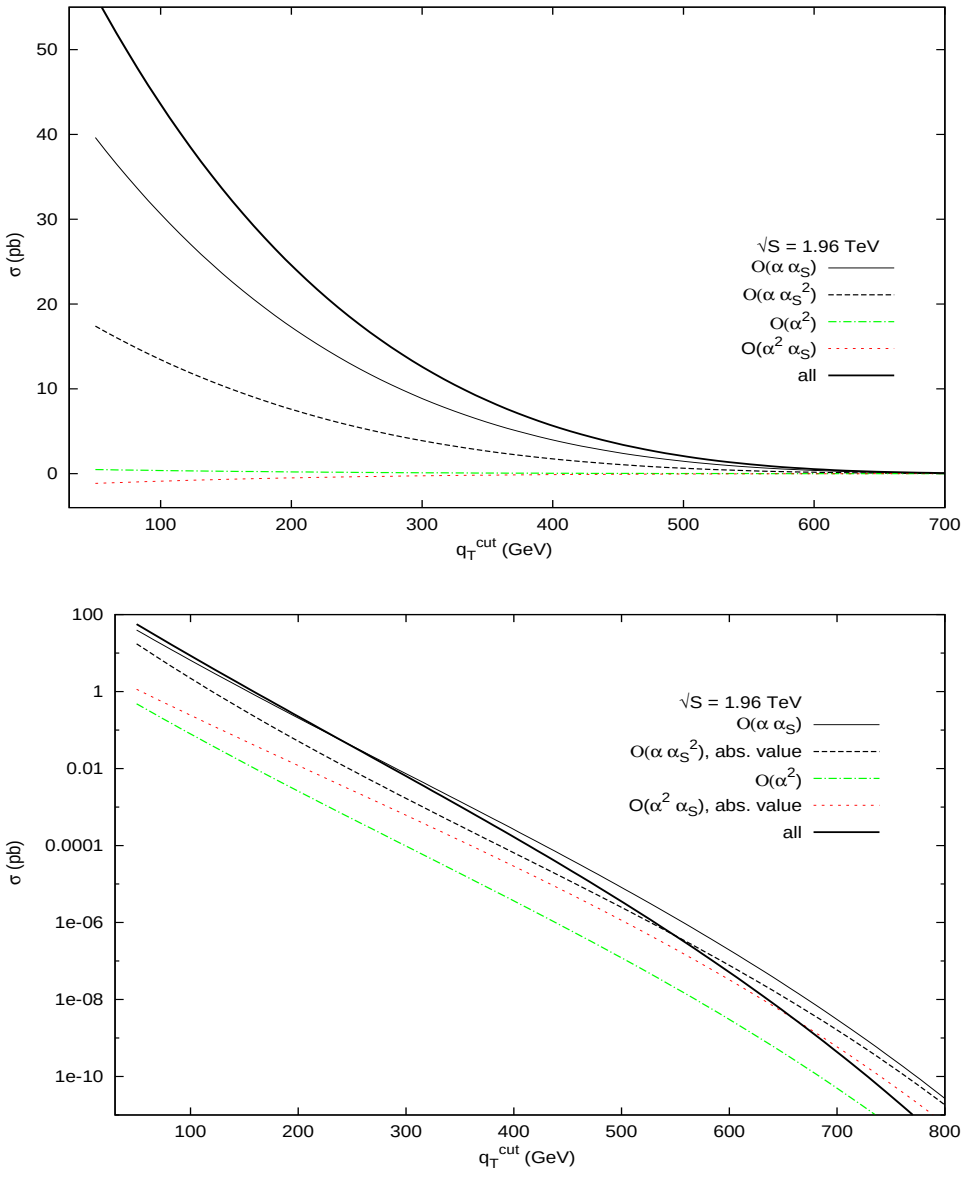

Figure 5.2: The same as Fig. (5.1) for $\sqrt{S} = 14\,\text{TeV}$ (Tevatron energy).

cross-section:

$$K = \frac{\sigma_{tot}}{\sigma_{Born}}. \tag{5.11}$$

Namely, we plotted $K-1$ factor as distribution in the momenta q_T^{cut} in the LHC and Tevatron energy ranges correspondingly and we separated the contributions in depending of orders and subprocesses.

In the upper plots pf the Fig. (5.3) and the Fig. (5.4) we can see the contribution of the QCD corrections of the order $O(\alpha_S^2\alpha)$ (marked with a black dashed line) and the EW corrections of the order $O(\alpha_S\alpha^2)$ (marked a blue dashed-point line). All other contributions are smaller, so we consider their individually close up at the upper plots. The red line shows the Born level of Z boson production of order $O(\alpha)^2$ (which comes from the diagrams a_5 and a_6 in the Fig. (3.1)), the green line shows contributions of the QED corrections which was calculated in the section (4.3), the blue dashed line presents the EW additional contributions from the subprocesses $q+q \to Z+q+q$ (see the section (4.4)) and the purple dashed line give us the contribution of the photoproduction (the diagrams a_7 and a_8 in the Fig. (3.1)).

From the Fig. (5.3) and Fig. (5.4) we can see that the QCD contributions dominate in the whole region of interest and can be larger as tens percents. The weak corrections can also achieve big values and grow up for large q_T. The QED corrections and the part of qq-Chanel of EW corrections appear to be surprisingly small. The naive counting of orders shows that formally these corrections are of the same order $O(\alpha_s\alpha^2)$ as pure weak corrections. However they appear to be highly suppressed. We can see that the distribution of order $O(\alpha_S^2\alpha)$ is about $10-20\%$, while the distribution of corrections of order $O(\alpha_S\alpha^2)$ give us only about 2%.

In the Fig. (5.5) and the Fig. (5.6) we plot the differential cross section to Z boson production in the transverse momentum q_T distributions at $\sqrt{S} = 14TeV$ (LHC energy) and for $\sqrt{S} = 1.86TeV$ (Tevatron energy) correspondingly. In the upper plots we show the real value of contributions, where we separate as usual results by orders of $O(\alpha_S^2\alpha)$ and $O(\alpha_S\alpha^2)$. The born result is presented in the black dashed-point line, the QCD corrections are shown with the black dashed line, the QED and the EW corrections are shown with the red line, the photoproduction we marked the with green dashed line. And the black heavy line present the sum of all contributions. To seeing also the small value of corrections at large transverse momentum q_T, we plot the logarithmic graphs. Note, that some NLO contributions are negative at large q_T, cause for this picture we take absolute values of corrections. We can see that at big value of transverse momentum q_T the contribution of order $O(\alpha_S\alpha^2)$ start to play bigger role.

And finally we present the rapidity distribution of the differential cross section at energies for LHC and Tevatron (the Fig. (5.7)).

We compared our result with results of others groups. The QCD contributions were in agreement with result of [7], [8], [9]. The QED corrections were calculated separately. To check this result we gone into the so-called "QED limit" for these subprocesses where it is possible. So, we considered limits $C_F \to 1$ and $C_A \to 0$ for known QCD loops corrections,

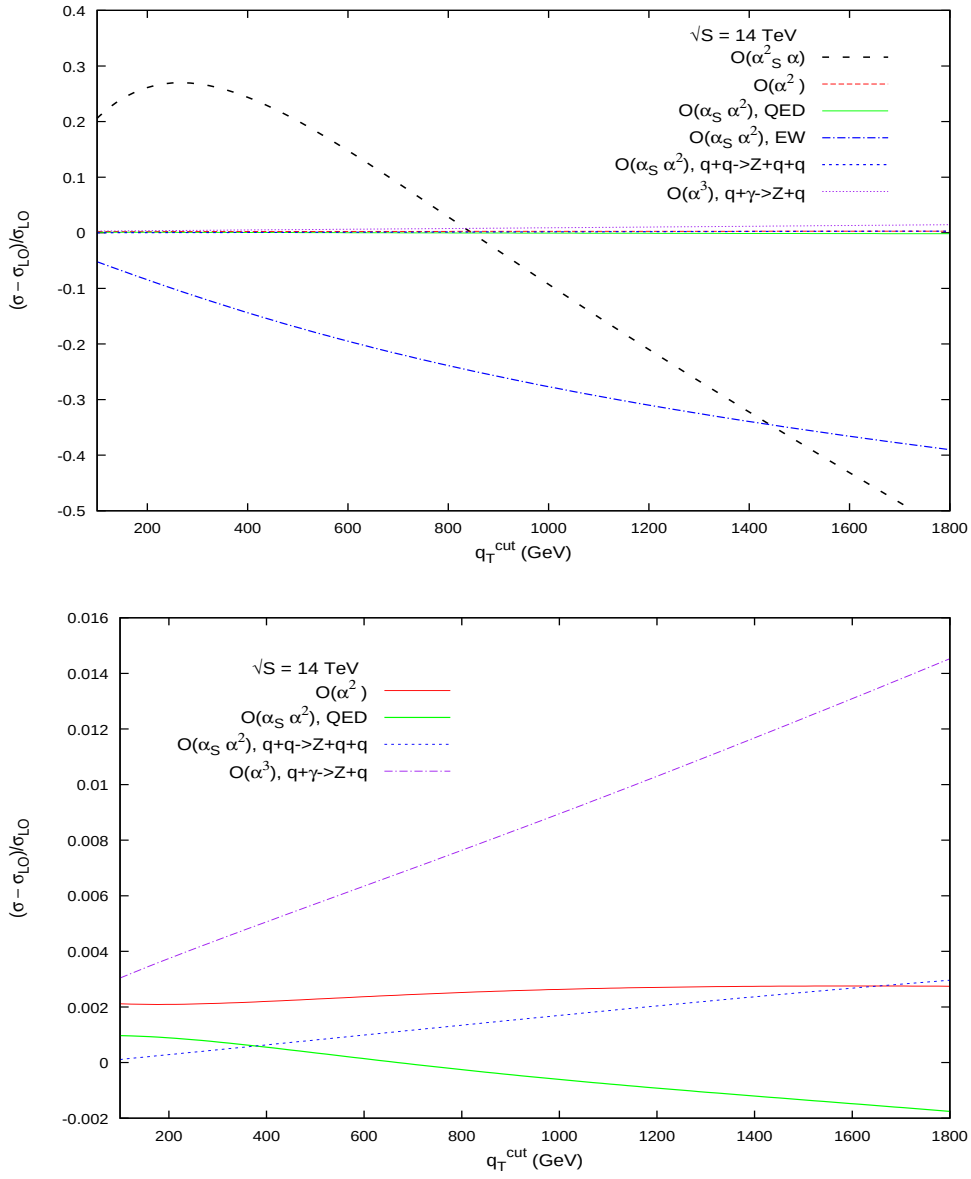

Figure 5.3: NLO QCD and EW corrections ($K-1$ factor) to the total σ for $p+p \longrightarrow Z+X$ for $\sqrt{S} = 14TeV$ (LHC). Upper plot includes all NLO contributions. Lower plot is the close up without QCD NLO.

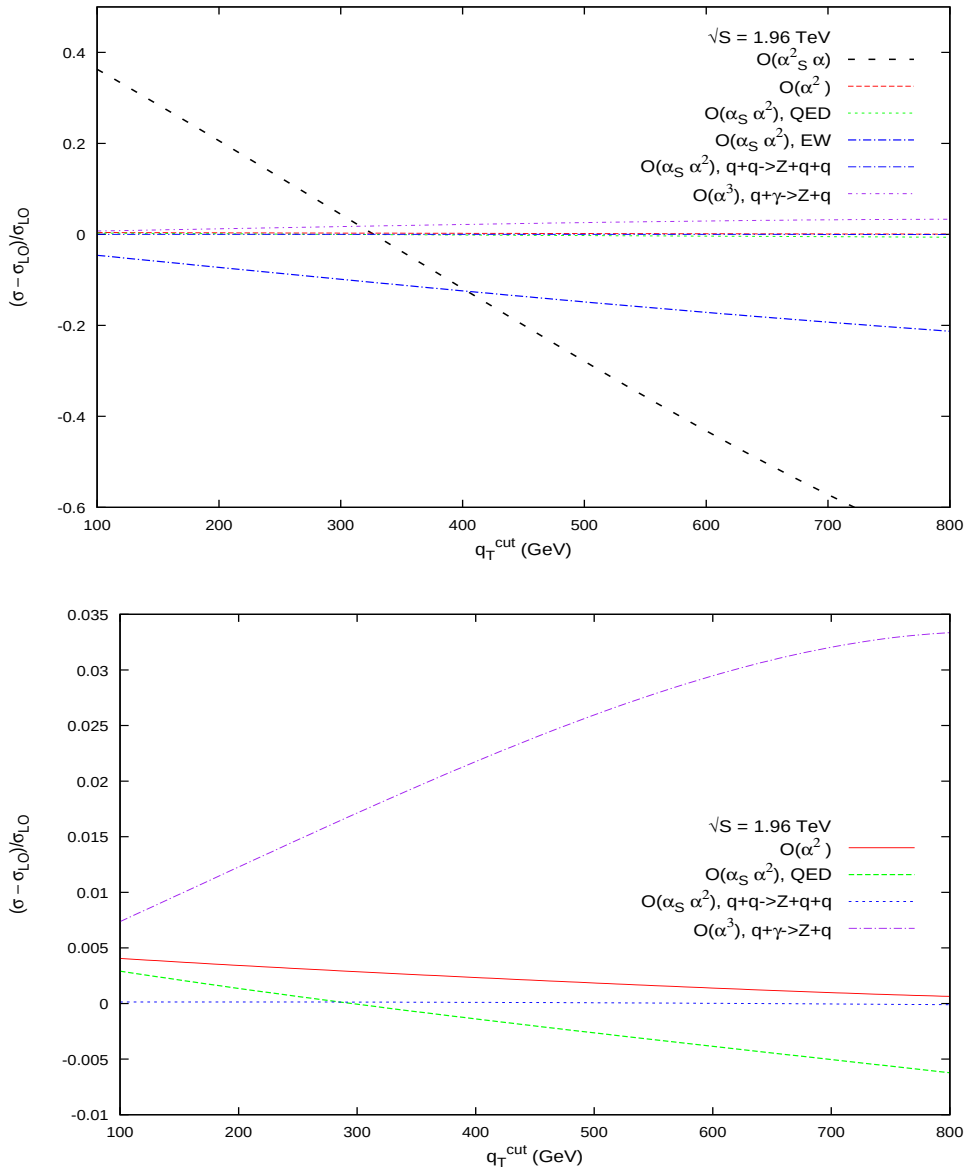

Figure 5.4: The same as Fig. (5.3) for $\sqrt{S} = 1.96TeV$ and for process $p + \bar{p} \longrightarrow Z + X$ (Tevatron).

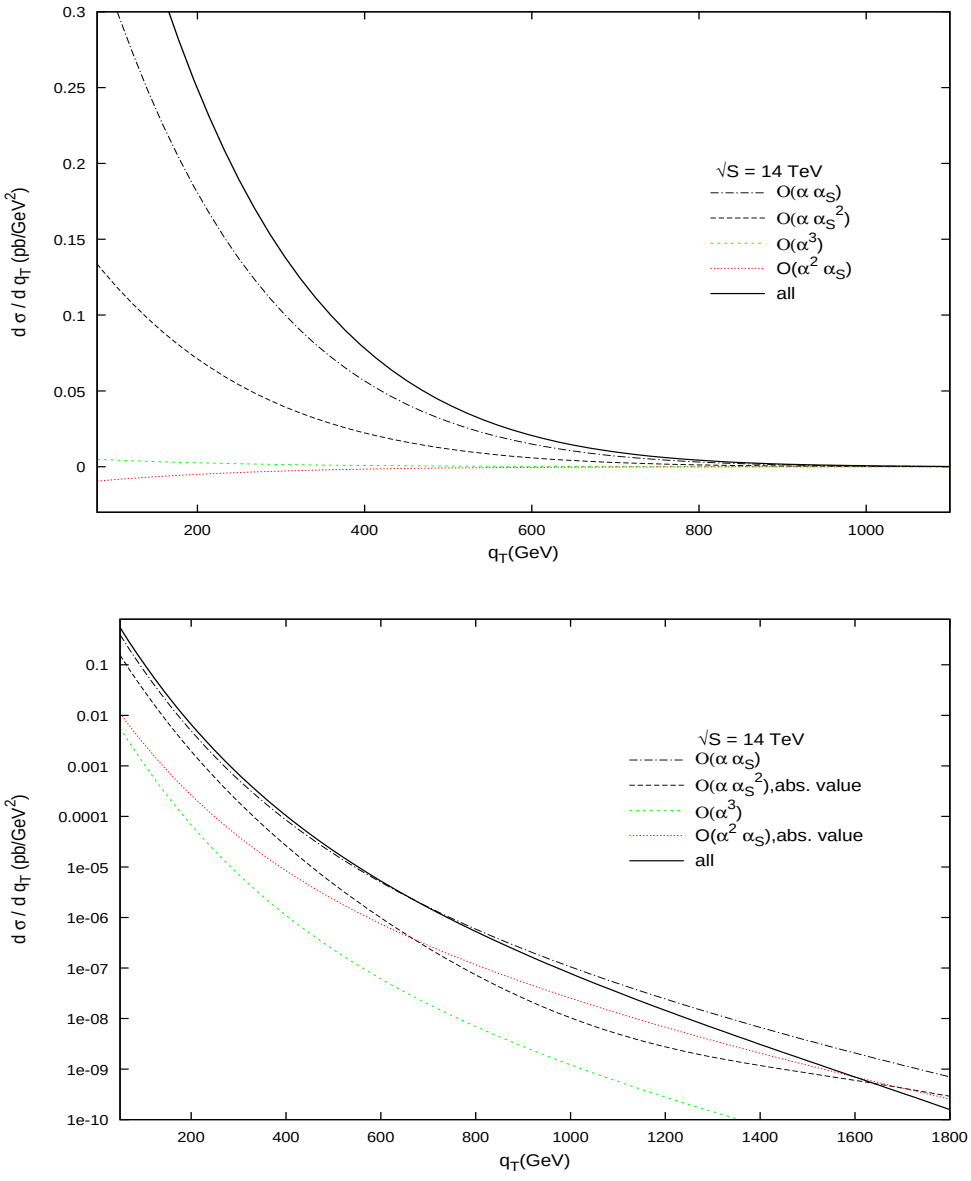

Figure 5.5: The q_T distributions to Z boson production at $\sqrt{S} = 14TeV$ (LHC). Upper picture shows the full value of cross section. Lower one shows the logarithmic values.

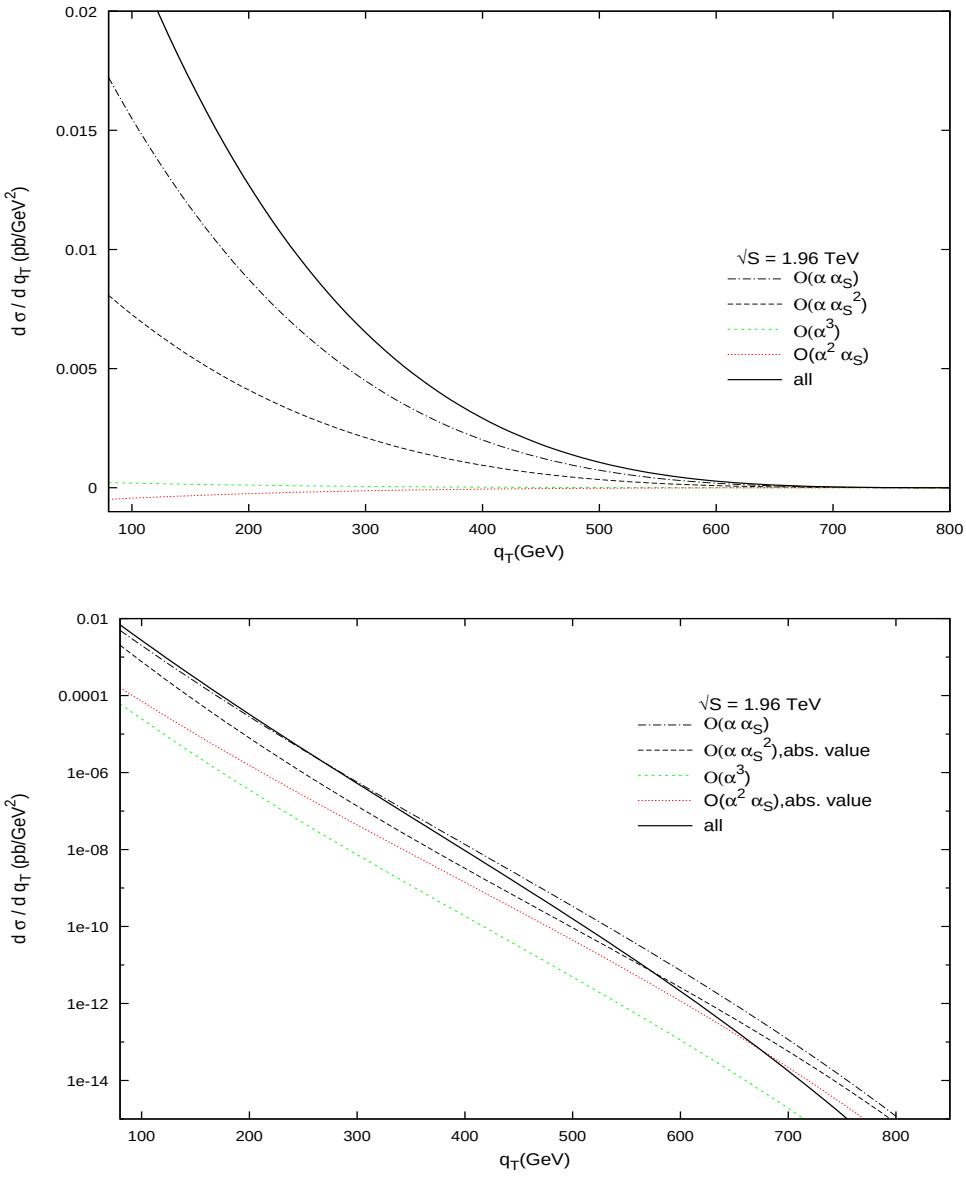

Figure 5.6: The same as Fig.(5.5) at $\sqrt{S} = 1.96TeV$ (Tevatron).

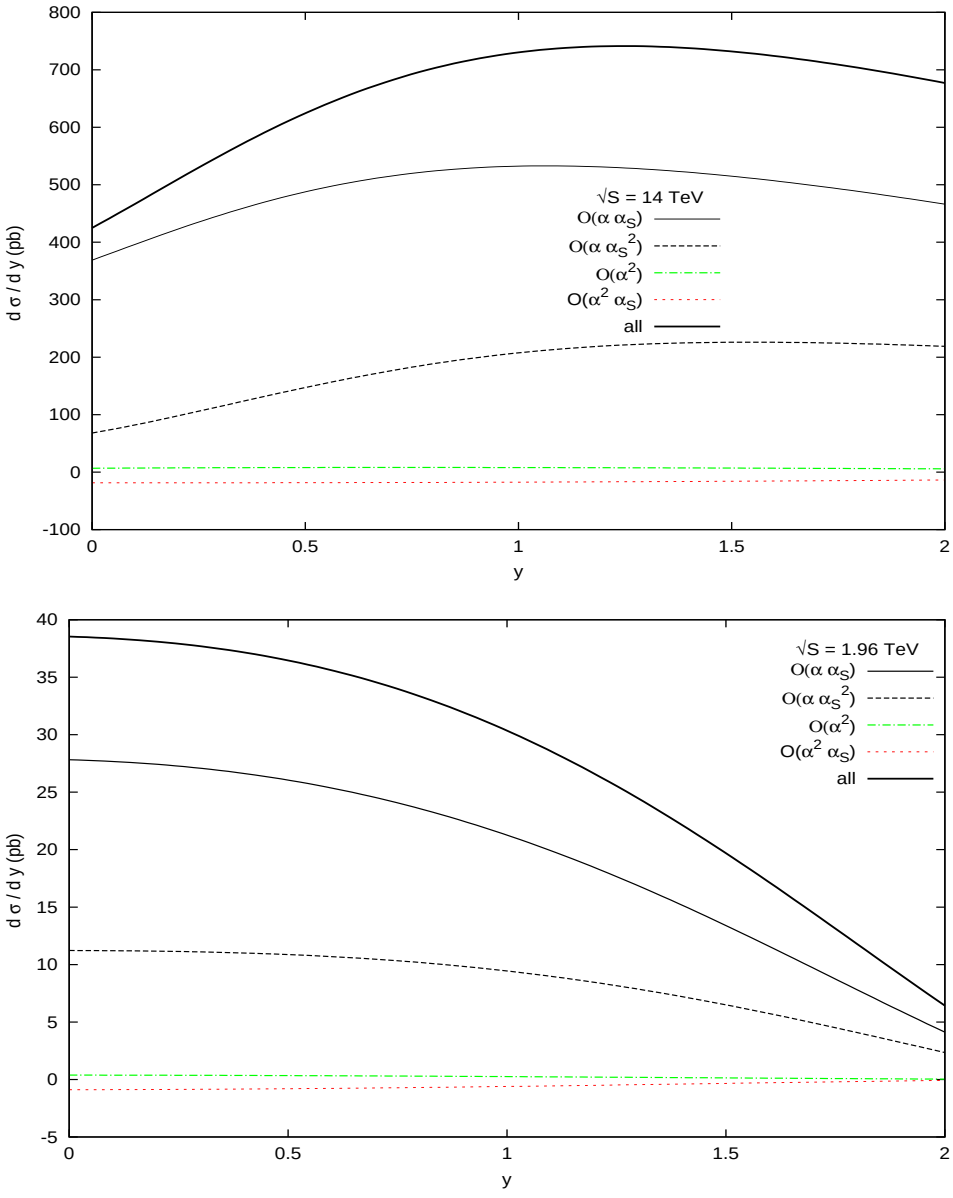

Figure 5.7: The rapidity distribution to Z boson production. Upper picture shows the value at energy $\sqrt{S} = 14TeV$ (LHC), the lower one shows the value at energy $\sqrt{S} = 1.96TeV$ (Tevatron).

this limiting formula given us correct result of QED case. The EW part, which was particularly calculated by Kuhn in [17] also was congruented with our result.

Chapter 6

Conclusion

In this thesis, we present the calculations of the differential as well as the total cross section for the Z boson production via the Drell-Yan process at the orders of the perturbation theory $O(\alpha_S^2\alpha)$ and $O(\alpha_S\alpha^2)$.

The production of Z boson in the hadron-hadron interactions plays very important role in the modern physics in relation with the development of the colliders technique and the building of new high energies hadron-hadron colliders like LHC. The leptonic decay modes of Z boson decay in this process can be very easily triggered in detectors. The accuracy of the calculated cross section give us good approximation in knowledge about the value of background and help us to separate important events.

Our result includes the QCD, QED and EW corrections to the main Born processes and has the general orders $O(\alpha_S\alpha, \alpha_S^2\alpha, \alpha_S\alpha^2)$. The calculations were done in the framework of the Standard Model. We adopted the $\overline{\text{MS}}$ scheme of renormalization and factorization. The integration over loop and bremsstrahlung momenta was done in the d dimension phase space. The traces with γ_5 matrix were accurately calculated using 't Hooft-Veltman definition of γ_5.

Our analytical result for the QCD corrections of the order $O(\alpha_S^2\alpha)$ is in good agreement with early calculation. The QED corrections of the order $O(\alpha_S\alpha^2)$ cannot be extracted directly from QCD formulae, because in the mixed $\alpha_S\alpha$ corrections the non-vanishing colour factor appears in the quark-quark processes like $q + q \to Z + q + q$. In this thesis, for the first time the analytical result for QED corrections of the Z boson production is presented. Our calculations of the EW corrections include the loop calculations and the bremsstrahlung subprocess, which are the new contributions and were never calculated before. Namely, we took into account the quark-quark interaction $q + q \to Z + q + q$ with an exchange of weak neutral boson and gluon. So, in this work the full order corrections up to the order $\alpha_S\alpha^2, \alpha_S^2\alpha$ were calculated for the first time.

As the result of our calculations, we gave the analytical formula for the partonic subprocess and the graphical output of our numerical calculation of the hadronic cross section. The convolution of the parton cross section to the hadron cross section was done with help of CTEQ6 and MRTSparton distribution functions. The numerical results are presented by plots of the total cross section σ^{tot} and of the distributions in the transverse momentum

$\frac{\mathrm{d}\sigma}{\mathrm{d}q_T}$ and in the rapidity distribution $\frac{d\sigma}{\mathrm{d}y}$ of the Z boson. We plotted the distribution of the total cross sections in dependence of the cut-momenta q_T^{cut} at the energies for LHC and Tevatron colliders.

For more detail presentation of the relative contributions of the different subprocesses to the total cross sections, we plotted the $K = \frac{\sigma_{\mathrm{tot}}}{\sigma_{\mathrm{Born}}}$ factor in dependence of the cut-momentum q_T^{cut}. The contribution of the QCD corrections of order $O(\alpha_S^2\alpha)$ is most important at small q_T^{cut}. At large values of the momentum q_T^{cut} (for LHC energies $q_T^{cut} > 1200GeV$ and for Tevatron energies $q_T^{cut} > 400GeV$) the EW contributions of the order $O(\alpha_S\alpha^2)$ play a significant role and achieve up to 30% for LHC and 20% for Tevatron energies. The contributions of order $O(\alpha_S\alpha^2)$ of the QED subrocesses are small and average out at $1-2\%$.

Our numerical calculations were done in C++ and FORTRAN codes, where for numerical integration was used the CUBA library. The next step of calculation of full order of corrections to the Z boson production in the Drell-Yan process is the including in the result the calculations of processes $q + \bar{q} \to Z$. Our code can be easy changed and used for calculation also of W boson, as well as Higgs boson production at the hadron-hadron interactions.

Appendix A

Operator definitions of Parton Distribution Functions

Here we collect the operators definitions [27, 45] of the parton distribution functions. All the definitions have ultraviolet divergences and that must be renormalized away to define finite parton distribution functions.

Quark Distribution Functions

The distribution function of the quark of flavor i in a hadron h with momentum p_μ in the plus direction is [45]:

$$\begin{aligned}\phi_{i/h}(x) &= \int \frac{dy^-}{2\pi} e^{-ixp^+y^-} \\ &\langle p\big|\bar{\psi}_i(0,y^-,0_\perp)\frac{y^+}{2}P\exp\Big[-ig\int_0^{y^-} dy'^- A_a^+(0,y'^-,0)\psi t^a\Big]\psi_i(0)\big|p\rangle,\end{aligned} \tag{A.1}$$

where t^a are generating matrices for the adjoined representation of color group $SU(N_c)$, p^+ is component to z-axis of momenta p, y^μ denote position in space-time, ψ is quark filed operator. The path ordered exponential of the gluon field A is needed to make the definition gauge invariant. This distribution was done for unpolarized case without to take into account a spin momenta transverse to collision axis.

Gluon Distribution Functions

The operator definition for the distribution function of gluons in a hadron h with momentum p_μ in the plus direction is:

$$\phi_{g/h}(x) = \sum_{j=1}^{2}\int \frac{dy^-}{2\pi x p^+} e^{-ixp^+y^-}\langle p\big|G^{+\,j}(0,y^-,0_\perp)PG^{+\,j'}(0)\big|p\rangle, \tag{A.2}$$

where G is gluon filed strength tensor and P denotes path-ordered exponential of the gluon filed along the light-cone that makes the operator gauge invariant:

$$P = P \exp\Big[\int_0^{y^-} dy'^- A_a^+(0, y'^-, 0_\perp) t^a\Big]. \tag{A.3}$$

Appendix B

Analytical result for QED corrections

Here we present the analytical result of the calculation of QED corrections to Z boson production in the Drell-Yan mechanism. The calculation was done independently of the QCD corrections and compared with them in limit $\alpha_S \to \alpha$, $C_F \to 1$, $C_A \to 0$ for this subprocesses were we don't have vanishing colour factors.

Partonic cross-section $\bar{q} + q \longrightarrow Z + X$

First part of the QED corrections is the distribution of $q\bar{q}$ channel of the hadron-hadron collisions. The partonic process $\bar{q}q \longrightarrow Z + X$ of the order $O(\alpha_S\alpha^2)$ contains following partonic subprocesses:

$$\bar{q}q \longrightarrow Z\gamma\,, \qquad \bar{q}q \longrightarrow Zg\gamma \qquad \text{and} \qquad \bar{q}q \longrightarrow Z\bar{q}q\,.$$

The first two processes were considered together in order to obtain the infrared finite cross-section. The last subprocess is finite and gauge invariant itself. Therefore we can present this contributions separately in the formulae below:

$$\frac{s\,d\sigma^{\bar{q}q}}{dt\,du} = \frac{2\pi\alpha^2 Q_q^2(v_q^2+a_q^2)}{N_c}\frac{1}{s}\left\{\delta(s_2)A_{q\bar{q}}(s,t,u) + C_F\frac{\alpha_s}{\pi}\left(\delta(s_2)B_1 + B_1' + B_1''\right)\right\} \quad \text{(B.1)}$$

where $A_{q\bar{q}}(s,t,u)$ is the Born contribution (4.2):

$$A_{q\bar{q}}(s,t,u) \;=\; \frac{u}{t} + \frac{t}{u} + \frac{2Q^2(Q^2-u-t)}{ut},$$

The functions B_1, B_1' and B_1'' are NLO terms of corrections which come from diagrams c_i and $v_{i=1..10}$ in the Fig. (3.4) and in the Fig. (3.2). The contribution B_1'' comes from the subprocess $\bar{q}+q \to Z+\bar{q}+q$ only (diagrams b_i in the Fig. (3.4)). The electroweak coupling constants v_q and a_q are given in the Eq. (3.13), Q_q is the electric charge of a quark.

For the NLO terms we obtained following expressions:

$$
\begin{aligned}
B_1 \;=\;& A_{q\bar{q}}\Bigg[L_{\mu_F}(2L_t+2L_u-4L_A-3)+4L_A(L_A+L_s-L_t-L_u-1)+(L_t+L_u)^2\Bigg]\\
&+L_s^2\left(-\frac{2s^2}{tu}-A_{q\bar{q}}\right)+L_s\left(\frac{8s}{t+u}+\frac{4s^2}{(t+u)^2}\right)\\
&+\left(2A_{q\bar{q}}+\frac{4s^2}{tu}\right)\left(L_s\ln\Big(\frac{s-Q^2}{Q^2}\Big)-\mathrm{Li}_2\Big(\frac{Q^2}{s}\Big)\right)+\zeta(2)\left(\frac{4s^2}{tu}+8A_0\right)\\
&+\Bigg\{L_t\left(\frac{t+4s}{s+u}+\frac{st}{(s+u)^2}\right)+L_sL_t\left(\frac{2(2s+t)}{u}-4A_{q\bar{q}}\right)\\
&+\frac{2(2s^2+2su+u^2)}{tu}\left(L_t\ln\Big(\frac{s+u}{Q^2}\Big)+\mathrm{Li}_2\Big(\frac{t}{Q^2}\Big)\right)\\
&-\frac{9t+17s}{u}-\frac{8s^2}{tu}+\frac{2s}{t+u}+\frac{s}{s+t}\Bigg\}+\Big\{u\leftrightarrow t\Big\}\,,
\end{aligned}
\tag{B.2}
$$

$$
\begin{aligned}
B_1' \;=\;& \left[4A_{q\bar{q}}\left(-\ln\Big(\frac{(s_2-t)(s_2-u)}{s^2}\Big)-L_{\mu_F}+2\ln\Big(\frac{s_2}{Q^2}\Big)-L_s\right)\frac{1}{s_2}\right]_{A+}\\
&+\ln\Big(\frac{tu-Q^2s_2}{(s_2-t)(s_2-u)}\Big)\left(\frac{4s^2(s-Q^2)}{tu(s_2-t)(s_2-u)}+\frac{2(2s+u-t)}{t(s_2-t)}+\frac{2(2s+t-u)}{u(s_2-u)}\right.\\
&\qquad\left.+\frac{4Q^2A_0-2u-2t-2Q^2-6s}{tu-Q^2s_2}+\frac{2(t+u+s+Q^2)}{tu}\right)\\
&+\ln\Big(\frac{(s_2-t)(s_2-u)}{ss_2}\Big)\left(\frac{4s^2(s-Q^2)}{tu(s_2-t)(s_2-u)}+\frac{2(2s+u-t)}{t(s_2-t)}+\frac{2(2s+t-u)}{u(s_2-u)}\right)\\
&+\ln\Big(\frac{\mu_F^2}{s_2}\Big)\left(\frac{s}{(s_2-t)^2}+\frac{s}{(s_2-u)^2}-\frac{2s+u+t}{t(s_2-t)}-\frac{2s+t+u}{u(s_2-u)}+\frac{Q^2}{t^2}+\frac{Q^2}{u^2}\right.\\
&\qquad\left.-\frac{4Q^2A_0-2u-2t-2Q^2-6s}{tu-Q^2s_2}\right)\\
&+\frac{s}{(s_2-t)^2}+\frac{s}{(s_2-u)^2}+\frac{2(u/t+s/t-s/u)}{s_2-t}+\frac{2(t/u+s/u-s/t)}{s_2-u}\\
&+\frac{2(s-Q^2+Q^2u/t+Q^2t/u)}{tu-Q^2s_2}+\frac{2(t+u-s)}{tu}\,,
\end{aligned}
\tag{B.3}
$$

$$
\begin{aligned}
B_1'' \;=\; & \frac{9}{4}\frac{1}{\lambda}L_\lambda\Bigg(\frac{3s(t-u)^2(t+u)(4Q^2s+(t+u)^2)}{2tu\lambda^4} \\
& -\frac{2s(t^3+u^3)+Q^2(-4s(t-u)^2+2s^2(t+u)-(t-u)^2(t+u))}{tu\lambda^2} \\
& +\frac{(t+u)(4s^2+t^2+u^2+2s(t+u))}{s_2tu}+\frac{6(s-Q^2)(t^2+u^2)}{stu}+\frac{2(6s+t+u)}{s+Q^2-s2} \\
& +\frac{(9s-18Q^2+8Q^4/s)(t+u)}{2tu}+\frac{3(t^3+t^2u+tu^2+u^3)}{stu}-\frac{4Q^2}{s}+2\Bigg) \\
& +\frac{9}{8st}L_{\lambda t}\left(\frac{4s^2+t^2+4su+u^2}{s+Q^2-s_2}+2Q^2-4s-t-3u\right) \\
& +\frac{9}{8su}L_{\lambda u}\left(\frac{4s^2+u^2+4st+t^2}{s+Q^2-s_2}+2Q^2-4s-u-3t\right) \\
& +\frac{9}{8t}L_{st}\Bigg(\frac{-2s_2+3t+u}{s}+\frac{2(2s^2+2su+u^2)}{s_2u} \\
& -\frac{2(2s-2s_2+t+2u)}{t}+\frac{4s^2+t^2+4su+u^2}{s(s+Q^2-s_2)}\Bigg) \\
& +\frac{9}{8u}L_{su}\Bigg(\frac{-2s_2+3u+t}{s}+\frac{2(2s^2+2st+t^2)}{s_2t} \\
& -\frac{2(2s-2s_2+u+2t)}{u}+\frac{4s^2+u^2+4st+t^2}{s(s+Q^2-s_2)}\Bigg) \\
& +\frac{27(t-u)^2(t+u)(-2Q^2(2s+t+u)+(t+u)(4s+t+u))}{8tu\lambda^4} \\
& -\frac{9(t^3+t^2u+tu^2+u^3-Q^2(t+u)(2s+t+u)+s(6t^2-4tu+6u^2))}{4tu\lambda^2} \\
& +\frac{9s^2}{4u(s_2-t)^2}+\frac{9s^2}{4t(s_2-u)^2}+\frac{9}{4}\left(2+\frac{3s^2}{tu}\right)\left(\frac{1}{s_2-t}+\frac{1}{s_2-u}\right) \\
& +\frac{9}{4s}\left(\frac{1}{t^2}+\frac{1}{u^2}\right)\Big(4Q^4+2tu-Q^2(7s+4(t+u))\Big)+\frac{9(3s(t+u)-4tu)}{8stu}\,. \qquad \text{(B.4)}
\end{aligned}
$$

In the above formulae we introduced the following notations for logarithms:

$$
\begin{aligned}
L_s &= \ln\Big(\frac{s}{Q^2}\Big), \\
L_t &= \ln\Big(\frac{-t}{Q^2}\Big), \\
L_u &= \ln\Big(\frac{-u}{Q^2}\Big), \\
L_A &= \ln\Big(\frac{A}{Q^2}\Big), \\
L_{\mu_F} &= \ln\Big(\frac{\mu_F^2}{Q^2}\Big), \\
L_{st} &= \ln\Big(\frac{st^2}{Q^2(s_2-t)}\Big), \\
L_{su} &= \ln\Big(\frac{su^2}{Q^2(s_2-u)}\Big), \\
L_{tu} &= \ln\Big(\frac{tu-s_2Q^2}{(s_2-t)(s_2-u)}\Big), \\
L_{\lambda} &= \ln\Big(\frac{s+Q^2-s_2+\lambda}{s+Q^2-s_2-\lambda}\Big), \\
L_{\lambda t} &= \ln\Big(\frac{sQ^2(s_2-t)^2}{(s_2(2Q^2-u)-Q^2t)^2}\Big), \\
L_{\lambda u} &= \ln\Big(\frac{sQ^2(s_2-u)^2}{(s_2(2Q^2-t)-Q^2u)^2}\Big).
\end{aligned}
\tag{B.5}
$$

Partonic cross-section $qg \longrightarrow Z + X$

For the partonic subprocess $qg \longrightarrow Z+X$ we can present the follow result of calculation of QED contributions:

$$
\frac{s\,d\sigma^{qg}}{dt\,du} = \frac{2\pi\alpha\alpha_s Q_q^2(v_q^2+a_q^2)C_F}{N_A}\frac{1}{s}\left\{\delta(s_2)A_{qg}(s,t,u) + \frac{\alpha}{\pi}\left(\delta(s_2)C_1 + C_1'\right)\right\} \tag{B.6}
$$

where $A_{qg}(s,t,u)$ is the Born contribution (diagrams a_3 and a_4 in Fig. 3.1) (4.2):

$$
A_{qg}(s,t,u) = -A_{q\bar{q}}(u,t,s) = -\frac{s}{t} - \frac{t}{s} - \frac{2Q^2u}{st},
$$

The NLO QED corrections, coming from crossed diagrams in the Figs. (3.4,3.2) are given by

$$
\begin{aligned}
C_1 &= A_{qg}\left[L_{\mu_F}(L_u - L_A - \frac{3}{4}) + \frac{1}{2}L_A^2 - \frac{3}{4}L_A\right] \\
&+\frac{(t+u)^2+u^2}{2st}\left(2\mathrm{Li}_2\Big(\frac{Q^2}{s}\Big) + L_s^2 + 2L_sL_u - 2L_s\ln\Big(\frac{s-Q^2}{Q^2}\Big)\right) \\
&-\frac{(s+u)^2+u^2}{st}\left(\mathrm{Li}_2\Big(\frac{t}{Q^2}\Big) - L_tL_u + L_t\ln\Big(\frac{s+u}{Q^2}\Big)\right) \\
&-\frac{(s+u)^2+(t+u)^2+2u^2}{st}\left(\mathrm{Li}_2\Big(\frac{u}{Q^2}\Big) + L_u\ln\Big(\frac{s+t}{Q^2}\Big)\right) \\
&+\frac{(s+u)^2+(t+u)^2}{2st}L_u^2 - \frac{2u(2s+2t+u)}{(s+t)^2}L_u + \left(-\frac{2u+t}{s+u} + \frac{st}{2(s+u)^2}\right)L_t \\
&-\left(\frac{s+4u}{2(t+u)} + \frac{su}{2(t+u)^2}\right)L_s - \frac{2(2s^2+4su+5u^2}{st}\zeta(2) - \frac{u}{2(t+u)} \\
&-\frac{2u}{s+t} + \frac{s}{2(s+u)} + \frac{11(s^2+t^2) - 2st + 20(su+tu) + 18u^2}{4st}\,. \qquad \text{(B.7)}
\end{aligned}
$$

The next contribution C_1' is quite big, we rewrite it in terms, proportional to logarithms:

$$
\begin{aligned}
C_1' &= \frac{L_\lambda}{\lambda}F_\lambda(s,t,u) + L_{su}F_{su}(s,t,u) + F_{A+}(s,t,u) \\
&+L_{tu}F_{tu}(s,t,u) + L_{\lambda t}F_{\lambda t}(s,t,u) - \ln\Big(\frac{\mu_F^2}{s_2}\Big)F_\mu(s,t,u) + F(s,t,u),
\end{aligned}
$$

where logarithm notations L_i was done in Eq. (B.5) and functions by logarithms $F_a(s,t,u)$ of Mandelstam variables are here:

$$
\begin{aligned}
F_\lambda(s,t,u) &= \frac{3s(t-u)^2(t+u)(-2Q^2+t+u)}{8t\lambda^4} \\
&+\frac{1}{\lambda^2}\left(\frac{(t-u)^2(t+u) - s(t^2+u^2)}{4t} + \frac{(t-u)(t+u)^2}{8s}\right. \\
&\left.+\frac{Q^2(-t^3+s^2(3t-u)+tu^2-2s(3t^2-4tu+u^2))}{4st}\right) \\
&+\frac{64Q^4+7s^2+7t^2+21tu+16u^2+2s(t+u)-2Q^2(30s+15t+16u)}{8st} \\
F_{tu}(s,t,u) &= \frac{1}{2s} - \frac{1}{2t} + \frac{Q^2}{st} + \frac{Q^2(Q^2-t-s)}{2su^2} \\
&-\frac{1}{u} + \frac{Q^2}{su} - \frac{t}{2su} + \frac{u}{st} - \frac{2Q^4-2Q^2(s+t)+(s+t)^2}{2st(Q^2-u)}
\end{aligned}
$$

$$
\begin{aligned}
F_{su}(s,t,u) &= +\Bigg(Q^2+t-\frac{2Q^2}{st}\Big((s-u)^2+(t-u)^2\Big) \\
&\quad +\frac{t^2+(t-2u)^2}{s}\Bigg)\frac{1}{tu-s_2Q^2}+\frac{2Q^2(u-s_2)+(s+t)^2}{st(Q^2-u)}+\frac{-2Q^2+3t-2u}{st} \\
F_{\lambda t}(s,t,u) &= \frac{2Q^2(u-s_2)+(s+t)^2}{2st(Q^2-u)}-\frac{s_2-2Q^2}{st} \\
F_{A+}(s,t,u) &= -\left[\frac{(s+u)^2+(t+u)^2}{sts_2}\ln\Big(\frac{s_2}{Q^2}\Big)\right]_{A+}+\frac{3(s^2+t^2+2su+2tu+2u^2)}{4st(s_2)_{A+}} \\
&\quad +L_{\mu_F}\frac{s^2+t^2+2su+2tu+2u^2}{st(s_2)_{A+}}-\frac{t^3+3t^2u+4tu^2+2u^3}{2st(s_2)_{A+}}\frac{L_\lambda}{\lambda} \\
&\quad -\frac{t^2+2tu+2u^2}{2st(s_2)_{A+}}L_{tu}-\frac{s^2+2su+2u^2}{st(s_2)_{A+}}L_{su} \\
F_{\mu}(s,t,u) &= \Bigg(-\frac{st}{(s_2-t)^3}+\frac{u+t}{(s_2-t)^2} \\
&\quad -\frac{3s^2-4st+2t^2+6su-4tu+4u^2}{2st(s_2-t)}-\frac{1}{s_2-u}+\frac{Q^2(u-s_2)}{2u^2s} \\
&\quad +\frac{t((s+t)^2+su+(t-4u)^2)-Q^2(2(s^2+t^2)+st+4(su-tu+u^2))}{st(tu-s_2Q^2)} \\
&\quad +\frac{5}{2s}-\frac{Q^2}{2t^2}+\frac{3}{2t}-\frac{1}{u}+\frac{Q^2}{su}-\frac{t}{2su}\Bigg) \\
F(s,t,u) &= \frac{3s(t-u)^2(t+u)}{4t\lambda^4} \\
&\quad +\frac{-2t^3-4Q^2(s-2t)(t-u)+2tu^2-2s^2(t+u)+s(7t^2-10tu+3u^2)}{8st\lambda^2} \\
&\quad +\frac{t(s^2+su+4(t-u)u)-Q^2(s(t-4u)+4u(t-u))}{2st(tu-s_2Q^2)}+\frac{4st}{(s_2-t)^3} \\
&\quad -\frac{4u+8t-3s}{2(s_2-t)^2}+\frac{-s^2-4st+3t^2+2su-2tu+u^2}{2st(s_2-t)}-\frac{s}{t(s_2-u)} \\
&\quad -\frac{3}{2s}-\frac{Q^2}{4t^2}+\frac{3}{8t}-\frac{Q^2(u-s_2)}{2u^2s}-\frac{1}{u}+\frac{Q^2}{su}-\frac{t}{su}\,.
\end{aligned}
$$

The "+" description is defined in this way:

$$\int\limits_0^{s_{2,\max}} ds_2 \frac{f(s_2)}{(s_2)_+} = \int\limits_0^{s_{2,\max}} \frac{ds_2}{s_2}[f(s_2)-f(0)],$$

$$\int\limits_0^{s_{2,\max}} ds_2 \frac{\ln(s_2)}{(s_2)_+} f(s_2) = \int\limits_0^{s_{2,\max}} \frac{ds_2}{s_2}[f(s_2)-f(0)]\ln(s_2)$$

Partonic cross-section $qq \longrightarrow Z + X$

Let us present the mixed QED/QCD contribution to the process $qq \longrightarrow Z+q+q$. This contributions are due to the interference of the diagrams, which shown in the Fig. (3.1) with the gluon exchange and the same diagrams but with the photon exchange. As discussed in the text, this contribution does not follows from the QCD calculation because of the zero color trace effect. We have follow differential partonic cross section:

$$\frac{s\, d\sigma^{qq}}{dt\, du} = \frac{2\pi\alpha_s\alpha^2 Q_q^2(v_q^2+a_q^2)C_F}{N_c} C_1', \tag{B.8}$$

where function C_1' is here:

$$\begin{aligned}
C_1' &= +\ln\Big(\frac{(s_2-t)(s_2-u)}{ss_2}\Big)\frac{9(2Q^4+2s^2+2s(t+u)+(t+u)^2-2Q^2(2s+t+u))}{4stu} \\
&+\frac{9(2s_2Q^2(t^2+u^2)-tu(t+u)^2)}{4st^2u^2} \\
&+\Bigg\{ L_{\lambda t}\frac{9(2s^2+(t+u-2s_2)(s+Q^2-s_2))}{8(s+Q^2-s_2)(s_2-t)t} \\
&+\frac{9}{4}L_{st}\Bigg(\frac{u-t}{2t(s_2-t)}+\frac{1}{s}+\frac{s-s_2+u}{t^2}+\frac{s_2^2}{stu}+\frac{t-2s_2}{2su}+\frac{u-2s_2}{2st} \\
&\quad +\frac{s^2}{t(s_2-t)(s+Q^2-s_2)}\Bigg)\Bigg\} + \Big\{ u \leftrightarrow t \Big\},
\end{aligned} \tag{B.9}$$

and logarithm notations L_i was done in Eq. (B.5).

Appendix C

Analytical result for EW corrections

In this Appendix we presented the analytical formula for EW correction to Z boson production. This result coincide with calculations in paper [17].

For subprocess $q + \bar{q} \to Zg$ the result can be given as in the below formula.

$$\frac{\mathrm{d}\sigma_{\bar{q}q}}{\mathrm{d}t\mathrm{d}u} = \tag{C.1}$$
$$\alpha_S \alpha K q q \left[\frac{K_1}{2s_{12}} A_{qq}(s,t,u) + \alpha_S \left(K_1 F_{K_1} + K_2 F_{K_2} + K_3 F_{K_3} + K_2 K_3 F_{K_2 K_3} + F_{rest} \right) \right],$$

where colour factors are here:

$$K_1 = \frac{4s^2}{9c^2} + \left(\frac{c}{2s} - \frac{s}{6c} \right)^2, \quad K_2 = \frac{16s^4}{81c^4} + \left(\frac{c}{2s} - \frac{s}{6c} \right)^2, \quad K_3 = \frac{3c^2 - s^2}{12s^4}, \tag{C.2}$$

$$F_{K_1} = \tag{C.3}$$
$$+ \ln(M_R^2) \frac{N_C}{m_Z^2 - 4m_t^2} \frac{-(m_t^2(8m_W^2 - 5Q^2)^2(2Q^2 s_{12} + t^2 + u^2))}{288 m_W^2 (m_W^2 - Q^2) tu}$$
$$+ \ln\left(\frac{M_R^2 m_Z^2}{m_H^2} \right) \frac{Q^6 (2Q^2 s_{12} + t^2 + u^2)}{8 m_W^2 (m_W^2 - Q^2)(m_H^2 - 4m_Z^2) tu}$$
$$+ \left(\ln(4\mu_R^2 \pi) \frac{7}{4} - \ln(4\mu_R^2 \pi) n_G \frac{1}{3} - \ln(4\mu_R^2 \pi) n_G N_C \frac{5}{27} \right) \frac{(2Q^2 s_{12} + t^2 + u^2)}{2tu}$$
$$+ N_C \left(B_0(m_Z^2, m_t^2, m_t^2, 1) + 1 \right) (2Q^2 s_{12} + t^2 + u^2) \frac{m_t^2 (8m_W^2 - 5Q^2)^2}{144 m_W^2 (m_W^2 - Q^2)(m_Z^2 - 4m_t^2) tu}$$
$$+ n_G (2Q^2 s_{12} + t^2 + u^2) \frac{72 m_W^2 (m_W^2 - m_Z^2)(32m_W^4 - 38m_W^2 m_Z^2 + 9m_Z^4) tu}{m_Z^8}$$
$$+ n_G N_C (2Q^2 s_{12} + t^2 + u^2) \frac{648 m_W^2 (m_W^2 - m_Z^2)(160m_W^4 - 166m_W^2 m_Z^2 + 33m_Z^4) tu}{m_Z^8}$$

$$F_{K_1K_2} = \tag{C.4}$$
$$+\frac{\zeta_2}{m_Z^2-t}\frac{3(m_W^2-Q^2)^2(2Q^4-2Q^2u+u^2)}{2(4m_W^2-Q^2)Q^2u}+\left\{u<->t\right\}$$

$$\begin{aligned}
F_{K_2} = \quad & +C_1(s_{12},m_Z^2)\frac{s_{12}(t^2+4tu+u^2-4Q^2(t+u))}{4tu} \qquad \text{(C.5)}\\
& +C_2(u,Q^2,m_Z^2)\frac{1}{(m_Z^2-u)^3}\frac{3Q^4s_{12}u}{2}\\
& +C_2(u,Q^2,m_Z^2)\frac{1}{(m_Z^2-u)^2}\frac{Q^2(4Q^4-2u(t+u)-Q^2(4t+3u)}{2}\\
& +C_2(u,Q^2,m_Z^2)\frac{1}{m_Z^2-u}\frac{Q^2s_{12}(Q^2+4u)}{2u}\\
& +C_2(u,Q^2,m_Z^2)\frac{-8Q^6+2Q^4(5t+8u)-5Q^2(t^2+2tu+2u^2)+u(t^2+2tu+2u^2)}{4tu}\\
& +C_2(t,Q^2,m_Z^2)\frac{1}{(m_Z^2-t)^3}\frac{3Q^4ts_{12}}{2}\\
& +C_2(t,Q^2,m_Z^2)\frac{1}{m_Z^2-t)^2}\frac{Q^2(4Q^4-2t(t+u)-Q^2(3t+4u)}{2}\\
& +C_2(t,Q^2,m_Z^2)\frac{1}{m_Z^2-t}\frac{Q^2(Q^2+4t)s_{12}}{2t}\\
& +C_2(t,Q^2,m_Z^2)\frac{-8Q^6+2Q^4(8t+5u)-5Q^2(2t^2+2tu+u^2)+t(2t^2+2tu+u^2)}{4tu}\\
& +B_0(u,m_Z^2,0,\epsilon)\frac{1}{m_Z^2-u}\frac{(2Q^2-(2Q^4)/t-t)}{4}+B_0(u,m_Z^2,0,\epsilon)\frac{-3Q^2+t+u}{2t}\\
& +B_0(t,m_Z^2,0,\epsilon)\frac{1}{m_Z^2-t}\frac{2Q^2-(2Q^4)/u-u}{4}+B_0(t,m_Z^2,0,\epsilon)\frac{-3Q^2+t+u}{2u}\\
& +\left\{\frac{D_1(s_{12},u,Q^2,m_Z^2)}{4tu}\Big(-8Q^6(t+2u)+4Q^4(t^2+6tu+6u^2)\right.\\
& \qquad \left.+u(t^3+3t^2u+4tu^2+2u^3)-Q^2(t^3+8t^2u+18tu^2+12u^3)\Big)\right.\\
& +\ln(m_Z^2-u)\frac{1}{(m_Z^2-u)^3}\frac{-3Q^2(Q^2-u)s_{12}}{2}\\
& +\ln(m_Z^2-u)\frac{1}{(m_Z^2-u)^2}\frac{-(Q^2-u)(5Q^4-u(t+u)-Q^2(5t+6u))}{4u}\\
& +\ln(m_Z^2-u)\frac{1}{m_Z^2-u}\frac{-(5Q^2-4t-3u)(Q^2-u)}{4u}\\
& \left.+\ln(m_Z^2-u)\frac{Q^6t-4Q^2u^2(t+2u)+Q^4u(-t+8u)+u^2(t^2+2tu+2u^2)}{2tu^3}\right\}+\left\{t<->u\right\}
\end{aligned}$$

$$
\begin{aligned}
F_{K_3} = {} & \frac{u}{(m_Z^2-u)^3}(-3m_W^2 t s_{12}) \qquad \text{(C.6)}\\
& + \frac{1}{6m_W^2 t(m_W^2-u)}\left(1+\frac{\zeta_2}{8}\right)\big(-Q^2(2Q^4-2Q^2t+t^2)\\
& \quad +2m_W^2(2Q^4-2t^2+Q^2(t-9u)+6tu-3u^2)\big)\\
& + \frac{C_1(s_{12},m_W^2)}{12m_W^2 tu}\big(s_{12}(4m_W^4(t+u)+Q^2(-t^2-4tu-u^2+2Q^2(t+u))\\
& \quad +m_W^2(6Q^2(t+u)-2(t^2+4tu+u^2))))\big)\\
& + C_2(u,Q^2,m_W^2)\frac{1}{m_Z^2-u}\frac{-(2m_W^2+Q^2)s_{12}(m_W^2+4u)}{12u}\\
& + C_2(u,Q^2,m_W^2)\frac{1}{(m_Z^2-u)^2}\frac{-(2m_W^2+Q^2)(m_W^2(4Q^2-4t-5u)+2s_{12}u)}{12}\\
& + C_2(u,Q^2,m_W^2)\frac{1}{(m_Z^2-u)^3}\frac{-m_W^2(2m_W^2+Q^2)s_{12}u}{4}\\
& + \frac{C_2(u,Q^2,m_W^2)}{24m_W^2 tu}\big((2m_W^2+Q^2)(2m_W^4 s_{12}+m_W^2(4Q^4-6Q^2t+4t^2-8Q^2u+6tu+4u^2)\\
& \quad +(Q^2-u)(2Q^2(s_{12}-u)+t^2+2tu+2u^2))\big)\\
& + C_3(u,Q^2,m_W^2,m_W^2)\frac{u}{(m_Z^2-u)^3}\frac{-3m_W^2 s_{12}}{2}\\
& + C_3(u,Q^2,m_W^2,m_W^2)\frac{1}{(m_Z^2-u)^2}\frac{-m_W^2(m_W^2(4Q^2-4t-5u)-2us_{12})}{2}\\
& + \frac{C_3(u,Q^2,m_W^2,m_W^2)}{4tu}\big(2m_W^4 s_{12}+Q^4(t-u)-u(t^2+u^2)+Q^2(-t^2+tu+2u^2)\\
& \quad +2m_W^2(2Q^2 s_{12}+2t^2+tu+u^2-Q^2(t+u))\big)\\
& + C_3(u,Q^2,m_W^2,m_W^2)\frac{1}{m_Z^2-u}\frac{m_W^2(-2u^2+m_W^2 s_{12})}{2u}\\
& + B_0(u,m_W^2,0,\epsilon)\frac{1}{m_W^2-u}\frac{Q^2(2Q^4-2Q^2t+t^2)+2m_W^2(2Q^4-2t^2+Q^2(t-9u)+6tu-3u^2)}{24m_W^2 t}\\
& + B_0(u,m_W^2,0,\epsilon)\frac{-(m_W^4+Q^2(Q^2-s_{12})+m_W^2(7Q^2-4t+2u))}{12m_W^2 t}\\
& + B_0(m_Z^2,m_H^2,m_Z^2,1)\frac{1}{m_H^2-4m_Z^2}\frac{(32m_W^4-40m_W^2Q^2+17Q^4)(2Q^2s_{12}+t^2+u^2)}{12c^4(4m_W^2-Q^2)tu}\\
& + B_0(m_Z^2,m_W^2,m_W^2,1)\frac{u}{(m_Z^2-u)^3}\frac{3m_W^2 s_{12}}{2}\\
& + B_0(m_Z^2,m_W^2,m_W^2,1)\frac{1}{(m_Z^2-u)^2}\frac{2m_W^2(4Q^2-4t-5u)-us_{12}}{4}\\
& + B_0(m_Z^2,m_W^2,m_W^2,1)\frac{1}{m_Z^2-u}\frac{2m_W^2 s_{12}+u(2Q^2-2t+u)}{4u}
\end{aligned}
$$

$$
\begin{aligned}
&+\frac{D_1(s_{12},u,Q^2,m_W^2)}{24m_W^2tu}\Big((2m_W^2+Q^2)(2m_W^6(t+u)+m_W^4(Q^2(4t+6u)-2(t^2+4tu+3u^2))\\
&\quad+m_W^2(t^3+5t^2u+10tu^2+6u^3+2Q^4(t+3u)-2Q^2(t^2+6tu+6u^2))\\
&\quad-u(-2Q^6+t^3+3t^2u+4tu^2+2u^3+Q^4(4t+6u)-Q^2(3t^2+8tu+6u^2)))\Big)\\
&+\frac{D_3(s_{12},t,Q^2,m_W^2,m_W^2)}{2tu}\Big(2m_W^6(t+u)-tu(t^2+u^2-Q^2(t+u))\\
&\quad+2m_W^4(-t^2-3tu-u^2+2Q^2(t+u))+m_W^2((t+u)^3-Q^2(t^2+6tu+u^2))\Big)\\
&+\ln(m_W^2)\frac{1}{m_W^2-u}\frac{Q^2(2Q^4-2Q^2t+t^2)+2m_W^2(2Q^4-2t^2+Q^2(t-9u)+6tu-3u^2)}{12m_W^2t}\\
&+\ln(m_W^2)\frac{1}{(m_Z^2-u)^3}\frac{m_W^2(4m_W^2-Q^2)s_{12}}{4}\\
&+\ln(m_W^2)\frac{1}{(m_Z^2-u)^2}\frac{4m_W^4(5Q^2-5t-7u)-4Q^2us_{12}+m_W^2(-5Q^4-4u(t+u)+Q^2(5t+11u))}{24u}\\
&+\ln(m_W^2)\frac{1}{m_Z^2-u}\frac{m_W^4+m_W^2(11Q^2-12t)-6Q^2s_{12}}{24u}\\
&+\ln(m_W^2)^2\frac{1}{m_W^2-u}\frac{-(Q^2(2Q^4-2Q^2t+t^2)+2m_W^2(2Q^4-2t^2+Q^2(t-9u)+6tu-3u^2))}{48m_W^2t}\\
&+\ln(m_W^2)^2\frac{4m_W^4(t+u)-Q^2(Q^2-s_{12})(t+u)+m_W^2(7Q^2(t+u)+2(t^2-4tu+u^2))}{12m_W^2tu}\\
&+\ln(m_W^2)\ln(M_R^2)\frac{1}{m_W^2-u}\frac{Q^2(2Q^4-2Q^2t+t^2)+2m_W^2(2Q^4-2t^2+Q^2(t-9u)+6tu-3u^2)}{24m_W^2t}\\
&+\ln(m_W^2)\ln(M_R^2)\frac{-4m_W^4(t+u)+Q^2(Q^2-s_{12})(t+u)-m_W^2(7Q^2(t+u)+2(t^2-4tu+u^2))}{6m_W^2tu}\\
&+\ln(m_W^2-u)\frac{1}{(m_Z^2-u)^3}\frac{-(4m_W^2-Q^2)(m_W^2-u)s_{12}}{4}\\
&+\ln(m_W^2-u)\frac{m_W^2-u}{(m_Z^2-u)^2}\frac{-4m_W^4(5Q^2-5t-7u)+Q^2s_{12}u+m_W^2(5Q^4+Q^2(-5t+u)-8u(t+u))}{24m_W^2u}\\
&+\ln(m_W^2-u)\frac{1}{m_Z^2-u}\frac{-(m_W^2-u)(4m_W^4+Q^2(-4Q^2+4t+3u)+m_W^2(3Q^2-4t+12u))}{24m_W^2u}\\
&+\frac{\ln(m_W^2-u)}{12m_W^2tu^3}\Big((4m_W^2-Q^2)(m_W^4Q^2t-m_W^2Q^2tu)+(8m_W^6+2m_W^4(7Q^2-4t)+4m_W^2(t^2-2Q^4)\\
&\quad-Q^2(2Q^4-2Q^2t+t^2))u^2-2(2m_W^2+Q^2)(m_W^2-2Q^2+t)u^3+2(m_W^2-Q^2)u^4\Big)
\end{aligned}
$$

$$
\begin{aligned}
&+\ln(M_R^2)\frac{1}{m_W^2-u}\frac{-(Q^2(2Q^4-2Q^2t+t^2)+2m_W^2(2Q^4-2t^2+Q^2(t-9u)+6tu-3u^2))}{2m_W^2t}\\
&+\ln(M_R^2)\frac{1}{(m_Z^2-u)^3}\frac{-3m_W^2s_{12}u}{2}\\
&+\ln(M_R^2)\frac{1}{(m_Z^2-u)^2}\frac{s_{12}u+m_W^2(-8Q^2+8t+10u)}{4}\\
&+\ln(M_R^2)^2\frac{1}{m_W^2-u}\frac{-(Q^2(2Q^4-2Q^2t+t^2)+2m_W^2(2Q^4-2t^2+Q^2(t-9u)+6tu-3u^2))}{48m_W^2t}\\
&+\left\{t<->u\right\}
\end{aligned}
$$

$$
\begin{aligned}
F_{rest} \quad = &\left[\frac{\ln(m_H^2)}{(m_Z^2-s_{12})^2}\Big(\frac{-m_H^4(t+u)}{Q^2}+\frac{m_H^4s_{12}}{Q^4}+\ln(m_H^2)\frac{m_H^4(2Q^2s_{12}+(t+u)^2)}{2Q^4tu}\Big)\right.\\
&\left.+\Big(\frac{m_H^4(t+u)}{Q^2(m_Z^2-s_{12})^2}-\frac{m_H^4s_{12}}{Q^4(m_Z^2-s_{12})}-\frac{m_H^4(2Q^2s_{12}+(t+u)^2)}{2Q^4tu}\Big)\Big(1+\ln(M_R^2)\Big)\right]\\
&\times\frac{-17+68c^2-88c^4+64c^6}{1728c^6s^2}\\
&+\left[\frac{N_C}{m_Z^2-s_{12}}\frac{m_t^4s_{12}}{Q^2m_W^2}-\frac{N_C}{(m_Z^2-s_{12})^2}\frac{m_t^4(t+u)}{m_W^2}+\frac{N_C}{2tu}\frac{m_t^4(2Q^2s_{12}+(t+u)^2)}{Q^2m_W^2}\right.\\
&+B_0(m_W^2,m_H^2,m_W^2,1)\Big(-\frac{m_H^4(t+u)}{2(m_Z^2-s_{12})^2m_W^2}\\
&\quad+\frac{m_H^2(m_H^2s_{12}+4m_W^2(t+u))}{2(m_Z^2-s_{12})Q^2m_W^2}+\frac{3m_W^4(-2ut)}{Q^2m_W^2tu}\Big)\\
&+\frac{(m_H^2(m_H^2-4m_W^2)+12m_W^4)(2Q^2s_{12}+(t+u)^2)}{4Q^2m_W^2tu}\\
&+\frac{(m_W^2m_t^2+m_t^4-2m_W^4)(2Q^2s_{12}+(t+u)^2)}{2Q^2m_W^2tu}\\
&+B_0(m_W^2,0,m_t^2,1)N_C\Big(-\frac{-2tu}{2Q^2m_W^2tu}+\frac{m_t^4(t+u)}{m_W^2}+\frac{m_t^2(m_W^2(t+u)-m_t^2s_{12})}{Q^2m_W^2(m_Z^2-s_{12})}\Big)\\
&+\ln(m_W^2)\frac{m_H^2(t+u)}{2Q^2(m_Z^2-s_{12})}-\ln(m_t^2)N_C\frac{m_t^4s_{12}}{Q^2m_W^2(m_Z^2-s_{12})}\\
&-\ln(m_t^2)N_C\frac{m_t^4}{2tuQ^2m_W^2}+\ln(M_R^2)N_C\frac{m_t^4s_{12}}{Q^2m_W^2(m_Z^2-s_{12})}\\
&\left.-\ln(M_R^2)N_C\frac{m_t^4(2Q^2s_{12}+(t+u)^2)}{2Q^2m_W^2tu}\right]\frac{17-34c^2+8c^4}{864c^4s^3}
\end{aligned}
$$

$$
\begin{aligned}
&+\left[\frac{2Q^2s_{12}+t^2+u^2}{tu}\Big(\ln(m_W^2)N_C-\ln(m_W^2)n_G-\ln(m_W^2)n_GN_C\Big)\right.\\
&\quad\left.+\ln\left(\frac{m_t^2}{M_R^2}\right)\frac{N_C}{(m_Z^2-s_{12})^2}\frac{m_t^4(t+u)}{Q^2}\right]\frac{17-34c^2+8c^4}{864c^2s^3}\\
&+\frac{4}{t^2}\frac{800c^8-1424c^6+1650c^4-1040c^2+257}{10368c^4s^2}\\
&+\frac{1}{tu}\frac{-2176c^{10}+21472c^8-31332c^6+18082c^4-3235c^2+51}{10368c^6s^2}\\
&+\frac{2}{tQ^2}\frac{16384c^{10}-45328c^8+63552c^6-39652c^4+8632c^2-51}{10368c^6s^2}\\
&+\frac{u}{tQ^4}\frac{-10624c^{10}+39424c^8-50268c^6+30274c^4-6319c^2+51}{10368c^6s^2}\\
&+\left[B_0(m_Z^2,m_H^2,m_Z^2,1)\Big(-\frac{m_H^4(2Q^2s_{12}+(t+u)^2)}{2Q^4tu}-\frac{m_H^4s_{12}}{Q^4(m_Z^2-s_{12})}\right.\\
&\quad\left.-\frac{s^3m_H^4(t+u)}{Q^2(m_Z^2-s_{12})^2}\Big)+\ln(m_Z^2)\frac{s^3m_H^2(t+u)}{(m_Z^2-s_{12})Q^2}\right]\frac{-51+148c^2-152c^4+64c^6}{1728c^4s^6}\\
&+B_0(m_Z^2,m_H^2,m_Z^2,1)\left(\frac{-m_H^2Q^2(t+u)}{Q^4(m_Z^2-s_{12})}+\frac{m_H^2(2Q^2s_{12}+(t+u)^2)}{2Q^2tu}\right)\frac{-153+421c^2-392c^4+160c^6}{1728c^4s^6}\\
&+B_0(m_Z^2,m_H^2,m_Z^2,1)\frac{(2Q^2s_{12}+t^2+u^2)}{tu}\frac{12(-34+91c^2-80c^4+32c^6)}{-3456c^4s^6}\\
&+B_0(m_Z^2,m_W^2,m_W^2,1)\left(\frac{2Q^4}{tu}\frac{1280c^{10}-2048c^8-8c^6+2212c^4-1222c^2+83}{1152c^2s^6}\right.\\
&\quad-\frac{2Q^2(t+u)}{tu}\frac{1280c^{10}-2144c^8+112c^6+2188c^4-1222c^2+83}{1152c^2s^6}\\
&\quad\left.+\frac{t^2+u^2}{tu}\frac{1280c^{10}-2240c^8+232c^6+2164c^4-1222c^2+83}{1152c^2s^6}\right)\\
&+B_0(m_Z^2,m_t^2,m_t^2,1)\Big(\frac{2N_Cm_t^2(2Q^2s_{12}+(t+u)^2)}{Q^2tu}-N_C\frac{m_t^2(t+u)}{Q^2(m_Z^2-s_{12})}\Big)\\
&\qquad\qquad\times\frac{-357+8155c^2-30520c^4+47136c^6-34816c^8+10240c^{10}}{15552c^4s^3}\\
&+\left(B_0(m_Z^2,m_t^2,m_t^2,1)N_C\big(1+\ln(m_Z^2)\big)\frac{2Q^2s_{12}+t^2+u^2}{tu}\right)\frac{409-2152c^2+4128c^4-3328c^6+1024c^8}{15552c^2s^3}\\
&-B_0(m_W^2,m_Z^2,m_W^2,1)\frac{2Q^2s_{12}+t^2+u^2}{tu}\frac{-17-238c^2+1692c^4-1624c^6-1088c^8+384c^{10}}{3456c^6s^3}
\end{aligned}
$$

$$
\begin{aligned}
&+\Bigg[\ln(m_Z^2)\Big(\frac{-s_{12}^2}{(m_Z^2-s_{12})^2}+\frac{3t}{4(m_z^2-t)}+\frac{3u}{4(m_z^2-u)}\Big)/2+\frac{s_{12}}{2(m_Z^2-s_{12})}\\
&\quad+\ln(s_{12})\frac{s_{12}^2}{2(m_Z^2-s_{12})^2}+\ln(s_{12})\frac{s_{12}}{m_Z^2-s_{12}}+\ln(m_Z^2)\frac{u(t+u)}{8(m_Z^2-u)^2}+\ln(m_Z^2)\frac{t(t+u)}{8(m_Z^2-t)^2}\\
&\quad+\Big(\ln^2(s_{12})-\ln(s_{12})\ln(M_R^2)\Big)\frac{3t^2+4tu+3u^2}{16tu}\Bigg]\frac{(257-1022c^2+1596c^4-1424c^6+512c^8)}{648c^4s^2}\\
&-\Big(\ln^2(s_{12})-\ln(s_{12})\ln(M_R^2)\Big)\frac{(257-1031c^2+1623c^4-1370c^6+440c^8)Q^2(t+u)}{864c^4s^2tu}\\
&+\Big(\ln(m_Z^2)^2-\ln(m_Z^2)\ln(M_R^2)-\ln^2(s_{12})+\ln(s_{12})\ln(M_R^2)\Big)\\
&\qquad\qquad\times\frac{(-514+2071c^2-3264c^4+2659c^6-862c^8+72c^{10})Q^4}{1296c^4s^2tu}\\
&+\Big[\ln(m_H^2)\frac{1}{m_Z^2-s_{12}}\frac{9m_H^2(t+u)}{Q^2}+\ln(m_H^2)\frac{6(2Q^2s_{12}+t^2+u^2)}{tu}\\
&\quad+\ln(m_H^2)\frac{-3m_H^2(2Q^2s_{12}+(t+u)^2)}{2Q^2tu}+\ln(M_R^2)\frac{-m_H^2}{m_Z^2-s_{12}}\frac{5(t+u)}{Q^2}\\
&\quad+\ln(M_R^2)\frac{5m_H^2(2Q^2s_{12}+(t+u)^2)}{2Q^2tu}-\frac{12}{m_H^2-4m_Z^2}Q^2(2Q^2s_{12}+t^2+u^2)\\
&\quad+\frac{1}{m_Z^2-s_{12}}\frac{-3m_H^2(t+u)}{4Q^2}+2m_H^2\frac{2Q^2s_{12}+(t+u)^2}{Q^2tu}\Big]\frac{(17-40c^2+32c^4)}{1728c^4s^2}\\
&+\ln(m_t^2)\frac{N_C}{m_Z^2-4m_t^2}\frac{m_t^2(2Q^2s_{12}+t^2+u^2)}{tu}\frac{-(5-8c^2)^2(17-40c^2+32c^4)}{10368c^4s^2}\\
&+\ln(m_Z^2)\left(\frac{u}{(m_Z^2-u)^3}+\frac{t}{(m_Z^2-t)^3}\right)\frac{-257+1040c^2-1650c^4+1316c^6-368c^8}{864c^4s^2}\\
&\Bigg\{+\frac{1}{(m_Z^2-u)^2}\Big(\frac{(257-1040c^2+1650c^4-848c^6-1504c^8)Q^4}{1728c^4s^2}+\frac{c^4(1-4c^2)u(t+u)}{24c^4s^2}\\
&\quad+\frac{Q^2(-257+1040c^2-1650c^4+848c^6+1504c^8)t}{1728c^4s^2}\\
&\quad+\frac{Q^2(-257+1040c^2-1722c^4+992c^6+2080c^8)u}{1728c^4s^2}\Big)\\
&+\frac{1}{m_Z^2-u}\Big(\Big(\frac{Q^2t}{u}-\frac{Q^4}{u}\Big)\frac{-257+1040c^2-1650c^4+1208c^6+64c^8}{2592c^4s^2}\\
&\quad+\frac{Q^2(-1285+5209c^2-7935c^4+5248c^6-2128c^8)}{2592c^4s^2}\\
&\quad+\frac{3t(257-1046c^2+1464c^4-512c^6+512c^8)}{5184c^4s^2}\\
&\quad+\frac{(u+7)(-257+1022c^2-1488c^4+992c^6-512c^8)}{5184c^4s^2}\Big)
\end{aligned}
$$

$$
\begin{aligned}
&+\ln(m_Z^2)\frac{1}{(m_Z^2-u)^2}\Big(+\frac{Q^2 4(257-1040c^2+1668c^4-1352c^6+224c^8)t}{5184c^4s^2}\\
&\quad+\frac{Q^2u(1285-5218c^2+8376c^4-6616c^6+1120c^8)}{5184c^4s^2}\\
&\quad-\frac{Q^4(2827-11440c^2+18096c^4-14368c^6+4480c^8)}{5184c^4s^2}\Big)\\
&+\ln(m_Z^2)\frac{1}{m_Z^2-u}\Big(\frac{(2(257-1004c^2+1560c^4-1568c^6+512c^8)t}{5184c^4s^2}\\
&+\frac{Q^4(1285-5200c^2+8124c^4-6328c^6+2848c^8)t}{5184c^4s^2tu}\\
&-\frac{4Q^2(257-1040c^2+1623c^4-1262c^6+584c^8)t}{5184c^4s^2u}\\
&+\frac{4Q^2(257-1022c^2+1587c^4-1406c^6+584c^8)}{5184c^4s^2}\Big)\Big\}+\Big\{t<->u\Big\}\\
&+\ln(m_Z^2)\frac{-s_{12}}{m_Z^2-s_{12}}\frac{-257+1279c^2-2618c^4+3020c^6-1936c^8+512c^{10}}{648c^4s^3}\\
&+\ln(m_Z^2)\Bigg(\frac{1028-5188c^2+10688c^4-11648c^6+7168c^8-2048c^{10}}{10368c^4s^3}\\
&\quad\times\frac{Q^4((Q^4(-1+Q^2/t))/t^2+(Q^4(-1+Q^2/u))/u^2)}{t^2}\\
&\quad+\frac{306-888c^2+912c^4-384c^6}{10368c^4s^3}\Big(\frac{m_H^2Q^2}{tu}-\frac{m_H^2}{t}-\frac{m_H^2}{u}+\frac{m_H^2}{Q^2}\Big)\\
&\quad-\frac{(-102-6474c^2+34626c^4-69456c^6+69336c^8-41712c^{10}+12864c^{12})(Q^2/t+Q^2/u)}{10368c^6s^6}\\
&\quad+\frac{102+16754c^2-86506c^4+176264c^6-185600c^8+113824c^{10}-33920c^{12}}{10368c^6s^3}\frac{Q^4}{tu}\\
&\quad+\frac{(51+1181c^2-6937c^4+13388c^6-11480c^8+6304c^{10}-2048c^{12})(t/u+u/t)}{10368c^6s^3}\\
&\quad+\frac{(153-444c^2+456c^4-192c^6)m_H^4(t/u+u/t)}{10368c^4s^3Q^4}\Bigg)\\
&+\ln(m_Z^2)n_G\frac{2Q^2s_{12}+t^2+u^2}{tu}\frac{-(51-262c^2+508c^4-416c^6+128c^8)}{864c^2s^3}\\
&+\ln(m_Z^2)n_GN_C\frac{2Q^2s_{12}+t^2+u^2}{tu}\frac{-(187-1174c^2+2508c^4-2080c^6+640c^8)}{7776c^2s^3}\\
&+\big(\ln(m_Z^2)^2-\ln(m_Z^2)\ln(M_R^2)\big)\Big(\Big(\frac{t}{u}+\frac{u}{t}\Big)\frac{(-1285+5146c^2-8052c^4+6832c^6-2560c^8)t}{10368c^4s^2u}\\
&\quad-\frac{8(257-1031c^2+1614c^4-1352c^6+512c^8)}{10368c^4s^2}
\end{aligned}
$$

$$
\begin{aligned}
&+\frac{(257-1034c^2+1626c^4-1340c^6+464c^8)Q^2(t+u)}{576c^4s^2tu}\Big)\\
&+\ln(m_Z^2)\ln(M_R^2)\frac{2Q^4-2Q^2u+u^2}{u(m_Z^2-t)}\frac{-512c^8+1280c^6-1632c^4+1040c^2-257}{5184c^4s^4}\\
&+\ln(m_W^2)\Big[-\frac{24(1-4c^2)^2c^2Q^6}{3456s^4t^3}+\frac{Q^6(24(1-4c^2)^2)}{3456s^4t^3}\\
&\quad-\frac{Q^4(-4608c^{12}+8640c^{10}-6696c^8+4152c^6-2354c^4+730c^2-17)}{3456c^4s^6tu}\\
&\quad-\frac{2(3840c^{12}-9024c^{10}+8040c^8-4212c^6+2198c^4-706c^2+17)Q^2}{3456c^4s^6t}\\
&\quad-\frac{-3840c^{12}u+9408c^{10}u+24c^8(48t-437u)-144c^6(10t-47u)}{3456c^4s^6t}\\
&\qquad\times\frac{c^4(288t-2690u)+706c^2u-17u}{3456c^4s^6t}\Big]\\
&+\ln(m_t^2)\frac{N_C}{m_Z^2-s_{12}}m_t^2\frac{m_W^2(663+8c^2(-1013+4c^2(705-768c^2+320c^4)))(t+u)}{15552c^4s^3Q^4}\\
&+\ln(m_t^2)N_Cm_t^2\frac{(2Q^2s_{12}+(t+u)^2)m_W^2}{tuQ^4}\frac{663-8767c^2+30664c^4-47136c^6+34816c^8-10240c^{10}}{31104c^6s^3}\\
&\Big\{+\ln(M_R^2)\frac{1}{m_Z^2-t}\Big(\frac{-2Q^2u((257-1040c^2+1578c^4-1010c^6+296c^8)t}{2592c^4s^2tu}\\
&\quad-\frac{2Q^2u54c^6(1-4c^2)}{2592c^4s^2t}+\frac{2Q^454c^6(1-4c^2)}{2592c^4s^2t}\\
&\quad+\frac{257u-1040c^2u+512c^8u-8c^6(27t+106u)+6c^4(9t+254u)}{2592c^4s^2}\Big)\Big\}+\Big\{t<->u\Big\}\\
&+\ln(M_R^2)\left(\frac{N_C}{m_Z^2-s_{12}}\frac{m_t^2(t+u)}{Q^2}+N_C\frac{m_t^2(2Q^2s_{12}+(t+u)^2)}{2Q^2tu}\right)\\
&\qquad\times\frac{-663+8767c^2-30664c^4+47136c^6-34816c^8+10240c^{10})}{15552c^4s^3}\\
&+\ln(M_R^2)\Big[\frac{(17-153c^2-798c^4+3124c^6-1944c^8-2304c^{10}+3840c^{12})Q^4}{1728c^6s^2tu}\\
&\quad+\left(\frac{t}{u}+\frac{u}{t}\right)\frac{(51-2515c^2+5782c^4-3396c^6+5992c^8-12736c^{10}+11520c^{12})}{10368c^6s^2}\\
&\quad-\frac{(257-1022c^2+1488c^4-992c^6+512c^8)}{648c^4s^2}\\
&\quad-\frac{(17-1181c^2+3314c^4-3044c^6+2672c^8-5024c^{10}+3840c^{12})Q^2(t+u)}{1728c^6s^2tu}\Big]\\
&+N_C(1+\ln(M_R^2)/2)\frac{2Q^2s_{12}+t^2+u^2}{tu}\frac{-(715-2764c^2+4272c^4-3328c^6+1024c^8)}{7776c^2s^3}
\end{aligned}
$$

$$
\begin{aligned}
&+\Bigg[\ln(M_R^2)^2\frac{1}{m_Z^2-u}\frac{2Q^4-2Q^2t+t^2}{t}+\ln(M_R^2)^2\frac{1}{m_Z^2-t}\frac{2Q^4-2Q^2u+u^2}{u}\\
&\quad+\ln(m_Z^2)\frac{12Q^4s_{12}}{(m_Z^2-u)^3}+\ln(m_Z^2)\frac{12Q^4s_{12}}{(m_Z^2-t)^3}\\
&\quad+\frac{1}{(m_Z^2-u)}\frac{Q^4}{t}+\frac{1}{(m_Z^2-t)}\frac{Q^4}{u}\\
&\quad+\ln(m_Z^2)\frac{1}{(m_Z^2-u)^2}\frac{10Q^6}{u}+\ln(m_Z^2)\frac{1}{(m_Z^2-t)^2}\frac{10Q^6}{t}\\
&\quad+\ln(m_Z^2)\frac{1}{(m_Z^2-u)^2}\frac{10Q^4t}{u}+\ln(m_Z^2)\frac{1}{(m_Z^2-t)^2}\frac{10Q^4u}{t}\\
&\quad+\ln(m_Z^2)\frac{1}{m_Z^2-u}\frac{8Q^4}{t}+\ln(m_Z^2)\frac{1}{m_Z^2-t}\frac{8Q^4}{u}+\ln(M_R^2)\frac{1}{m_Z^2-t}\frac{8Q^4}{u}+\ln(M_R^2)\frac{1}{m_Z^2-u}\frac{8Q^4}{t}\\
&\quad+\ln(m_Z^2)^2\frac{1}{m_Z^2-u}\frac{2Q^4-2Q^2t+t^2}{t}+\ln(m_Z^2)^2\frac{1}{m_Z^2-t}\frac{2Q^4-2Q^2u+u^2}{u}\\
&\quad-\ln(m_Z^2)\ln(M_R^2)\frac{1}{m_Z^2-u}\frac{2(2Q^4-2Q^2t+t^2)}{t}\Bigg]\frac{(257-1040c^2+1632c^4-1280c^6+512c^8)}{10368c^4s^2}\\
&+\left(\ln(M_R^2)^2+\zeta_2\right)\left(-\frac{257-1022c^2+1488c^4-992c^6+512c^8}{2592c^4s^2}\right.\\
&\quad\left.+\frac{(257-1028c^2+1542c^4-1136c^6+608c^8)Q^2(t+u)}{1728c^4s^2tu}\right)\\
&+\left(\ln(M_R^2)^2+\zeta_2\right)\left(\frac{t}{u}+\frac{u}{t}\right)\frac{(-257+1022c^2-1596c^4+1424c^6-512c^8)t}{5184c^4s^2u}.
\end{aligned}
$$

In our formula we denoted by $s=\sin\theta_W$, $c=\cos\theta_W$, s_{12} is Mandelstam variable and equal to the squared momenta of incoming particle $(p_1+p_2)^2$. The integrals, which come from bubble, triangle and box diagrams are here:

$$
\begin{aligned}
B_0(s,m_1^2,m_2^2) &= 2-\frac{1}{2}\ln\frac{m_1^2m_2^2}{M^4}+\frac{m_2^2-m_1^2}{2s}\ln\frac{m_1^2}{m_2^2}+\phi, \qquad \text{(C.7)}\\
&\text{where}\quad \phi=-\frac{\sqrt{a}}{2s}\ln\frac{m_1^2+m_2^2-s-\sqrt{a}}{m_1^2+m_2^2-s+\sqrt{a}},\ \text{if } a>0\\
&\qquad\quad \phi=-\frac{\sqrt{-a}}{2s}\arctan\frac{\sqrt{-a}}{m_1^2+m_2^2-s},\ \text{if } a<0\\
&\qquad\quad a=(m_1^2+m_2^2-s)^2-4m_1^2m_2^2;
\end{aligned}
$$

$$
\begin{aligned}
B_0(s,m_1^2,m_2^2,1) &= 1-\frac{1}{2}\ln\frac{m_1^2m_2^2}{M^4}+\frac{m_1^2+m_2^2}{2(m_2^2-m_1^2)}\ln\frac{m_1^2}{m_2^2} \qquad \text{(C.8)}\\
B_0(t,m^2,0,\epsilon) &= 4-2(L-L_M)+\frac{1}{2}(L+L_M)^2+' \, fracm^2t\left(2L-\frac{1}{2}L^2-LL_M-\mathrm{Li}_2\left(\frac{t}{m^2}\right)\right),\\
&\qquad L=\ln\left(\frac{m^2-t}{m^2}\right), \qquad L=\ln\left(\frac{m^2}{M^2}\right);\\
B_0(0,0,m^2) &= 1-\ln\frac{m^2}{M^2},
\end{aligned}
$$

$$
\begin{aligned}
C_1(s,m^2) &= \frac{1}{s}\Big(\mathrm{Li}_2\left(\frac{-m^2}{s}\right)+\ln\left(\frac{s}{m^2}\right)\ln\left(\frac{s+m^2}{m^2}\right)-\frac{1}{2}\ln^2\left(\frac{s}{m^2}\right)-\zeta_2\Big) \qquad \text{(C.9)}\\
C_1(t,m^2) &= \zeta_2-\frac{1}{t}\mathrm{Li}_2\left(1+\frac{t}{m^2}\right)
\end{aligned}
$$

$$
\begin{aligned}
C_2(t,Q^2,m^2) &= \frac{1}{Q^2-t}\Big(\frac{1}{2}\ln^2\left(\frac{m^2-t}{m^2}\right)-\frac{1}{2}\ln^2\left(\frac{m^2Q^2}{(m^2-t)(m^2-t+Q^2)}\right) \qquad \text{(C.10)}\\
&\quad +\frac{1}{2}\ln^2\left(\frac{m^2-t+Q^2}{m^2}\right)+\mathrm{Li}_2\left(\frac{t}{m^2}\right)-\mathrm{Li}_2\left(\frac{t-m^2}{Q^2}\right)-\zeta_2\Big),\\
C_2(s,Q^2,m^2) &= \frac{1}{Q^2-s}\Big(-\zeta_2+\frac{1}{2}(\ln^2(m^2)-\ln^2(Q^2))+\ln(|m^2-s|)\ln\left(\frac{Q^2}{m^2}\right)\\
&\quad +\ln\left(\left|\frac{Q^2}{m^2-s}\right|\right)\ln\left(\left|\frac{m^2+Q^2-s}{m^2}\right|\right)+Re\mathrm{Li}_2\left(\frac{s}{m^2}\right)-Re\mathrm{Li}_2\left(\frac{s-m^2}{Q^2}\right),
\end{aligned}
$$

$$
\begin{aligned}
C_3(t,Q^2,m^2,m^2) &= \frac{1}{Q^2-t}\Bigg[\mathrm{Li}_2\left(\frac{t}{m^2}\right)-2\mathrm{Re}\,\mathrm{Li}_2\left(\frac{Q^2}{2Q^2}+i\frac{a}{2m^2}\right) \qquad \text{(C.11)}\\
&\quad -\mathrm{Re}\,\mathrm{Li}_2\left(\frac{m^2Q^2}{z}\right)+\mathrm{Re}\,\mathrm{Li}_2\left(\frac{(m^2-t)Q^2}{z}\right)\\
&\quad +2\left(\pi-2\arctan\left(\frac{a}{Q^2}\right)\right)\arctan\left(\frac{a}{Q^2-2t}\right)+\ln\left(\frac{Q^2}{m^2}\right)\ln\left(\frac{Q^2-t}{t}\right)\\
&\quad +\ln\left(\frac{m^2-t}{m^2}\right)\ln\left(\frac{t^2}{m^2Q^2-tQ^2+t^2}\right)\\
&\quad +2\mathrm{Re}\,\mathrm{Li}_2\left(\frac{-Q^2(Q^2-2t)+a^2}{w}+i\,2a\,\frac{Q^2-2}{w}\right)\\
&\quad -2\mathrm{Re}\,\mathrm{Li}_2\left(\frac{+Q^2(Q^2-2t)+a^2}{w}-i\,a\,\frac{2t}{w}\right)\\
&\quad a=\sqrt{Q^2(4m^2-Q^2)}\\
&\quad z=m^2Q^2-Q^2t+t^2\\
&\quad w=(Q^2-2t)^2+a^2.
\end{aligned}
$$

$$
\begin{aligned}
D_1(s,t,Q^2,m^2) \;=\; & \frac{1}{st+m^2(t+u)}\Bigg[\mathrm{Li}_2\left(1+\frac{m^2-t}{Q^2}\right)-\mathrm{Li}_2\left(1+\frac{m^2}{s}\right) \\
& +2\mathrm{Li}_2\left(\frac{t}{m^2}\right)-2\mathrm{Li}_2\left(1-\frac{Q^2}{s}\right) \\
& +2\mathrm{Li}_2\left(1-\frac{Q^2m^2}{s(m^2-t)}\right)+\ln\left(\frac{m^2Q^2}{s(m^2-t)}\right)\ln\left(\frac{m^2M^2}{(m^2-t)^2}\right)\Bigg]
\end{aligned}
\tag{C.12}
$$

For calculating of the next four-point diagram, the formula (4.37) in [35] was used:

$$
\begin{aligned}
D_3(s,t,Q^2,m_2^2,m_3^2) \;=\; & \frac{1}{\delta}\Big(-2\mathrm{Li}_2\left(\frac{1-m_2^2}{m_2^2-u}\right)-2\mathrm{Li}_2\left(\frac{1-m_3^2}{m_3^2-t}\right) \\
& -\mathrm{Re}\,\mathrm{Li}_2(1-w_2x_{34}-iw_2y_{34})-\mathrm{Re}\,\mathrm{Li}_2(1-w_2x_{34}+iw_2y_{34}) \\
& -\mathrm{Re}\,\mathrm{Li}_2(1-w_3x_{43}-iw_3y_{43})-\mathrm{Re}\,\mathrm{Li}_2(1-w_3x_{43}+iw_3y_{43}) \\
& +2\mathrm{Li}_2\left(1-\frac{m_2^2m_3^2}{(m_2^2-u)(m_3^2-t)}\right) \\
& +\ln\left(\frac{m_2^2-u}{M^2}\right)\ln\left(\frac{m_3^2-t}{m_3^2}\right) \\
& +\ln\left(\frac{m_3^2-t}{M^2}\right)\ln\left(\frac{m_2^2-u}{m_2^2}\right)-x^2+y^2\Big);
\end{aligned}
\tag{C.13}
$$

$$
\begin{aligned}
&\delta = tu-m_2^2t-m_3^2u \quad w_2=\frac{m_2^2}{m_3^2-t} \quad w_3=\frac{m_3^2}{m_2^2-u} \\
&x_{34}=\frac{a_{34}(a_{34}-1)+b_{34}b_{34}}{(a_{34}-1)^2+b_{34}^2} \quad y_{34}=-\frac{b_{34}}{(a_{34}-1)^2+b_{34}^2} \\
&x_{43}=\frac{a_{43}(a_{43}-1)+b_{43}b_{43}}{(a_{43}-1)^2+b_{43}^2} \quad y_{43}=-\frac{b_{43}}{(a_{43}-1)^2+b_{43}^2} \\
&a_{34}=\frac{1-r_{23}}{2} \quad b_{34}=-\frac{\sqrt{(4m_3^2/Q^2-(1-r_{23})^2)}}{2} \\
&a_{43}=\frac{1+r_{23}}{2} \quad b_{43}=-\frac{\sqrt{(4m_2^2/Q^2-(1+r_{23})^2)}}{2} \\
&r_{23}=\frac{m_2^2-m_3^2}{Q^2} \\
&x=\frac{1}{2}\ln(x_{34}x_{34}+y_3y_{34}) \quad y=phase\{x_{34},y_{34}\}
\end{aligned}
$$

The results for other chanels ($q+g\to q+z$, $\bar{q}q\to Z+g$ etc.) can be found by crossing procedure.

Appendix D

Analytical result for EW corrections, $qq \to Zqq$ part

Here we present the mixed QCD/weak partonic differential cross-section for $qq \longrightarrow Z+q+q$ process. It comes from the interference of the diagrams which shown in the Fig. (3.1) with gluon exchange and the same diagrams with Z boson exchange.

$$\begin{aligned}
\frac{s d\sigma^{qq}_{\rm QCD/weak}}{dt\,du} &= \frac{2\alpha^2\alpha_s(v_u^4+6u^2a_u^2+a_u^6)C_F}{N_c s}\times \\
&\quad \Big[\Big\{ f_{ln}(s,t,u) + I_4(1,1,t,1) f_1^{1,1}(s,t,u) \\
&\quad + I_4(1,1,t,-1) f_{-1}^{1,1}(s,t,u) - I_4(1,2,t,-1) f_{-1}^{1,2}(s,t,u) \Big\} \\
&\quad + \Big\{ t \leftrightarrow u \Big\}\Big] .
\end{aligned} \tag{D.1}$$

In the above formula I_4 represent some phase space integrals given in Appendix C of Ref. [36]. The explicit expressions read

$$\begin{aligned}
I_4(1,1,t,1) &= \frac{1}{\sqrt{X_+}} \ln\Big(\frac{u(Q^2-s_2)+2Q^2s+\sqrt{X_+}}{u(Q^2-s_2)+2Q^2s-\sqrt{X_+}}\Big), \\
I_4(1,1,t,-1) &= \frac{1}{\sqrt{X_-}} \ln\Big(\frac{2Q^4-Q^2(t+u)-st+\sqrt{X_-}}{2Q^4-Q^2(t+u)-st-\sqrt{X_-}}\Big), \\
I_4(1,2,t,-1) &= 2\frac{4Q^6+st(t+u)-2Q^4(s+2(t+u))+Q^2(-2s^2-2s(t+u)+(t+u)^2)}{4Q^2sX_-} \\
&\quad + \frac{2Q^6-s(s+u)t+Q^2u(s+t+u)-Q^4(2s+3u+t)}{2X_-} I_4(1,1,t,-1), \\
X_+ &= (u(Q^2-s_2)+2Q^2s)^2 - 4Q^4s(s+u), \\
X_- &= (2Q^4-Q^2(t+u)-st)^2 - 4Q^4s(s+u).
\end{aligned} \tag{D.2}$$

And kinematics's factors are here:

$$
\begin{aligned}
f_{ln}(s,t,u) &= -\ln\frac{(Q^2t-s_2(s+Q^2))^2}{Q^2(s+t)(s_2-t)^2}\frac{Q^2(s_2^2+(s_2-t)^2-u(2s+u))+s(2s_2(s-Q^2)+(t+u)^2}{4(Q^2+s)^2tu} \\
&\quad + L_{st}\Bigg[\frac{-s^2}{2(Q^2+s)^2t}+\frac{s^2}{2(Q^2+s-s_2)t(s+u)}-\frac{s+t}{4t(s+u)}-\frac{1}{4t} \\
&\quad + \frac{t^2-u^2+2s_2^2-2s_2t}{4(Q^2+s)tu}+\frac{s_2Q^2}{2t^2(s+u)}\Bigg]+\frac{L_{\lambda t}(s^2+(Q^2-s_2)^2)}{4(Q^2+s-s_2)t(s+u)} \\
&\quad + \ln\Big(\frac{Q^2}{s+t}\Big)\frac{Q^2(s+t-Q^2)}{2u^2(s+t)} \\
f_1^{1,1}(s,t,u) &= \frac{s^2(Q^2-s-s_2)}{4(Q^2+s-s_2)(s+u)} \\
&\quad + \frac{(2s_2^2-2ts_2+t(Q^2+s2))s}{4t(s+u)}-\frac{(-2s_2+t+u)^2}{4t} \\
f_{-1}^{1,1}(s,t,u) &= -\frac{s^3}{2(Q^2+s-s_2)(s+u)}-\frac{s^2Q^2}{2(Q^2+s)^2}+\frac{s(Q^2-u)}{Q^2+s} \\
&\quad + \frac{s_2s(u-Q^2)}{2(Q^2+s)u}-\frac{s(u-t)^2}{4t(Q^2+s)}+\frac{s_2s(u-s_2)}{2(Q^2+s)t}+\frac{s^2(2t-s_2)}{4t(s+u)} \\
&\quad - \frac{5s_2t}{4(s+u)}+\frac{s_2^2(2t-s_2)}{t(s+u)}+\frac{t^2}{4(s+u)}+\frac{s(2s_2-t)}{4(s+u)}+\frac{u^2}{2t}-\frac{5s_2}{2}+\frac{t}{2}+u \\
&\quad - \frac{9s_2u}{4t}+\frac{3s_2^2}{t}-\frac{s_2^2}{u}-\frac{t^2}{4u}+\frac{s_2t}{u}-\frac{5s_2s}{4t}+\frac{s_2s}{2u} \\
f_{-1}^{1,2}(s,t,u) &= \frac{Q^2s^2}{Q^2+s}+\frac{s_2(Q^2-u)}{t^2(Q^2+s)}+\frac{2s_2t-u(t+u)}{2(Q^2+s)u^2}
\end{aligned}
\tag{D.3}
$$

Bibliography

[1] ATLAS Collaboration, The ATLAS Experiment at the CERN LHC, JINST 3:S08003, 2008

[2] CMS Collaboration, The CMS Experiment at the CERN LHC, JINST 3:S08004, 2008

[3] S. D. Drell and T. M. Yan, Phys. Rev. Lett. **25** (1970) 316 [Erratum-ibid. **25** (1970) 902].

[4] J. H. Christenson, G. S. Hicks, L. M. Lederman, P. J. Limon, B. G. Pope and E. Zavattini, Phys. Rev. Lett. **25**, 1523 (1970).

[5] G. Arnison *et al.* [UA1 Collaboration], Phys. Lett. B **122** (1983) 103;
G. Arnison *et al.* [UA1 Collaboration], Phys. Lett. B **126** (1983) 398;
M. Banner *et al.* [UA2 Collaboration], Phys. Lett. B **122** (1983) 476;
P. Bagnaia *et al.* [UA2 Collaboration], Phys. Lett. B **129** (1983) 130.

[6] G. Altarelli, R. K. Ellis and G. Martinelli, Nucl. Phys. B **157** (1979) 461.
G. Altarelli, R. K. Ellis and G. Martinelli, Nucl. Phys. B **143** (1978) 521 [Erratum-ibid. B **146** (1978) 544].
G. Altarelli, G. Parisi and R. Petronzio, Phys. Lett. B **76**, 356 (1978).

[7] R. K. Ellis, G. Martinelli and R. Petronzio, Nucl. Phys. B **211** (1983) 106.

[8] R. J. Gonsalves, J. Pawlowski and C. F. Wai, Phys. Rev. D **40** (1989) 2245.

[9] P. B. Arnold and M. H. Reno, Nucl. Phys. B **319** (1989) 37 [Erratum-ibid. B **330** (1990) 284].

[10] R. Hamberg, W. L. van Neerven and T. Matsuura, Nucl. Phys. B **359** (1991) 343 [Erratum-ibid. B **644** (2002) 403];
P. J. Rijken and W. L. van Neerven, Phys. Rev. D **51** (1995) 44 [arXiv:hep-ph/9408366].

[11] R. V. Harlander and W. B. Kilgore, Phys. Rev. Lett. **88** (2002) 201801 [arXiv:hep-ph/0201206].

[12] W. T. Giele, E. W. N. Glover and D. A. Kosower, Nucl. Phys. B **403** (1993) 633 [arXiv:hep-ph/9302225];
J. M. Campbell and R. K. Ellis, Phys. Rev. D **65** (2002) 113007 [arXiv:hep-ph/0202176] ;
J. M. Campbell, R. K. Ellis and D. L. Rainwater, Phys. Rev. D **68** (2003) 094021 [arXiv:hep-ph/0308195].

[13] T. Matsuura, S. C. van der Marck and W. L. van Neerven, Nucl. Phys. B **319** (1989) 570.

[14] Y. L. Dokshitzer, D. Diakonov and S. I. Troian, Phys. Lett. B **79** (1978) 269.
P. B. Arnold and R. P. Kauffman, Nucl. Phys. B **349** (1991) 381.
G. Altarelli, R. K. Ellis, M. Greco and G. Martinelli, Nucl. Phys. B **246** (1984) 12.
G. Parisi and R. Petronzio, Nucl. Phys. B **154** (1979) 427.

[15] C. Balazs and C. P. Yuan, Phys. Rev. D **56** (1997) 5558 [arXiv:hep-ph/9704258].
R. K. Ellis and S. Veseli, Nucl. Phys. B **511** (1998) 649 [arXiv:hep-ph/9706526].
H. L. Lai, J. Huston, Z. Li, P. Nadolsky, J. Pumplin, D. Stump and C. P. Yuan, Phys. Rev. D **82** (2010) 054021 [arXiv:1004.4624 [hep-ph]];
J. Pumplin, D. R. Stump, J. Huston, H. L. Lai, P. M. Nadolsky and W. K. Tung, JHEP **0207** (2002) 012 [arXiv:hep-ph/0201195];
P. M. Nadolsky *et al.*, Phys. Rev. D **78** (2008) 013004 [arXiv:0802.0007 [hep-ph]].

[16] C. Anastasiou, L. J. Dixon, K. Melnikov and F. Petriello, Phys. Rev. Lett. **91** (2003) 182002 [arXiv:hep-ph/0306192];
C. Anastasiou, K. Melnikov and F. Petriello, Phys. Rev. D **69** (2004) 076010 [arXiv:hep-ph/0311311];
K. Melnikov and F. Petriello, Phys. Rev. D **74** (2006) 114017 [arXiv:hep-ph/0609070];
C. Anastasiou, K. Melnikov and F. Petriello, Nucl. Phys. B **724** (2005) 197 [arXiv:hep-ph/0501130]. C. Anastasiou, K. Melnikov and F. Petriello, Nucl. Phys. B **724** (2005) 197 [arXiv:hep-ph/0501130].

[17] J. H. Kuhn, A. Kulesza, S. Pozzorini and M. Schulze, Nucl. Phys. B **727** (2005) 368 [arXiv:hep-ph/0507178].

[18] J. H. Kuhn, A. Kulesza, S. Pozzorini and M. Schulze, Phys. Lett. B **609** (2005) 277 [arXiv:hep-ph/0408308].

[19] A. Kotikov, J. H. Kuhn and O. Veretin, Nucl. Phys. B **788** (2008) 47 [arXiv:hep-ph/0703013].

[20] J. Fleischer, A. V. Kotikov and O. L. Veretin, Nucl. Phys. B **547** (1999) 343 [arXiv:hep-ph/9808242].

[21] G. Passarino and M. J. G. Veltman, Nucl. Phys. B **160** (1979) 151.

[22] W. Beenakker, W. L. van Neerven, R. Meng, G. A. Schuler and J. Smith, Nucl. Phys. B **351** (1991) 507.

[23] H1 Collaboration: C. Adloff *et al.* [H1 Collaboration], Eur. Phys. J. C **13** (2000) 609 [arXiv:hep-ex/9908059]. C. Adloff *et al.* [H1 Collaboration], Eur. Phys. J. C **21** (2001) 33 [arXiv:hep-ex/0012053].

[24] S. Chekanov *et al.* [ZEUS Collaboration], Eur. Phys. J. C **21** (2001) 443 [arXiv:hep-ex/0105090];
A. M. Cooper-Sarkar, arXiv:hep-ph/0110386.

[25] H. L. Lai, M. Guzzi, J. Huston, Z. Li, P. M. Nadolsky, J. Pumplin and C. P. Yuan, Phys. Rev. D **82** (2010) 074024 [arXiv:1007.2241 [hep-ph]];
J. Pumplin, D. R. Stump, J. Huston, H. L. Lai, P. M. Nadolsky and W. K. Tung, JHEP **0207** (2002) 012 [arXiv:hep-ph/0201195].

[26] A. D. Martin, W. J. Stirling, R. S. Thorne and G. Watt, Eur. Phys. J. C **70** (2010) 51 [arXiv:1007.2624 [hep-ph]];
A. D. Martin, R. G. Roberts, W. J. Stirling and R. S. Thorne, Eur. Phys. J. C **39** (2005) 155 [arXiv:hep-ph/0411040];
A. D. Martin, W. J. Stirling, R. S. Thorne and G. Watt, Phys. Lett. B **652** (2007) 292 [arXiv:0706.0459 [hep-ph]];
A. D. Martin, W. J. Stirling, R. S. Thorne and G. Watt, Eur. Phys. J. C **63** (2009) 189 [arXiv:0901.0002 [hep-ph]].

[27] A. H. Mueller, Phys. Rev. D **18** (1978) 3705.
G. Curci, W. Furmanski and R. Petronzio, Nucl. Phys. B **175** (1980) 27.

[28] V. N. Gribov and L. N. Lipatov, Sov. J. Nucl. Phys. **15** (1972) 438 [Yad. Fiz. **15** (1972) 781];
L. N. Lipatov, Sov. J. Nucl. Phys. **20** (1975) 94 [Yad. Fiz. **20** (1974) 181];
G. Altarelli and G. Parisi, Nucl. Phys. B **126** (1977) 298;
Y. L. Dokshitzer, Sov. Phys. JETP **46** (1977) 641 [Zh. Eksp. Teor. Fiz. **73** (1977) 1216].

[29] K. G. Chetyrkin and F. V. Tkachov, Nucl. Phys. B **192** (1981) 159.

[30] F. V. Tkachov, Phys. Lett. B **100** (1981) 65.

[31] S. Laporta, Int. J. Mod. Phys. A **15** (2000) 5087 [arXiv:hep-ph/0102033].

[32] C. Anastasiou and A. Lazopoulos, JHEP **0407** (2004) 046 [arXiv:hep-ph/0404258].

[33] G. 't Hooft and M. J. G. Veltman, Nucl. Phys. B **44** (1972) 189;
G. 't Hooft and M. J. G. Veltman, Nucl. Phys. B **153** (1979) 365.

[34] G. J. van Oldenborgh and J. A. M. Vermaseren, Z. Phys. C **46** (1990) 425;
A. Denner, U. Nierste and R. Scharf, Nucl. Phys. B **367** (1991) 637;
W. Beenakker and A. Denner, Nucl. Phys. B **338** (1990) 349;
J. Fleischer, F. Jegerlehner and O. V. Tarasov, Nucl. Phys. B **672** (2003) 303 [arXiv:hep-ph/0307113].

[35] R. K. Ellis and G. Zanderighi, JHEP **0802** (2008) 002 [arXiv:0712.1851 [hep-ph]].

[36] W. Beenakker, H. Kuijf, W. L. van Neerven and J. Smith, Phys. Rev. D **40** (1989) 54.

[37] M. E. Peskin and D. V. Schroeder, An Introduction to Quantum Field Theory, 1995, Addison-Wesley Advanced Book Program.

[38] S. Weinberg, The Quantum Theory of Fields, (three volumes: 1995, 1996, 2003).

[39] M. Tentyukov and J. Fleischer, Comput. Phys. Commun. **132** (2000) 124 [arXiv:hep-ph/9904258];
M. Tentyukov and J. Fleischer, Nucl. Instrum. Meth. A **502** (2003) 570 [arXiv:hep-ph/0210179].

[40] B. A. Kniehl, Phys. Lett. B **254** (1991) 267.

[41] M. Gluck, M. Stratmann and W. Vogelsang, Phys. Lett. B **343** (1995) 399.

[42] K. Nakamura et al. (Particle Data Group), J. Phys. G **37**, 075021 (2010) http://pdg.lbl.gov/

[43] F. Jegerlehner, M. Y. .Kalmykov, O. Veretin, Nucl. Phys. **B658** (2003) 49-112, F. Jegerlehner [hep-ph/0105283].

[44] T. Hahn, Nucl. Instrum. Meth. **A559** (2006) 273-277. [hep-ph/0509016].

[45] J. C. Collins and D. E. Soper, Nucl. Phys. B **194** (1982) 445.

Acknowlegements

I would like to thank my supervisor Prof. Bernd A. Kniehl for discussions and for contionuous support. I would like to thank prof. Jochen Bartels for support.

I am very grateful for Oleg Veretin for collaboration and especially for his help and science discussion. I thank for discussions and friendship Anatoliy Kotikov, Zakaria Merebashvili, Oleg Tarasov, Simon Albino, Mathias Butenschn, Mikhail Kalmykov, Paolo Bolzoni.

I am thankful to the members of the II. Institute of Theoretical Physics and DESY Theory Group for the pleasant athmosphere. I am grateful Elizabeth Monteiro Duarte for help in questions about studing and living in Hamburg.

I would like to thank my friends, who support me all these years: Oleg, Lyudmila, Denis, Julia, Anastasia, Hayk, Aziz, Igor, Mikhail, Mayya, Vitalij, Nikolaj, Irina, Denis, Elena, Tatyana, Oleksandr, Patrick, Mariam, Pavel, Maks, Polina, Lola, Ekaterina.

Finnally, I would like say many thanks to Alexey for the love and tender loving care and to my parents and sister for daily support and friendly sympathy.

I acknowledge the Deutsche Forschungsgemeinschaft (DFG), the Sonderforschungsbereich (SFB) and Hamburg Univeristy for the financial support.